

UNCLASSIFIED

AD NUMBER

AD819153

LIMITATION CHANGES

TO:

Approved for public release; distribution is unlimited. Document partially illegible.

FROM:

Distribution authorized to U.S. Gov't. agencies and their contractors; Critical Technology; JUL 1967. Other requests shall be referred to Air Force Rome Air Development Center, EMLI, Griffiss AFB, NY 13440. Document partially illegible. This document contains export-controlled technical data.

AUTHORITY

radc usaf ltr, 31 jan 1974

THIS PAGE IS UNCLASSIFIED

AD819153

RADC-TR-67-347  
Final Report



WIDEBAND ELEMENT SPACING AND WEIGHTING

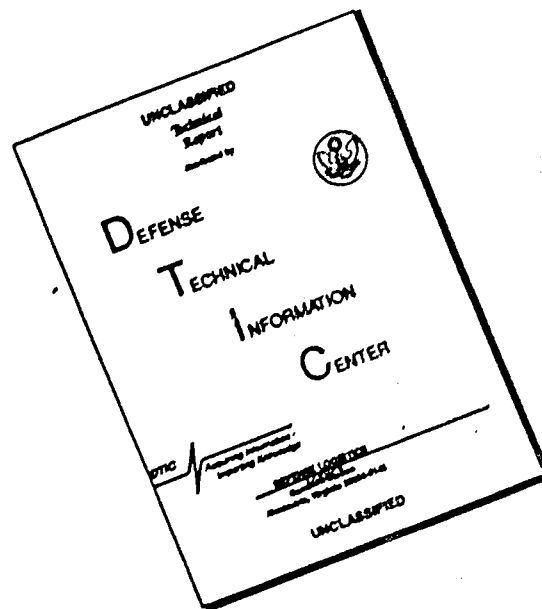
William E. Rupp  
Wilfred E. Schneider  
Philip L. Randolph  
The Bendix Corporation

TECHNICAL REPORT NO. RADC-TR-67-347  
July 1967

This document is subject to special  
export controls and each transmittal  
to foreign governments, foreign na-  
tionals or representatives thereto may  
be made only with prior approval of  
RADC (EMLI), GAFB, N.Y. 13440

Rome Air Development Center  
Air Force Systems Command  
Griffiss Air Force Base, New York

# DISCLAIMER NOTICE



THIS DOCUMENT IS BEST QUALITY AVAILABLE. THE COPY FURNISHED TO DTIC CONTAINED A SIGNIFICANT NUMBER OF PAGES WHICH DO NOT REPRODUCE LEGIBLY.

When US Government drawings, specifications, or other data are used for any purpose other than a definitely related government procurement operation, the government thereby incurs no responsibility nor any obligation whatsoever; and the fact that the government may have formulated, furnished, or in any way supplied the said drawings, specifications, or other data is not to be regarded, by implication or otherwise, as in any manner licensing the holder or any other person or corporation, or conveying any rights or permission to manufacture, use, or sell any patented invention that may in any way be related thereto.

Do not return this copy. Retain or destroy.



## WIDEBAND ELEMENT SPACING AND WEIGHTING

William E. Rupp  
Wilfred E. Schneider  
Philip L. Randolph  
The Bendix Corporation

This document is subject to special  
export controls and each transmittal  
to foreign governments, foreign na-  
tionals or representatives thereto may  
be made only with prior approval of  
RADC (EMLI), GAFB, N.Y. 13440

## FOREWORD

This final report covers a twelve month study program entitled "Wideband Array Element Spacing and Weighting". The period of the study extended from 4 April 1966 to 4 April 1967. The report is submitted by The Bendix Corporation, Communications Division, Baltimore, Maryland in May 1967. There were no subcontractors engaged in the investigation.

The effort covered by this report was accomplished under Contract AF30(602)-4206, issued by Rome Air Development Center, Griffiss Air Force Base, New York. The program monitor was Mr. Joseph A. Lovecchio (EMATS).

The authors acknowledge the efforts of Messrs. R. Jones, H. Gruenberger, and K. Hnat in computational assistance and evaluation of computed data. The contributions of many other Bendix engineers as consultants are also acknowledged.

The use of references has been confined to unclassified material. This report contains no classified information extracted from classified documents.


This technical report has been reviewed by the Foreign Disclosure Policy Office (EMLI). It is not releasable to the Clearinghouse for Federal Scientific and Technical Information because it contains information embargoed from release to Sino-Soviet Bloc Countries by AFR 400-10, Strategic Trade Control Program.

This technical report has been reviewed and is approved.


Approved:

  
JOSEPH LOVECCHIO  
Project Engineer

Approved:

  
THOMAS S. BOND, JR.  
Colonel, USAF  
Chief, Surveillance  
and Control Division

FOR THE COMMANDER.

  
IRVING J. GABELMAN  
Chief, Advanced Studies Group

## ABSTRACT

This study was initiated to determine the effects of antenna element weighting (amplitude control) and spacing on the signal-to-noise ratio of wideband systems. The initial analysis is directed toward the linear array operating in an environment of white noise, uniformly distributed in space. These confinements are later removed to illustrate application to planar arrays, and non-uniform noise conditions.

It is shown that the signal-to-noise ratio of an antenna system operating in a uniform noise environment is optimized when the array directivity is maximum. Optimization involves the application of a specific illumination function which can be achieved by element weighting, element spacing or a combination.

The application of wideband signals modifies the array pattern in the time space domain. Although the nature of the modification is dependent on waveform, the sidelobe displacement in time and space is a function of the number of elements comprising the array.

An iterative technique of mathematical analysis is developed which permits solutions to large array problems where matrix inversion is difficult. Several examples of possible applications of the analysis are presented including a spectral detection technique, an approach to secure communications, and a concept of array adaptation to a non-uniform noise environment.

## EVALUATION

Much study has been devoted to optimization of element spacing and element weighting for narrow band arrays, but comparatively little equivalent study has been devoted to the wideband array.

The study herein has looked at the wideband array and has further developed the theory of wideband arrays by considering not only radiation patterns but also the processed array signal.

Work in the area of wideband arrays will continue to put the theory and techniques of the wideband array on the same firm basis as the narrow band array.

*Joseph Lovecchio*  
JOSEPH LOVECCHIO  
Project Engineer  
EMATS/330-3685

*Thomas Maggio*  
THOMAS MAGGIO  
Chief, Signal Processing Section  
Techniques Branch

## TABLE OF CONTENTS

	Page
SECTION I - INTRODUCTION	1
SECTION II - SUMMARY	2
SECTION III - DESIGN PARAMETERS IN THE LINEAR ARRAY -- NARROW BAND ARRAYS	4
1. Array Design	4
1.1 Uniform Weighting	9
1.2 Homming Function	9
1.3 Cosine <sup>n</sup> Illumination	9
1.4 Modified Sin X/X	9
1.5 Triangular Function	9
1.6 Tchebycheff Distribution	9
1.7 Taylor's Distribution	9
2. Graphical Analysis	10
3. Space Taper Arrays	16
SECTION IV - SIGNAL NOISE CONSIDERATIONS IN ARRAY ANTENNAS	21
1. Signal Power in the Antenna Array	21
2. Noise Power	27
2.1 External Noise	28
2.2 Antenna Noise Power ( $N_a$ )	30
2.3 Network Noise Power ( $N_r$ )	30
3. Maximization of Signal-to-Noise Ratio	31
4. Maximization of Array Directivity through Element Spacing	40
SECTION V - WIDEBAND EFFECTS	45
1. Aperture Effects	45
2. Signal-to-Noise Ratio Effects	50
3. Space-Frequency Equivalence	66
SECTION VI - APPLICATIONS	77
1. Signal-to-Noise Ratio in Directive Arrays	77
2. Spectral or Waveform Detection	77
3. Secure Communications	78
4. Adaptation in a Non-Uniform Noise Environment	81
5. Application to Planar Arrays	85
SECTION VII - COMPUTATIONAL TECHNIQUES	89
1. A Method for Controlling Pattern Sidelobe Level Through Space and Amplitude Tapering	89
2. An Exact Method of Determining the Array Output Waveform for any Specified Input Waveform	90
3. Maximization Techniques	93

TABLE OF CONTENTS (Continued)

	Page
SECTION VIII REFERENCES	99
APPENDIX A - DERIVATION OF THE PATTERN SYNTHESIS TECHNIQUE	103
APPENDIX B - NOISE ANALYSIS	105
APPENDIX C - CORRELATION COEFFICIENTS	110

# LIST OF ILLUSTRATIONS

Figure		Page
1	Radiator Pattern-Uniform Illumination with Sidelobe Envelopes for Other Illumination Functions	11
2	Beamwidth of Uniform Linear Array (Beam Normal to Array Axis)	12
3	Illumination Efficiency in Amplitude Tapered Linear Array	13
4	Beamwidth Relative to Uniformly Illuminated Linear Array	14
5	Linear Array Nomograph	15
6	Array Element Gain in Linear Arrays	17
7	Amplitude Tapered Array of 24 Element Sidelobe Control in $u < 1.00$	18
8	Space Tapered Array of 24 Elements Sidelobe Control in $u < 1.00$	19
9	Basic Concept	22
10	Equivalent Circuit	22
11	Array Equivalent Circuit	25
12	Noise Temperature vs. Frequency	29
13	Array Directivity as a Function of Element Spacing, $N = 10$ Elements	33
14	Linear Array of Isotropic Sources, Array Length = $5\lambda$	34
15	Time-Space Response of Wideband Array	48
16	Near Boresight Response (Expanded) Wideband Array	51
17	Near Boresight Response Contour Plot-Uniform Frequency	52
18	Maximum Response in Time-Space Domain	53
19	Near Boresight Response Contour Plot-Cosine Frequency	54
20	Maximum Response in Time-Space Domain-Cosine Frequency	55
21	Near Boresight Response Contour Plot	56
22	Maximum Response in Time-Space Domain	57
23	Near Boresight Response Contour Plot	58
24	Maximum Response in Time-Space Domain	59
25	Near Boresight Response Contour Plot	60
26	Near Boresight Response Contour Plot	61
27	Near Boresight Response Contour Plot	62
28	Near Boresight Response Contour Plot	63
29	The Correlation Coefficient for Band-Limited White Noise	65
30	Maximized Antenna Directivity by Amplitude Control	67
31	Maximized Antenna Directivity by Element Spacing	69
32	Space-Frequency Equivalence	70
33	Thirty Element Array Space-Frequency Equivalence	72
34	Time Response of Thirty Element Array	73
35	Thirty Element Space Tapered Array	74
36	Time Response of Modified Thirty Element Array	77
37	Transmitted Waveform and Spectrum	79
38	Direct Signal Processing	80
39	Parallel Signal Processing	80
40	Optimized S/N for a 20 DB Noise Increase in the Sidelobe Region	82
41	Optimized S/N for a 20 DB Noise Increase in the Far-out Sidelobe Region	83
42	Optimized S/N for a 10 DB Noise Increase Near Boresight	84

## LIST OF ILLUSTRATIONS (Continued)

Figure		Page
43	Optimized Planar Array - Narrow Band	87
44	Optimized Planar Array - Wideband	88

## LIST OF TABLES

Table		Page
1	Continuous Aperture Weighting	5/6
2	Discrete Aperture Weighting	7/8
3	Results of Element Spacing Computations	44
4	Illustrated Time-Space Response Functions	50
5	Maximum Antenna Directivity by Amplitude Control, Element Spacing and Array Length	68
6	Algorithm for Iterative Pattern Synthesis	91
7	Maximization Algorithm	94
C-1	Array Conditions and Correlation Function	115



# LIST OF SYMBOLS AND DEFINITIONS (ARABIC)

<u>Symbol</u>	<u>Unit</u>	<u>Function</u>	<u>Location*</u>
A		Factor determining the pattern for a Taylor distribution function	Section III
A	Degrees	Extended element aperture	Appendix C
$a_K$		Impulse function magnitude	
$A_n, A_m$	Volts	n-th or m-th element amplitude coefficients for a linear array	
B	Hz	Bandwidth	Section IV, Appendix B
B		Factor which determines the value of the highest sidelobe in the modified Sin X/X pattern	
B		Parameter determining non-isotropic noise characteristics	Appendix C
BW	Degrees	Beamwidth measured at the half power points	Section III
C	Cm/Sec	Velocity of light = $3 \times 10^{10}$ Cm/Sec	
D		Array directivity	
$d, d_k$	Cm or inches	Element spacing for a linear array	
$d_x, d_y$	Cm or inches	Element spacing for a planar array	Appendix C
$E(u, t)$	Volts	Linear array voltage pattern (function of indicated variables)	
$\epsilon_m$	Degrees	m-th element deviation from uniform spacing for a space-tapered array	
$F_k$		Amplitude weighting of the k-th frequency (Discrete frequency analysis)	Sections IV, V
$F(d_k)$		Element spacing optimization function	Section VII
F		Noise figure	
f		Frequency	
$f_o$		Center frequency of a wide-band signal	Section V
$G(x)$	Volts	Continuous aperture distribution function	Section III
$G(f)$		Aperture function with variable frequency	Section V

<u>Symbol</u>	<u>Unit</u>	<u>Function</u>	<u>Location*</u>
$G(\Theta, \phi)$		Element power pattern	Appendix C
$G$		Gain (denoted by subscript)	
$g_e(u)$		Element gain function in an array	Section III
$H(f)$		Frequency - noise response in bandwidth B	Appendix B
$I$	Amperes	Current	Section IV
$I_0(x)$		Modified Bessel function of zero order	Section III
$I(\Theta, \phi)$	Watts/Steradian	Relative noise power distribution in space	Appendix C
$I$		Inverse directivity function used in obtaining optimal directivity	
$[I]$		Identity matrix	
$J_m(x)$		m-th order Bessel function of first kind	Appendix C
$K$		Number of components in discrete frequency band	Section V
$K$	Joule/degree K	Boltzman's constant = $1.38 \times 10^{-23}$	
$L$		Loss ratio in passive circuits	Appendix B
$N$		Total no. of elements in array	
$N$	Watts	Noise power	Section IV, Appendix B
$\bar{n}$		Factor determining the pattern for a Taylor distribution function	Section III
$\eta$	Watts/Cm <sup>2</sup>	Noise power density	Section IV
$P$	Watts	Power	
$P(\Theta, \phi)$	Watts/Steradian	Signal power distribution in space	Section IV
$Q$		Quality factor	Section IV
$R$	Ohms	Resistance	
$R_{ij}, R_{m,n}$		Linear array cross-correlation coefficients (between ith and jth elements, or nth and mth elements)	
$R_{n,m,i,j}$		Planar array cross-correlation coefficients	Section V Appendix C
$S$	Watts	Signal power	Section IV
$Si$		Sine integral	
$S/N$		Signal-to-Noise ratio	
$T$	Degrees, Kelvin	Temperature	

<u>Symbol</u>	<u>Unit</u>	<u>Function</u>	<u>Location*</u>
T(t)	Volts	Linear array input time waveform	Section VII
T	Sec/cycle	Period of repeating waveform	Section V
t	Sec	Universal time variable	
u		Array observation angle (denoted by subscripts)	
u		Efficiency factor	Section IV
V	Volts	Voltage (Potential) (Electromotive force)	
V(u, t)	Volts	Array output time waveform	Section VII
W	Watts	Signal power	
W(f)	Watts/cycle	Power spectral density of an array	Appendix C
X	Ohms	Reactance	
Z	Ohms	Impedance	

#### LIST OF SYMBOLS AND DEFINITIONS (GREEK)

<u>Symbol</u>	<u>Unit</u>	<u>Function</u>	<u>Location</u>
$\alpha$		Parameter determining non-isotropic noise characteristics	Appendix C
$\alpha_{ij}$		Terms of unity matrix	Section VII
$\beta_{n,m}$		Correlation coefficients for a linear array	
$\gamma_{n,m}$		Function of $\beta_{n,m}$	Section VII
$\delta$		Bandwidth factor in wideband analysis	Section V
$\delta_n$	Degrees	Variable element spacing for use in the space tapering synthesis tech- nique	Section VII
$\Delta$		Deviation variable	
$\eta$		Antenna efficiency relative to 100% uniformity	
$\Theta$	Degrees	Angle off array boresight	
$\Theta_0$	Degrees	Position of major lobe	
$\lambda$	Cm or inches	Wavelength	
$\lambda_0$	Cm or inches	Wavelength corresponding to the center frequency for the wideband case	
$\lambda_{\max}$		Maximum eigenvalue of a non-singular matrix	Section VII

<u>Symbol</u>	<u>Unit</u>	<u>Function</u>	<u>Location*</u>
$\xi$		Sidelobe ratio parameter	Section III
$\sigma$		A factor determining the pattern for a Taylor distribution function	Section III
$\Phi_0$	Volts/meter	Field intensity	Section IV
$\phi_n$		Relative phase	Section IV
$\Omega$	Steradian	Solid angle	Section IV

\*Location designated only where usage of symbol is confined to the particular section.

## SECTION I

### INTRODUCTION

A wideband array is defined as one in which the excitation consists of something other than a pure continuous wave sinusoid. In general, the excitation may take any form, from a pair of discrete frequency components to a continuous spectrum defined in terms of its waveform.

The purpose of this investigation is to determine the response characteristics of array antennas excited by wideband signals. The array and the applied excitation are considered variables in an attempt to optimize the signal-to-noise ratio of the processed array output. The primary array variables are the separation between elements (spacing), and the relative amplitude coefficients at the element terminals (weighting).

In order to provide a basis for comparison, a set of initial conditions is assumed which confines the extent, but not the scope, of the investigation.

- a. Linear arrays are to be considered, although no restraint is placed on size, number of elements, or spacing.
- b. Only fixed beam arrays with a broadside beam are considered. Analysis must be carried over sufficient coverage to detect the presence of any grating lobes.
- c. A point signal source is assumed to be aligned with the beam maximum.
- d. The source of noise is assumed to be "white" (evenly distributed in frequency) and uniformly distributed over all space.
- e. Control of the signal-to-noise ratio is effected by manipulation of the element spacing and element weighting.
- f. Wideband signals are applied to determine the effects of bandwidth, waveform, and spectral content.

The major portion of this report concerns array response within these conditions; however, the linear array restriction (a), and the uniform noise restriction, (d), are removed to illustrate the general applicability of the results.

Evaluation of the array modification techniques is achieved in comparison with a standard model array. The standard model is defined as a linear array of  $N$  uniformly illuminated isotropic elements located on half-wavelength centers at a fixed frequency. The gain, beamwidth, sidelobe level, and signal-to-noise ratio (in white noise) are fixed by  $N$  for this standard array.

In an attempt to provide a coherent presentation of the results obtained during the investigation, a step-by-step reporting procedure is incorporated. This procedure begins with an analysis of narrow band linear arrays, with control provided through amplitude weighting. Element displacement, to effect a "space taper" is also discussed. The next step is to consider the effect of noise on array performance and to establish signal-to-noise relationships utilizing the array parameters. The array conditions thus developed are subjected to the effect of wideband signals so that a composite picture of the wideband optimized array is produced. The results of this investigation have provided several features of the wideband array which suggest application in practical array systems. These applications are discussed in a separate section.

## SECTION II

### SUMMARY

The principal objective of the Wideband Element Spacing and Weighting investigation is to determine the procedure whereby the signal-to-noise ratio of a wideband antenna array can be optimized by means of antenna element amplitude control and spacing. A subsequent objective is to determine the array response as these parameters, along with bandwidth, are varied over a prescribed range of values.

Some of the results of this investigation can be expressed as statements which are substantiated in the body of the report.

- a. Maximum signal-to-noise ratio is synonymous with maximum array directivity when external noise is uniformly distributed in frequency and space.
- b. Maximum signal-to-noise ratio in narrow band arrays can be specified by an optimum illumination function for a specified sidelobe level.
- c. The optimum illumination can be applied as an amplitude weighting function, a space taper function, or a combination function.
- d. An improvement in signal-to-noise ratio, over the uniform model, can be obtained by applying the super-gain effect if the resulting array parameters can be established.
- e. The application of bandwidth modifies the array function in the time-space domain.
- f. Beamwidth can be incorporated with amplitude or space weighting to produce specifically shaped array patterns.
- g. Increased bandwidth reduces the optimum array signal-to-noise ratio, but permits optimization within a confined aperture.
- h. Optimized amplitude weighting deviates from uniform only slightly, even in wideband arrays.
- i. An iterative technique can be used to solve large array problems where matrix inversion becomes cumbersome.
- j. The optimized array response of the planar array is similar to its counterpart linear array.
- k. Waveform distortion is prevalent in the sidelobe response of wideband arrays.
- l. The array signal-to-noise ratio can be optimized for non-uniform noise conditions by amplitude control, resulting in a modified array pattern.

The design parameters, which control the performance of a linear array, are discussed in Section III. Most of the information is presented in graphical form so that an estimate of array performance can be obtained without computation. An example is provided to illustrate the process.

The effects of noise on array performance is discussed in Section IV. A general noise analysis is followed by signal-to-noise ratio considerations and several optimization techniques based on element amplitude weighting and spacing.

Bandwidth is considered in Section V. The effect of bandwidth on the radiation patterns in the time-space domain is illustrated by a three-dimensional model and a series of contour diagrams. The effect of bandwidth on array signal-to-noise ratio is presented in graphical form. An application of the space-frequency equivalence theorem applied to a space tapered array is presented as an example of utilizing bandwidth in array design.

Several possible applications of the principles evolving from the analytical investigation are discussed in Section VI. These applications are intended to illustrate the manner in which the information developed during this project can be applied in future development effort.

Several computational techniques have been developed during the course of investigation. Since these methods are general in nature, they are discussed separately in Section VII.

Considerable information and several mathematical formulations have evolved which supplement the data and statements in the body of this report. These are collected as appendices to the report.

A list of references and a bibliography are provided to permit further evaluation of the general topics covered in this report.

## SECTION III

### DESIGN PARAMETERS IN THE LINEAR ARRAY -- NARROW BAND ARRAYS

An application of wideband element spacing and weighting techniques to a specific antenna array problem, requires information concerning the performance of the array for the specified parameters. In this section, the parameters which determine the performance of an array are examined with emphasis on their interdependence. The narrow band restriction is applied to permit an independent exploration of array parameters, so that the application of bandwidth (Section V) can be considered in proper perspective.

An antenna array is usually specified in terms of its gain, beam width, and sidelobe level. There are other parameters which may be specified such as polarization, available aperture, method of excitation, input impedance, power handling capability and form factor, but these are either related to the three primary parameters or can be considered independently. One parameter which is an overriding function in any antenna design is efficiency. Efficiency includes all factors which represent a departure from maximized directivity, which in this report is defined as a lossless uniformly illuminated array.

In a practical design, the array efficiency affects all of the above parameters either directly or indirectly. For purposes of discussion in this section only the illumination efficiency will be considered in analysis since system losses can be applied on a discrete basis.

#### 1. ARRAY DESIGN

The gain of an array is always a function of the aperture available. Within the specified aperture, beam width and sidelobe level can be controlled by means of the applied illumination function.

The radiation pattern of an array (which provides beam width and sidelobe level) can be synthesized from a known or assumed illumination function and the geometrical properties of the array. The illumination function can be described as a continuous function or as a pattern of discrete weighting factors. The illumination function can be implemented as an amplitude weighting on individual elements (amplitude taper), as a non-uniform distribution of equal amplitude elements within the array (space or density taper) or as a combination of these techniques.

The details of antenna array synthesis have been adequately covered in the available literature\* and will not be repeated here. An analytical technique which is applicable to array analysis and has not been previously reported appears in Section VII. The purpose of this discussion is to illustrate the application of specific illumination functions to the general form of the radiation pattern. The selected functions are briefly described below and are tabulated in numerical form in Tables 1 and 2 for continuous and discrete weighting respectively.

---

\*An excellent survey of the theory of antenna arrays is contained in Reference (1).

NOTE: Reference numbers noted refer to references listed in Section VIII.



TABLE 1. CONTINUOUS APERTURE WEIGHTING

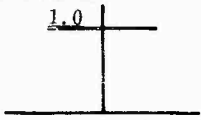
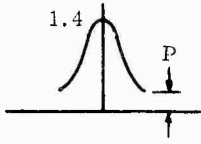
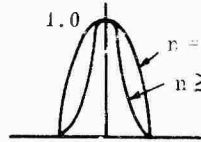
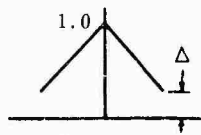
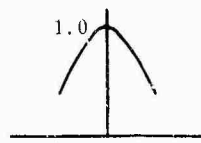
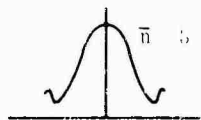

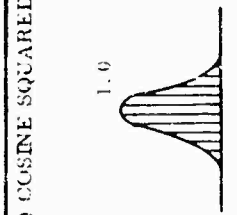
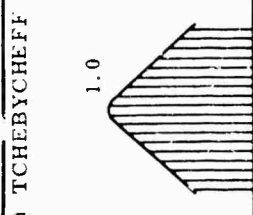
ILLUMINATION FORM	ILLUMINATION FUNCTION - $-\frac{1}{2} \leq x \leq \frac{1}{2}$	RAY PATTERN E(u) NORMALIZED TO UNITY
(1) GENERAL EVEN FUNCTION	$G(x)$ $G(x) = G(-x)$	$E(u) = \int_{-\frac{1}{2}}^{\frac{1}{2}} G(x) e^{j2\pi ux} dx$ $E(u) = 2 \int_0^{\frac{1}{2}} G(x) \cos(2\pi ux) dx$
(2) UNIFORM 	$G(x) = 1$	$E(u) = \frac{\text{SIN} \pi u}{\pi u}$
(3) HAMMING 	$G(x) = 1 + P \cos 2\pi x$ $0 \leq P \leq 1$	$E(u) = \frac{\text{SIN} \pi u}{\pi u} \left[ \frac{1 + (P-1)u^2}{1 - u^2} \right]$ AT INDETERMINATE POINTS: $u = \pm 1$ $E(\pm 1) = \frac{P}{2}$
(4) COSINE <sup>n</sup> 	$G(x) = \cos^n x$	$E(u) = \left[ \frac{n!}{\pi(n+2u)(n+2u-2) \cdots (2+2u-n)} \right] \frac{\text{SIN} \left[ (2u-n)\pi \right]}{(2u-n)\pi}$
(5) TRIANGULAR 	$G(x) = \begin{cases} (2-2\Delta)x + 1: & -\frac{1}{2} \leq x \leq 0 \\ -(2-2\Delta)x + 1: & 0 \leq x \leq \frac{1}{2} \end{cases}$	$E(u) = \frac{1-\Delta}{1+\Delta} \left( \frac{\text{SIN} \frac{\pi u}{2}}{\frac{\pi u}{2}} \right)^2 + \frac{2\Delta}{1+\Delta} \frac{\text{SIN} \pi u}{\pi u}$
(6) MODIFIED $\text{SIN} x/x$ 	$G(x) = I_0 \left( 2\pi B \sqrt{\frac{1}{4} - x^2} \right)$	$E(u) = \frac{B \text{SIN} \left( \pi \sqrt{1 - \frac{u^2}{B^2}} \right)}{\text{SINH}(\pi B) \sqrt{u^2 - B^2}}$ AT INDETERMINATE POINTS $u = \pm B$ , $E(\pm B) = \frac{\pi B}{\text{SINH}(\pi B)}$
(7) TAYLOR 	$G(x) = 1 + 2 \sum_{m=1}^{n-1} F(m) \cos(2\pi mx)$ WHERE: $F(m) = \frac{[(n-1)!]^2}{(n-1+m)! (n-1-m)!} K$ $K = \frac{\pi^{n-1}}{n-1} \left\{ 1 - \frac{m^2}{u^2 - (n-\frac{1}{2})^2} \right\}$	$E(u) = \frac{\cos \sqrt{\left( \frac{u}{u_0} \right)^2 - A^2}}{\cosh \pi A}$

TABLE 1. CONTINUOUS APERTURE WEIGHTING

	RAY PATTERN E(u) NORMALIZED TO UNITY	REMARKS
	$E(u) = \int_{-\frac{1}{2}}^{\frac{1}{2}} G(x) e^{j2\pi ux} dx$ $E(u) = 2 \int_0^{\frac{1}{2}} G(x) \cos \{2\pi ux\} dx$	E(u) IS THE VOLTAGE PATTERN, POWER PATTERN IS GIVEN BY 20 LOG( E(u) )
	$E(u) = \frac{\text{SIN} \pi u}{\pi u}$	
	$E(u) = \frac{\text{SIN} \pi u}{\pi u} \left[ \frac{1 + (P - 1)u^2}{1 - u^2} \right]$ <p>AT INDETERMINATE POINTS: <math>u = \pm 1</math></p> $E(\pm 1) = -\frac{P}{2}$	THE PARAMETER P DETERMINES THE SIDELOBE RATIO ( $\xi$ ) : $\xi = \frac{1 + (P - 1) u^2}{1 - u^2}$ WHERE u IS NOMINALLY THE POINT AT WHICH THE 1st SIDELOBE OCCURS
	$E(u) = \left[ \frac{n!}{\pi(n + 2u)(n + 2u - 2) \cdots (2 + 2u - n)} \right] \frac{\text{SIN} \left[ (2u - n) \frac{\pi}{2} \right]}{(2u - n)}$	E(u) IS VALID ONLY FOR INTEGER VALUES OF n. INDETERMINATE POINTS DEPEND ON THE VALUE OF n.
$x \leq 0$ $x \leq \frac{1}{2}$	$E(u) = \frac{1 - \Delta}{1 + \Delta} \left( \frac{\text{SIN} \frac{\pi u}{2}}{\frac{\pi u}{2}} \right)^2 + \frac{2 \Delta}{1 + \Delta} \frac{\text{SIN} \pi u}{\pi u}$	
	$E(u) = \frac{B \text{SIN} \left( \pi \sqrt{u^2 - B^2} \right)}{\text{SINH}(\pi B) \sqrt{u^2 - B^2}}$ <p>AT INDETERMINATE POINTS <math>u = \pm B</math>,</p> $E(\pm B) = \frac{\pi B}{\text{SINH}(\pi B)}$	$I_0$ = MODIFIED ZERO-ORDER BESSEL FUNCTION $\xi$ (SIDELOBE RATIO)* = 4.60333 $\frac{\text{SINH} \pi B}{\pi B}$ $\theta$ (3DB BEAMWIDTH)* = $2B \sqrt{1 + \frac{2 \text{SIN}^2 \left[ \pi \sqrt{\left(\frac{3}{2}\right)^2 - B^2} \right]}{\text{SINH}^2(\pi B)}}$  *SOLUTION BY ITERATION PROCESS
$\sigma$ K }	$E(u) = \frac{\cos \sqrt{\left(\frac{u}{\sigma}\right)^2 - A^2}}{\cosh \pi A}$	SIDELOBE RATIO IS DENOTED BY $\xi$ : $\xi = \cosh \pi A$  PARAMETERS $\sigma$ , $\pi$ , A, MODIFY THE APERTURE DIST. FUNCTION BEAM- WIDTH IS APPROXIMATELY, $\beta = \frac{2\sigma}{\pi} \sqrt{\left[ \cosh^{-1}(\xi) \right]^2 - \left[ \cosh^{-1} \left( \frac{\xi}{\sqrt{2}} \right) \right]^2}$

TABLE 2. DISCRETE APERTURE WEIGHTING

ILLUMINATION FORM	ILLUMINATION WEIGHTING	RAY PATTERN E(u) NORMALIZED TO UNITY
(1) GENERAL	$A_n = A_{-n}$ $n = 1, 2, \dots, \frac{M-1}{2}; M \text{ EVEN}$ $n = 1, 2, \dots, \frac{M-1}{2}; M \text{ ODD}$	$M \text{ EVEN, } \frac{1}{2} \sum_{n=1}^{\frac{M-1}{2}} A_n \cos \left[ \pi \left( n - \frac{1}{2} \right) u \right]$ $M \text{ ODD, } \frac{M-1}{2} \sum_{n=1}^{\frac{M-1}{2}} A_n \cos \pi n u + \frac{A_0}{2}$ <p>SEE NOTE "A"</p>
(2) UNIFORM	$A_n = 1, \text{ FOR ALL } n$	$E(u) = \frac{\sin \left( \frac{\pi M u}{2} \right)}{M \sin \left( \frac{\pi u}{2} \right)}$
(3) HAMMING	$\text{FOR } M \text{ ODD, } n = 0, 1, 2, \dots, \frac{M-1}{2}$ $A_n = 1 + P \cos \frac{2\pi n}{M}$ $\text{FOR } M \text{ EVEN, } n = 1, 2, \dots, \frac{M}{2}$ $A_n = 1 + P \cos \frac{\pi(2n-1)}{M}$	$E(u) = \frac{P \sin \frac{M \pi u}{2} \sin \frac{\pi u}{2} \cos \frac{\pi}{M} \frac{\pi u}{2} + \sin \frac{\pi M u}{2}}{M \sin \left( \frac{\pi}{M} + \frac{\pi u}{2} \right) \sin \left( \frac{\pi}{M} - \frac{\pi u}{2} \right)} + \frac{\sin \frac{\pi M u}{2}}{M \sin \frac{\pi u}{2}}$ <p>AT INDETERMINATE POINTS, <math>v = \pm \frac{2}{M}</math>,  <math>E \left( \pm \frac{2}{M} \right) = \frac{P}{2}</math></p>
(4) COSINE	$\text{FOR } M \text{ ODD } n = 0, 1, 2, \dots, \frac{M-1}{2}$ $A_n = \cos \frac{\pi n}{M}$ $\text{FOR } M \text{ EVEN, } n = 1, 2, \dots, \frac{M}{2}$ $A_n = \cos \frac{\pi(n-1)}{M}$	$E(u) = \frac{\cos \frac{\pi u}{2} \cos \frac{M \pi u}{2} \sin^2 \frac{\pi}{2M} \frac{\pi u}{2}}{\sin \left( \frac{\pi}{2M} + \frac{\pi u}{2} \right) \sin \left( \frac{\pi}{2M} - \frac{\pi u}{2} \right)}$ <p>AT INDETERMINATE POINTS, <math>u = \pm \frac{1}{M}</math>,  <math>E \left( \pm \frac{1}{M} \right) = \frac{M}{2} \sin \frac{\pi}{2M}</math></p>
(5) COSINE SQUARED	$\text{FOR } M \text{ ODD } n = 0, 1, \dots, \frac{M-1}{2}$ $A_n = \cos^2 \frac{\pi n}{M}$ $\text{FOR } M \text{ EVEN, } n = 1, 2, \dots, \frac{M}{2}$	$E(u) = \frac{\sin \frac{M \pi u}{2} \sin \frac{\pi u}{2} \cos \frac{\pi}{M} \frac{\pi u}{2}}{M \sin \left( \frac{\pi}{M} + \frac{\pi u}{2} \right) \sin \left( \frac{\pi}{M} - \frac{\pi u}{2} \right)} + \frac{\sin \frac{M \pi u}{2}}{M \sin \frac{\pi u}{2}}$

	<p>FOR M EVEN, <math>n = 1, 2, \dots, \frac{M}{2}</math></p> $A_n = \cos \frac{\pi (n - \frac{1}{2})}{M}$	<p>AT INDETERMINATE POINTS, <math>u = \pm \frac{1}{M}</math>,</p> $E(\pm \frac{1}{M}) = \frac{M}{2} \sin \frac{\pi}{2M}$
<p>(5) COSINE SQUARED</p> 	<p>FOR M ODD <math>n = 0, 1, \dots, \frac{M-1}{2}</math></p> $A_n = \cos^2 \frac{\pi n}{M}$ <p>FOR M EVEN, <math>n = 1, 2, \dots, \frac{M}{2}</math></p> $A_n = \cos^2 \frac{\pi (n - \frac{1}{2})}{M}$	$E(u) = \frac{\sin \frac{M \pi u}{2}}{M \sin \left( \frac{\pi}{M} + \frac{\pi u}{2} \right)} \cos \frac{\pi}{M} \sin \left( \frac{\pi}{M} - \frac{\pi u}{2} \right)$ $+ \frac{\sin \frac{M \pi u}{2}}{M \sin \frac{\pi u}{2}}, \quad E\left(\pm \frac{2}{M}\right) = \frac{1}{2}$
<p>(6) TCHEBYCHEFF</p> 	<p>FOR M ODD <math>n = 1, 2, \dots, \frac{M+1}{2}</math></p> $A_n = \frac{M-1}{2} F(Z) \cos \frac{2\pi K (n-1)}{M}$ <p>FOR M EVEN <math>n = 1, 2, \dots, \frac{M}{2}</math></p> $A_n = \frac{M}{2} F(Z) \cos \frac{\pi K (2n-1)}{M}$ <p>WHERE:</p> $Z_0 = \frac{1}{2} \left[ \left( \xi + \sqrt{\xi^2 - 1} \right)^{\frac{1}{M-1}} + \left( \xi - \sqrt{\xi^2 - 1} \right)^{\frac{1}{M-1}} \right]$ $Z = Z_0 \cos \frac{K \pi}{M}$ $F(Z) = \left( Z + \sqrt{Z^2 - 1} \right)^{M-1} + \left( Z - \sqrt{Z^2 - 1} \right)^{M-1}; \quad  Z  > 1$ $F(Z) = 2 \cos \left[ (M-1) \cos^{-1}(Z) \right]; \quad  Z  < 1$	<p>SEE NOTE "B"</p>

NOTE A

E(u) IS THE VOLTAGE PATTERN.  
THE POWER PATTERN IS CALCULATED  
FROM  $20 \log (E(u))$

NOTE B

SIDELobe RATIO  $\xi$  GIVEN BY  $\xi = \cosh \pi A$   
FOR LARGE M, THE BEAMWIDTH IS GIVEN  
APPROXIMATELY BY

$$\beta = \frac{2}{\pi} \sqrt{\left[ \cosh^{-1} \xi \right]^2 - \left[ \cosh^{-1} \left( \frac{\xi}{\sqrt{2}} \right) \right]^2}$$

THE PARAMETERS Z,  $Z_0$  DETERMINE THE FORM  
OF THE ILLUMINATION FUNCTION AND ARE  
CHARACTERISTIC OF THE TCHEBYCHEFF  
FUNCTION.

### 1.1 UNIFORM WEIGHTING

This condition represents maximum directivity and is assigned an illumination efficiency of 100 percent. Uniform illumination can be effected on a continuous or discrete basis. In either case the first sidelobe is approximately 13 DB below the major lobe. The difference in the two forms of uniform illumination is observed in the far out sidelobe pattern where the continuous illumination exhibits a lower level. This difference is accentuated as the total number of elements is reduced. A discrete array of only four elements, for example, will produce a sidelobe only 11 DB below the beam maximum rather than the characteristic 13 DB of larger arrays. Kraus, Reference ( 2 ) has recorded the space patterns for discrete uniform illumination in an array of N elements where N is any integer from 1 through 24.

### 1.2 HAMMING FUNCTION

Named for R.W. Hamming - Bell Laboratories, Reference ( 3 ), the Hamming Function like uniform weighting can be applied on a uniform or discrete basis. The function is essentially a cosine variation in a form which represents a compromise between major lobe broadening, sidelobe suppression, illumination efficiency and ease of implementation.

### 1.3 COSINE<sup>n</sup> ILLUMINATION

The cosine function is a basic form of illumination. Sidelobe control is exercised by variation of the exponent "n". Characteristics of cosine<sup>n</sup> illumination are significant beam broadening and low efficiency. These undesirable characteristics can be improved by placing the function on a pedestal, i. e. restricting the edge term to a non-zero value. The cosine<sup>n</sup> on a pedestal resembles the Hamming function.

### 1.4 MODIFIED SIN X/X

The name applied to the resulting radiation pattern rather than the illumination function. This method of array excitation was suggested by Taylor, Reference ( 4 ), as a means of achieving the rapid sidelobe decay of the uniform array without the high first sidelobe level.

### 1.5 TRIANGULAR FUNCTION

This is included primarily for comparison purposes. The triangular illumination function is seldom used in practice although the sidelobe level can be controlled by establishing the magnitude of the edge illumination. For low sidelobes, a broad beam with low efficiency results.

### 1.6 TCHEBZCHEFF DISTRIBUTION

A technique developed by Dolph, Reference ( 5 ), of applying the Tchebzecheff polynomials to antenna design results in uniform sidelobes with a minimum beam width. This form of excitation has found extensive application despite its low illumination efficiency.

### 1.7 TAYLOR'S DISTRIBUTION, (Reference ( 6 ))

An adaptation of the Dolph-Tchebzecheff form which controls a specified number of sidelobes to a uniform level while the remainder decay with increased displacement from the major lobe is a distribution form which has found extensive use in radar antennas.

The above described functions serve to illustrate the pattern control which is available through array illumination. There are many other illumination functions which can be applied including modifications of the above. The selection must be based on the desired radiation characteristics which are governed by application.

## 2. GRAPHICAL ANALYSIS

The analytical forms presented in Tables 1 and 2 are complete and permit direct numerical analysis for the functions tabulated. For a complete array design, the specified parameters should be applied through the selected illumination function to produce the design array function. For purposes of preliminary analysis, however, it is often desirable to determine the approximate characteristics before proceeding with a detailed design. This is particularly true when other factors are to be considered, such as those presented in subsequent sections of the report.

The pattern characteristics resulting from applied illumination functions can be displayed in graphic and nomographic form provided a reference is established. The reference used in this section is the uniformly illuminated array. The calculated array function is illustrated in Figure 1 along with the sidelobe envelopes for other illumination functions.

The illumination efficiency of the uniformly illuminated array is taken to be 100 percent. The sidelobe behavior is shown in Figure 1 and the beam width as a function of array length as can be determined from Figure 2. The relative illumination efficiency for other illumination functions can be determined from Figure 3 as a function of design sidelobe level. The half-power beam width of the array can be determined from Figure 4 which gives the beam width multiplication factor as a function of sidelobe level for several illumination functions.

The directive gain of the linear array is determined by the number of elements comprising the array, the illumination efficiency, and the gain of the individual elements. This relationship is presented as a nomograph in Figure 5

Figures 1 through 5 can be used to provide a rapid approximate solution to various array design problems, and provide a visual display of parameters. To illustrate the usefulness of the graphical analysis, consider a sample problem.

### a. Illustrative Example

It is desired to determine the gain and beam width of a 70 element linear array with half wavelength element spacing designed to provide a maximum sidelobe level of 25 DB below the major lobe. Assume that sidelobe control can be achieved through application of the Hamming illumination function. The array element gain is 8 DB.

### b. Procedure

- (1) Determine the array length by multiplying the quantity of elements (70) by the element spacing ( $\lambda/2$ ).  $L = 35\lambda$
- (2) From Figure 2 determine the half-power beam width for a  $35\lambda$  linear uniformly illuminated array. Beam width = 1.4 degrees

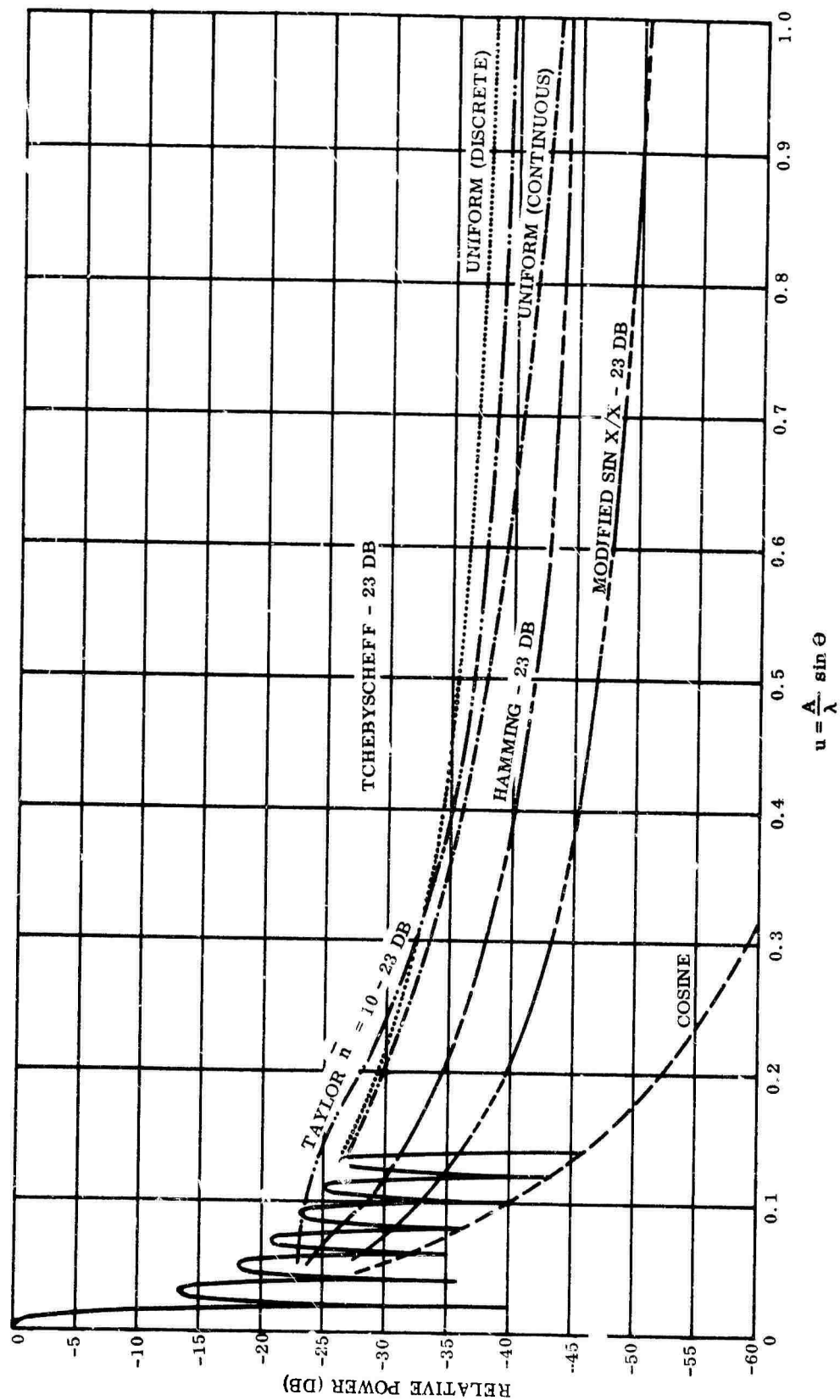


Figure 1. Radiator Pattern-Uniform Illumination with Sidelobe Envelopes for Other Illumination Functions

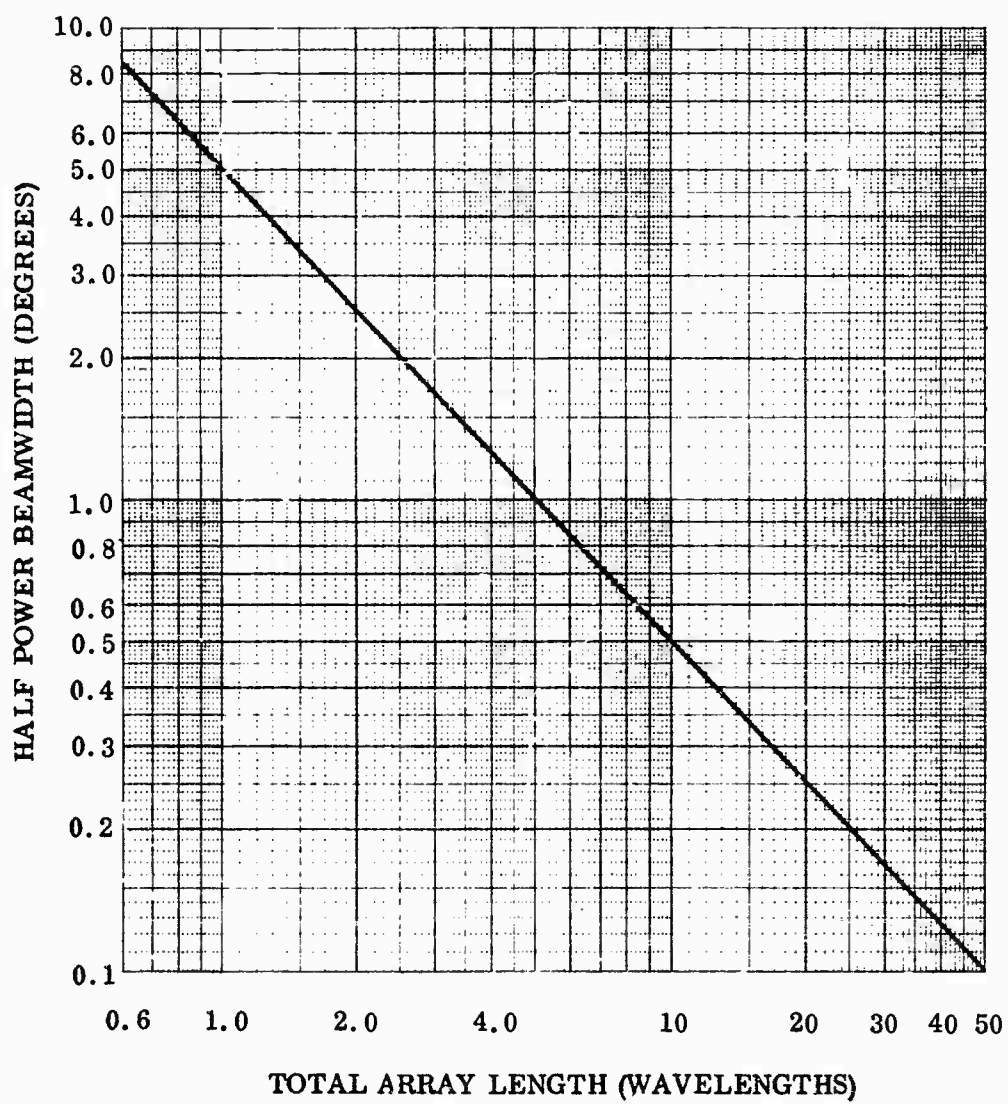


Figure 2. Beamwidth of Uniform Linear Array (Beam Normal to Array Axis)



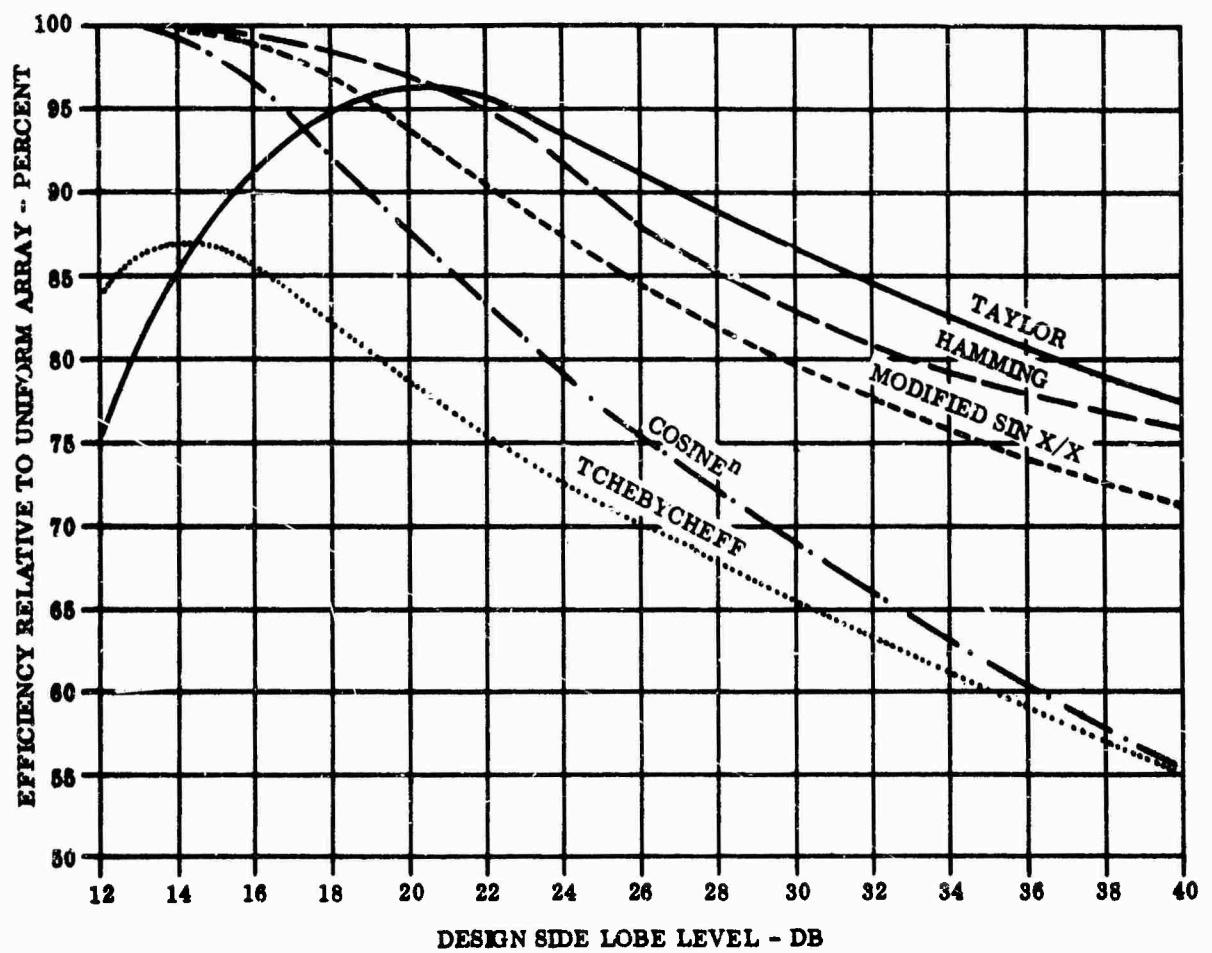


Figure 3. Illumination Efficiency in Amplitude Tapered Linear Array

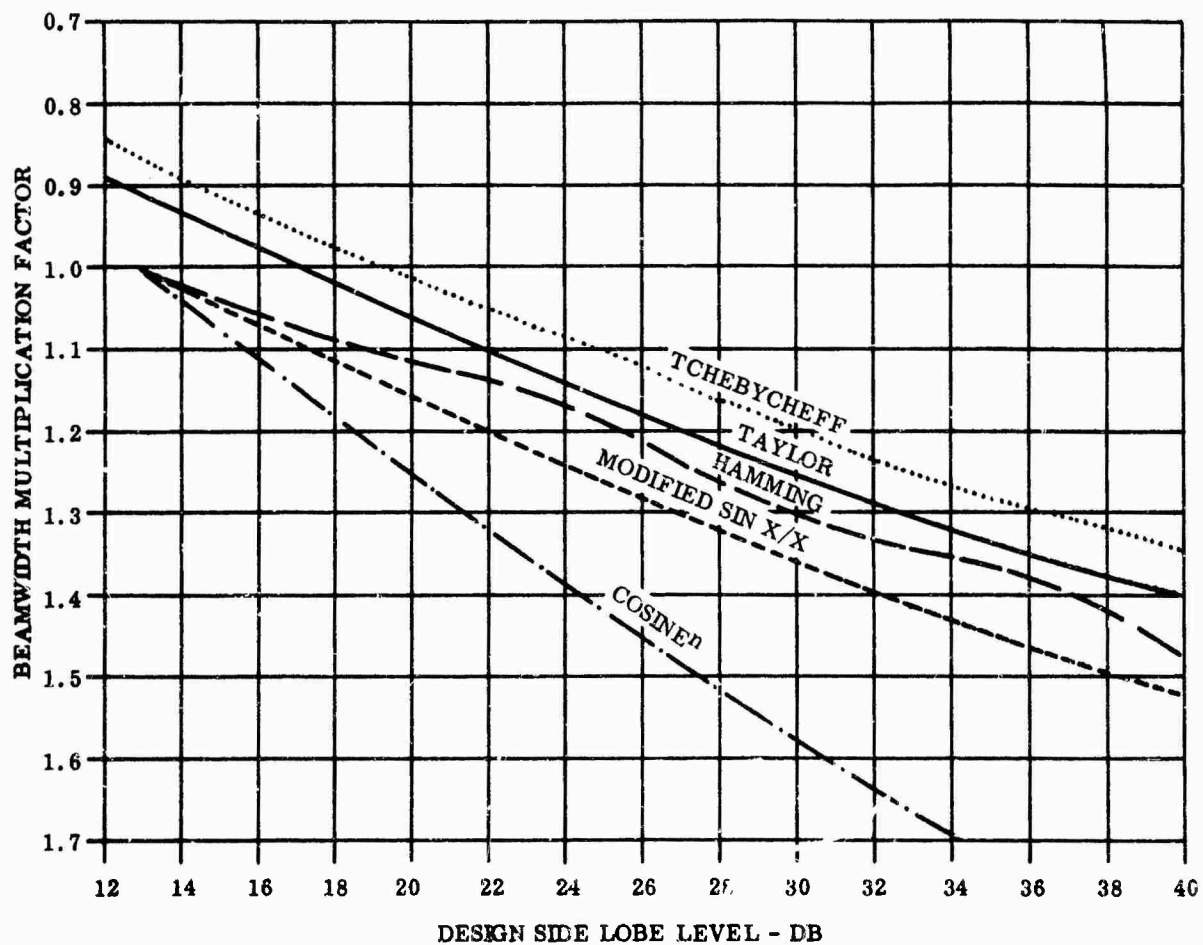
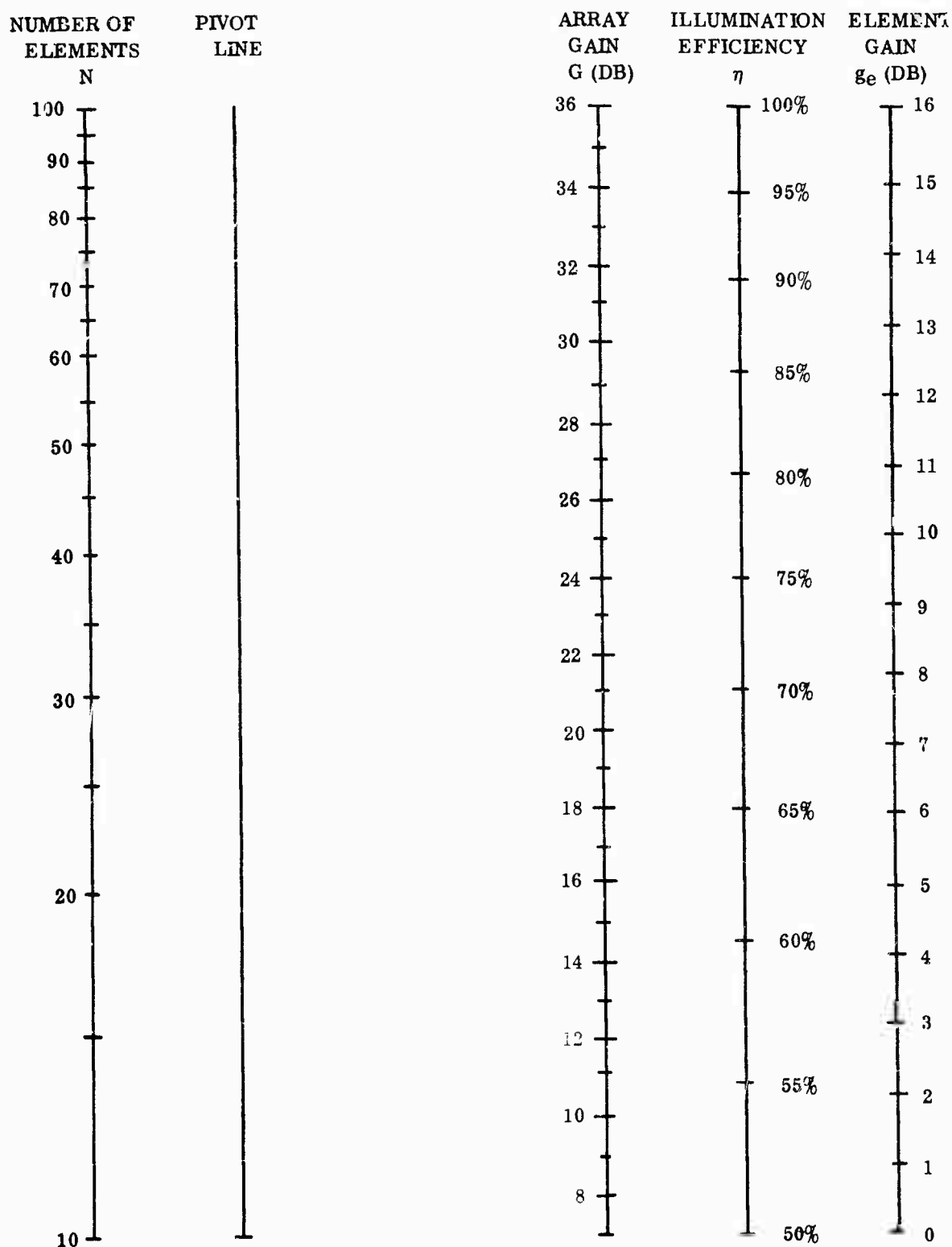


Figure 4. Beamwidth Relative to Uniformly Illuminated Linear Array



**PROCEDURE:**

1. CONNECT  $N$  AND  $\eta$  WITH A STRAIGHT LINE WHICH INTERSECTS THE PIVOT LINE.
2. CONNECT THE PIVOT LINE INTERSECTION WITH THE ELEMENT GAIN AND READ ARRAY GAIN FROM THE INTERSECTION WITH THE  $G$  SCALE.

Figure 5. Linear Array Nomograph

- (3) From Figure 4 determine the beam width multiplication factor for a Hamming function of 25 DB sidelobe level design. Multiplier = 1.19
- (4) The product of steps (2) and (3) gives the approximate half-power beam width. BW (3 DB) = 1.68 degrees
- (5) From Figure 3 determine the relative efficiency for the 25 DB sidelobe Hamming function.  $\eta = 90\%$
- (6) Using the nomograph (Figure 5), connect 75 on the N scale with 90 percent on the  $\eta$  scale.
- (7) Mark the point where this line intersects the pivot line and connect this point to 8 on the  $g_e$  scale.
- (8) Read the approximate array gain from the G scale.  $G = 26.3$  DB

The general shape of the radiation pattern in the sidelobe region can be seen in Figure 1. The Hamming function sidelobe envelope is for a sidelobe maximum of 23 DB, but the general distribution is indicative of other design levels.

The parameter  $g_e$  -- element gain, requires a word of explanation in application to linear arrays. In a two dimensional planar array, the individual radiating element is confined to a physical area which confines the effective area; hence the gain. In the linear array, confinement is limited to one dimension only, therefore it is possible to utilize high gain elements in the linear array. An approximation of the array element gain can be established from a knowledge of a separation between elements and the half-power beam width in the plane normal to the array. Figure 6 illustrates this relationship. Using the above example where the element separation was  $0.5\lambda$  and the element gain given as 8 DB, the half-power beam width of the array in the orthogonal plane can be found from Figure 6 to be 60 degrees. The depicted relationship is only an approximation, since the gain of any antenna element is affected by factors other than beam width and element separation.

### 3. SPACE TAPER ARRAYS

The graphical method of array analysis outlined above applies only to the amplitude tapered array. It is also possible to effect a taper function by the displacement of elements along the line of the array while the magnitude of excitation is uniform. In general this procedure consists of estimating the amplitude or spacing coefficients necessary to produce a desired pattern and calculating correction factors from the observed pattern necessary to produce the desired result.

The calculated patterns shown in Figures 7 and 8 illustrate the results of the iterative process for a 24 element array designed for 24 DB sidelobes. The two figures represent the amplitude and space tapered cases respectively. Comparison of these two methods of pattern control reveals the following characteristics:

- a. The space tapered pattern is more sensitive to small deviations in displacement, than the amplitude tapered pattern is to small variations in amplitude.
- b. An exact sidelobe level is more easily obtained with the amplitude taper.

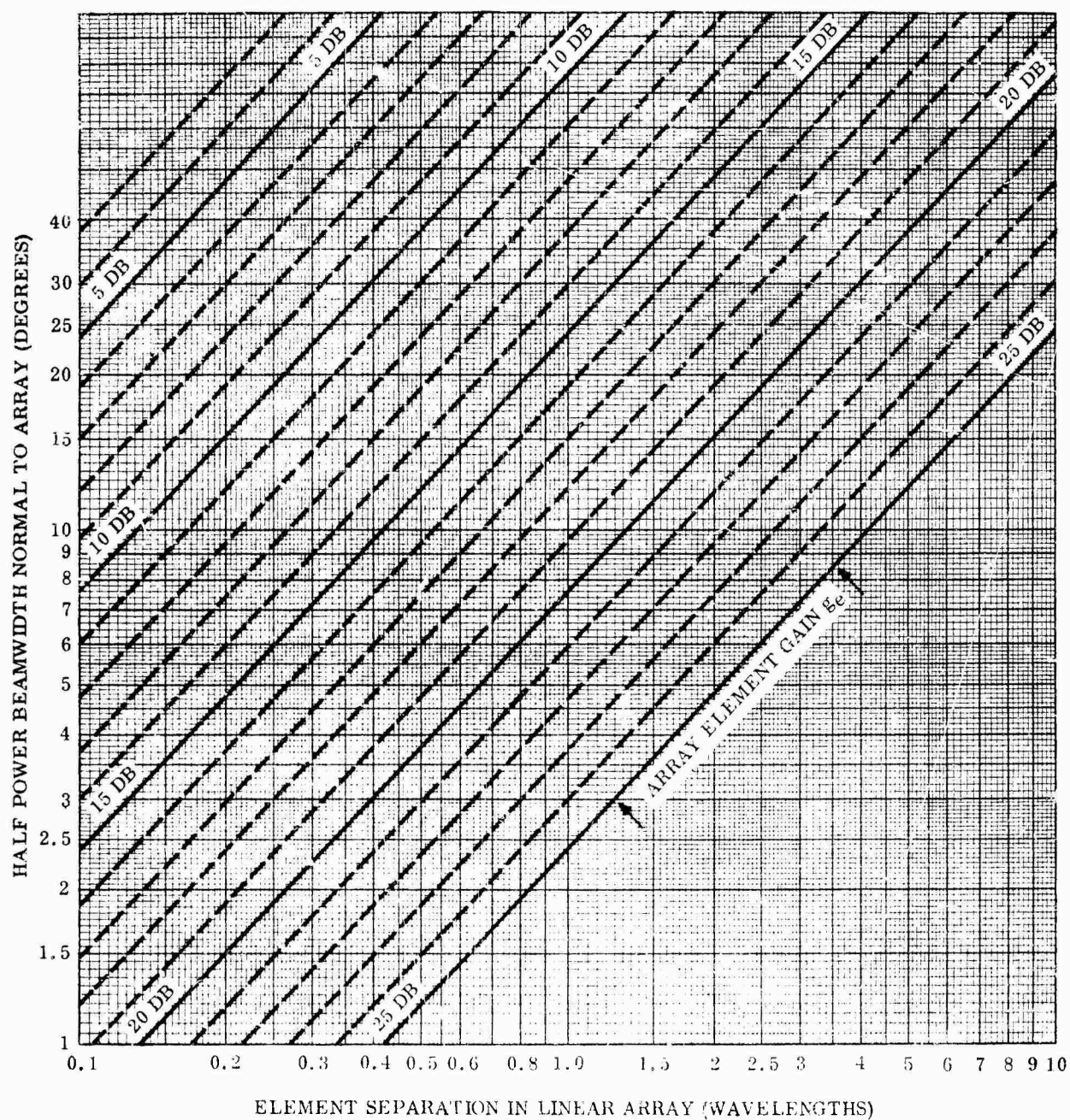


Figure 6. Array Element Gain in Linear Arrays

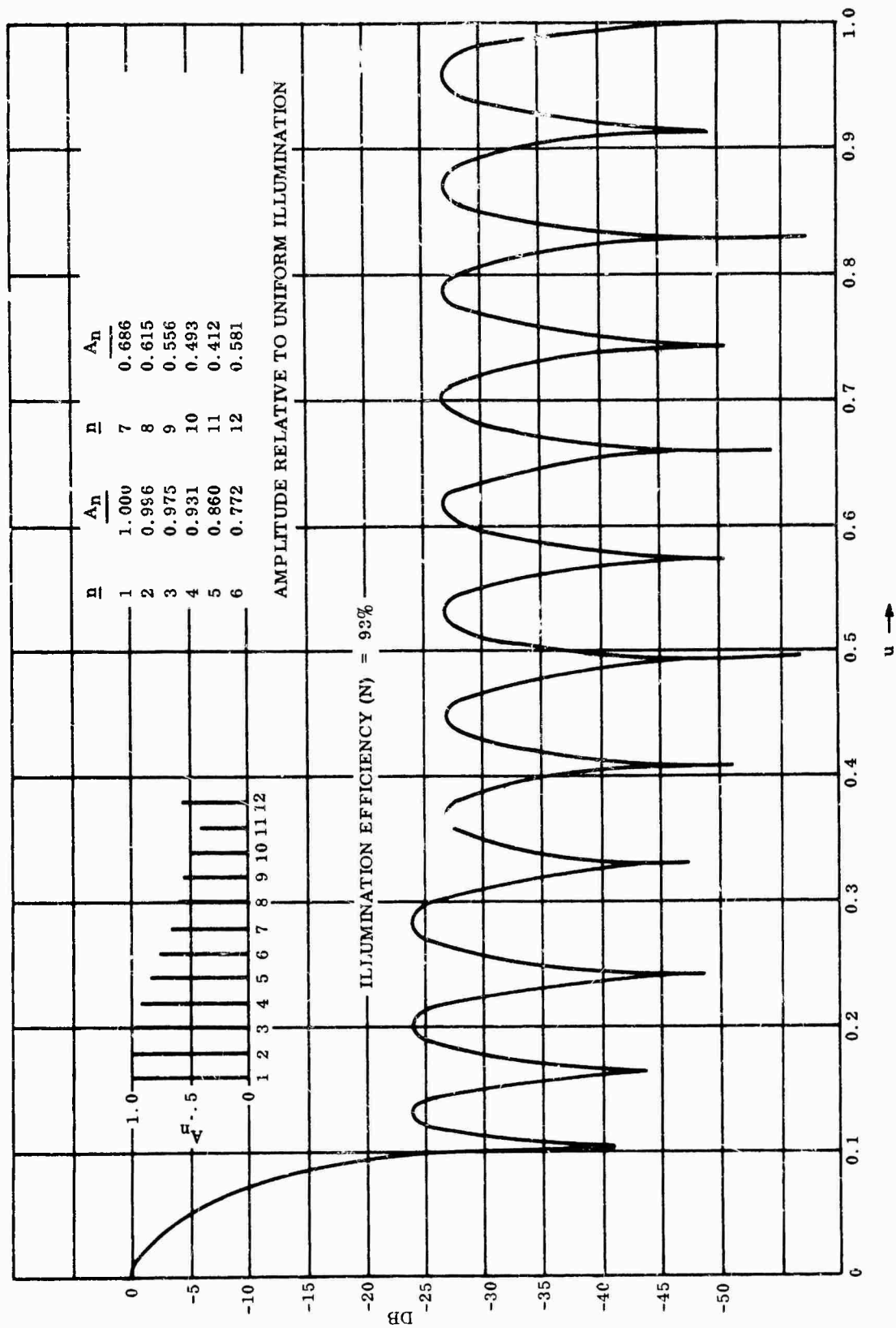


Figure 7. Amplitude Tapered Array of 24 Element Sidelobe Control in  $/u/<1.00$

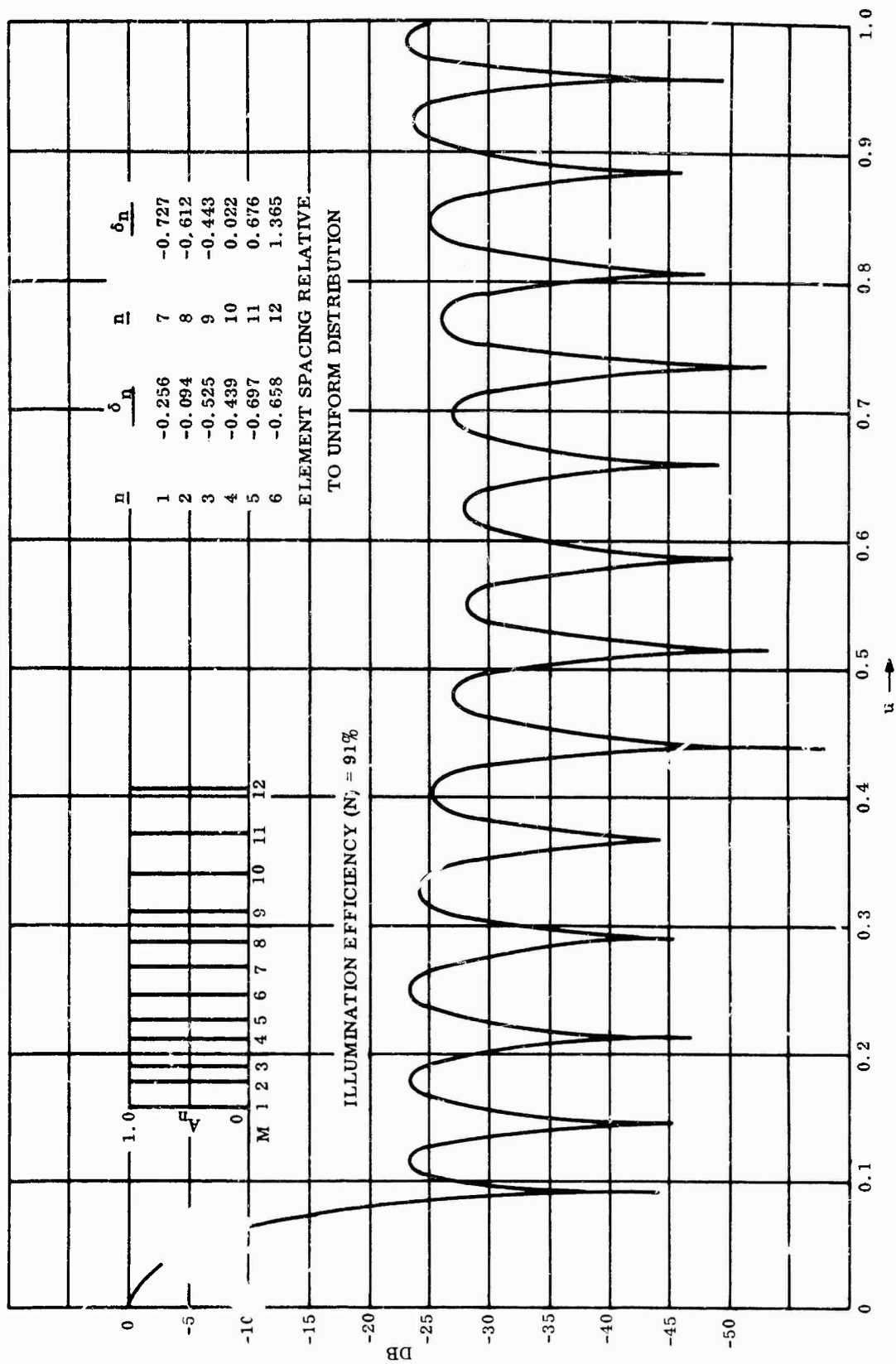


Figure 8. Space Tapered Array of 24 Elements Sidelobe Control in  $u < 1.00$

- c. The beam width of the amplitude tapered array increases as a function of sidelobe level more than the space tapered array. The beam width in the space tapered array is only slightly wider than the uniformly spaced, uniformly illuminated array.
- d. The illumination efficiency for the space tapered array is lower than for the amplitude tapered array with a common sidelobe level.
- e. The element gain in the space tapered array is not constant since the spacing between elements is not constant. Except in severely tapered arrays this is not a serious factor in array response.

Although the graphical method of array evaluation does not apply to the space tapered array, a fair estimate for performance can be obtained by assuming an equivalent amplitude taper condition and applying the above difference conditions.



## SECTION IV

### SIGNAL-NOISE CONSIDERATIONS IN ARRAY ANTENNAS

The procedure for antenna array analysis described in the preceding section considered only the signal aspect of antenna performance. The antenna radiation pattern is an expression of the relative signal strength (with respect to the beam maximum) as a function of observation angle. The absolute value of signal available for use in a detection circuit is dependent on a number of other factors associated with the antenna system. These include: (1) the spatial power density at the array aperture, (2) the impedance of the antenna and its associated components, and (3) the loss or gain of any subsequent components. Reference (7).

In addition to the signal available for detection, the noise associated with the system and its environment must be considered since the practical usefulness of any detector is its ability to separate signal from the input noise. The figure of merit which is generally used in analyzing circuits with noise is the signal-to-noise ratio (S/N).

Signal and noise parameters are considered in this section as they relate to narrow band array antennas. The bandwidth restriction is temporary and is removed in Section V. The object of this analysis is to determine what control of the overall signal-to-noise ratio can be obtained through manipulation of element weighting (amplitude control) and spacing (density control).

#### 1. SIGNAL POWER IN THE ANTENNA ARRAY

For purposes of analysis the antenna array can be represented as a "black box" with  $N$  inputs and a single output. The concept is illustrated in Figure 9. The antenna signal response can be defined as value of signal power ( $W$ ) which can be dissipated in a terminating impedance ( $Z_t$ ) for an applied constant fixed field density ( $\Phi_0$ ).

Since the antenna response is a function of angle, it is appropriate to utilize the concept of a gain function which is defined in terms of the array operating as a receiving antenna. Assuming reciprocity, the expressions are also valid for the transmitting case. The definition of gain is the ratio of the power available for dissipation in a load resistor ( $R_l$ ), to the total power available to the antenna. In antenna work it is convenient to express this ratio as a relative ratio using an isotropic source as the reference (7).

$$\text{The gain of any antenna relative to an isotropic source is then } G = \frac{W}{W'} \quad (1)$$

where:  $W$  = power delivered to load

$W'$  = power delivered to load if antenna is an isotropic source.

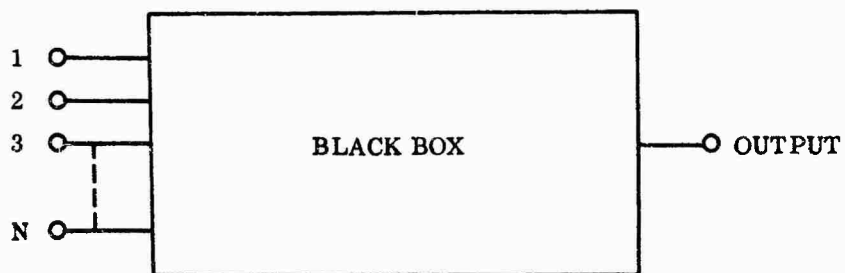
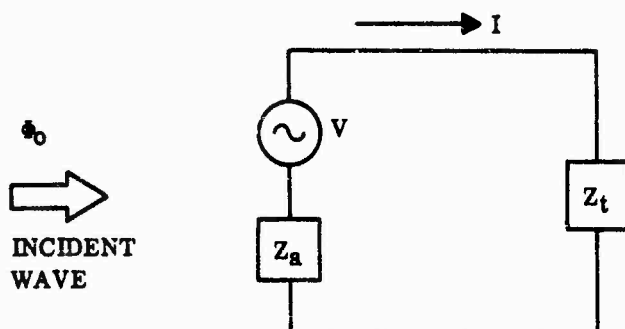


Figure 9. Basic Concept



$V$  = VOLTAGE INDUCED BY THE INCOMING WAVE

$Z_a$  = ANTENNA IMPEDANCE =  $R_a + jX_z$

$I$  = CURRENT FLOWING AS A RESULT OF THE INDUCED VOLTAGE  $V$

$Z_t = R_t + jX_t$  (TERMINATING IMPEDANCE)

$$I = \frac{V}{Z_a + Z_t}$$

Figure 10. Equivalent Circuit

The absolute gain of any antenna is a function of the effective area of the antenna aperture. But the effective area of an isotropic source is  $\lambda^2/4\pi$  therefore the power received by the unknown antenna relative to that which would have been received by an isotropic source is related to the gain of the antenna relative to the gain of the isotropic source (unity), assuming a constant fixed field intensity  $\Phi_0$ .

$$G \propto 4\pi W \quad (2)$$

In the simple aperture case the antenna can be represented by the equivalent circuit of Figure 10.

Considering a lossy antenna  $R_a = R_r + R_e$  where  $R_r$  is the antenna radiation resistance and  $R_e$  is the loss in the antenna and circuit.

The total power available to the antenna from the incoming wave is

$$P = VI = \frac{I^2}{(Z_a + Z_t)}$$

but the power available for dissipation in the load impedance ( $Z_t$ ) is

$$W = I^2 R_t = \frac{P^2 R_t}{V^2}$$

$$\frac{P^2}{W} = \frac{V^2}{R_t} = \frac{I^2 (Z_a + Z_t)^2}{R_t}$$

if  $P = uW$

$$W = \frac{I^2 (Z_a + Z_t)^2}{u^2 R_t}$$

where  $u$  is an efficiency factor. (NOTE: Kraus, Reference (7), refers to  $u$  as a scattering coefficient in the lossless antenna.)

Substituting for  $Z_a$  and  $Z_t$

$$W = \frac{I^2}{u^2 R_t} \left[ (R_r + R_e + R_t)^2 + (X_a + X_t)^2 \right] \quad (3)$$

The maximum power which can be dissipated in the load is  $I^2 R_t$ . This condition exists only when  $X_a = X_t$ ,  $R_e = 0$ , and  $R_t = R_r$  which, from equation 3, renders

$u = 2$ . That is to say that under optimum receiving conditions (conjugate matching)

only half of the available power can be absorbed in the load. The remainder is scattered from the antenna (absorbed in  $R_r$ ). Under these conditions, the maximum value of incident power which can be absorbed in the load is

$$W = \frac{I^2}{4R_t} \left[ (R_r + R_e + R_t)^2 + (X_a + X_t)^2 \right] \quad (4)$$

Extending this simple analysis to the array depicted in Figure 5 we can consider each element as an incremental collector as shown in Figure 11.

Following the preceding analysis, the power available in terminating impedance of the  $n^{\text{th}}$  element is

$$W_n = \frac{i_n^2}{4R_{tn}} \left[ (R_{rn} + R_{en} + R_{tn})^2 + (X_{an} + X_{tn})^2 \right] \quad (5)$$

and 
$$W = \sum_n W_n.$$

Before proceeding with the applicability of equation 5 to array antennas, it will be helpful to establish a physical understanding of some of the terms involved.

- a.  $i_n$  is the current in the  $n^{\text{th}}$  element. This current is a function of the antenna element radiation pattern. Further, the pattern used to modify  $i_n$  (expressed as  $g_e(u)$ ), must be considered the pattern of the element as it exists in the array; i.e., all mutual coupling effects in pattern modification are included.
- b. If the array is an amplitude tapered array, the values of  $i_n$  must be multiplied by the tapering coefficients,  $a_n$ . If the network provides tapering in a lossless manner, this must be accounted for in the basic expression.
- c.  $Z_{tn} = R_{tn} + jX_{tn}$  is, in general, not a function of scan in steerable arrays. The load impedance is usually adjusted to provide the best average match over the sector of scan.
- d. In a large array of equally spaced (or near equally spaced) identical elements, the element pattern function  $g_e(u)$  and the element impedance function  $Z_{an}$  can be considered a constant for all elements. The large array stipulation implies that the edge effects are negligible.
- e. The power available in the receiver ( $W$ ) is always a maximum when the receiver impedance ( $Z_t$ ) is the complex conjugate of the antenna impedance ( $Z_a$ ). The current induced by the incident wave, however, is a function of the terminal impedance of the array element which is, in turn, a function of the self and mutual impedances in the array. It has been shown, Reference (8), that the input impedance of the  $n^{\text{th}}$  element is related to the self and mutual impedances by the following relationship

$$Z_{an} = Z_{nn} + \sum_{p=1}^m Z_{np} \text{EXP}(\theta_p) \quad (6)$$

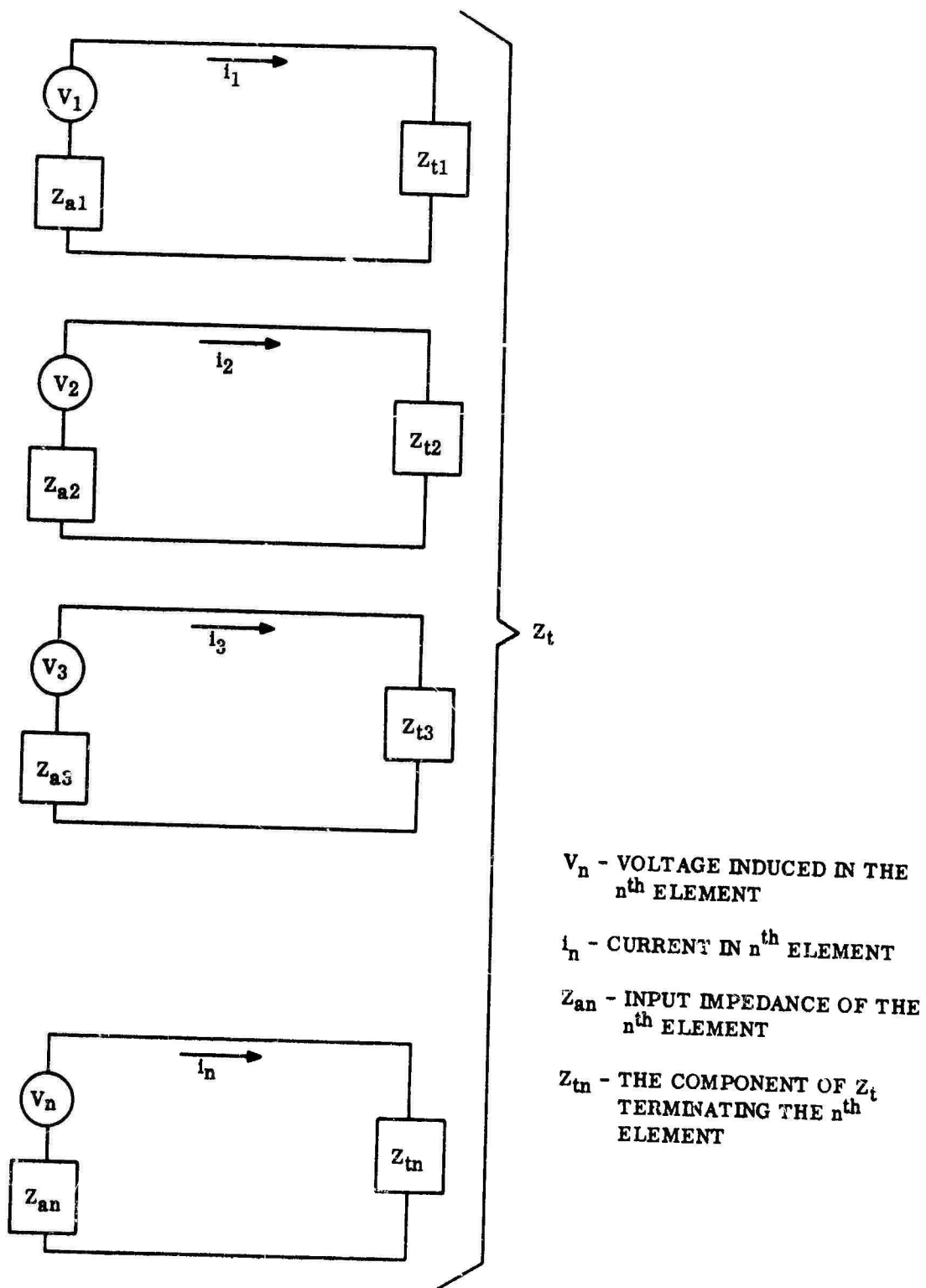


Figure 11. Array Equivalent Circuit

where  $Z_{np}$  is the mutual impedance between the  $n^{\text{th}}$  and the  $p^{\text{th}}$  element and  $\phi_p$  is the phase of the current in the  $p^{\text{th}}$  element relative to that in the  $n^{\text{th}}$  element.

It must be noted that  $Z_{np}$  is a function of antenna element spacing and therefore must be considered a variable whenever element spacing is employed as a means of controlling the array radiation pattern.

Utilizing these comments, it is now possible to establish a generalized expression of the signal power which is available in the receiver.

From e., above

$$(W_n)_{\max} = i_n^2 R_{rn} \quad (7)$$

From a., b., and e., above,

$$i_n = \frac{g_{en}(u) a_n}{Z_{an}} \text{EXP}(\phi_n) \quad (8)$$

where:  $g_{en}(u)$  is the element pattern function of the  $n^{\text{th}}$  element,  $a_n$  is the relative voltage amplitude of the  $n^{\text{th}}$  element in an amplitude tapered array.  $Z_{an}$  is the input impedance of the  $n^{\text{th}}$  element given by equation 6.

$\phi_n$  is the relative phase of the  $n^{\text{th}}$  element.

The maximum value of signal in the  $n^{\text{th}}$  receiver is therefore

$$(W_n)_{\max} = \frac{|g_{en}(u)|^2 a_n^2 R_{rn}}{|Z_{an}|^2} \text{EXP}(\phi_n)$$

or the total receiver power becomes

$$W_{\max} = \sum_n \frac{|g_{en}(u)|^2 |a_n \text{EXP}(\phi_n)|^2}{|Z_{an}|^2 a_n^2} R_{rn} \quad (9)$$

the  $a_n^2$  term in the denominator is required to meet the lossless (efficient) tapering condition of comment b.

The signal power expression, equation 9, is general in that the power is a function of  $u$  for any position of the array beam specified by  $\phi_n$ . In a large fixed beam array the conditions of comment d are met and the signal is a maximum when the array beam is aligned with the direction of the source. In the fixed beam broadside array the signal power becomes

$$W(u_0) = \frac{|g_e(u_0)|^2 R_t}{|Z_a|^2} \frac{\left| \sum_n a_n \right|^2}{\sum_n a_n^2} \quad (10)$$

Allen, Reference (9), has shown that the summation of equation 10 is simply the total number of array elements (N) multiplied by an amplitude taper efficiency factor ( $\eta$ ) so that

$$W(u_0) = \frac{|g_e(u_0)|^2}{|Z_a|^2} R_t \eta N \quad (11)$$

Equation 11 states that the total signal power present in the receiver is the signal power per element multiplied by the total number of elements in the array.

## 2. NOISE POWER

In the black box concept depicted in Figure 9, there are three conceivable sources of noise power which can be observed at the output terminal (dissipated in the load resistor  $R_t$ ). These three sources have been identified by Waldman and Wooley, Reference 10, and are classified as follows:

### a. External Noise

Noise which is external to the system but is transferred to the terminals as power collected by the array. This power is a function of antenna gain ( $G_a$ ) and the spatial distribution of noise power density ( $\eta$ ). This is correlated noise power.

### b. Antenna Noise

Noise generated in the antenna is taken to be the noise generated in each antenna element and transferred to the black box output by means of the network. This is uncorrelated noise power.

### c. Black Box Noise

The internal noise power of the network is transferred to the output and can be evaluated as an equivalent circuit noise factor.

The total noise power ( $N_t$ ) is considered to be the sum of these incremental contributions. Each contribution must be considered separately in terms of the influencing factors.

A generalized analysis of noise in active and passive circuits is contained in Appendix B. An expression of the noise power contributed by a network is given by:

$$\Delta N = K T_e B G \quad \text{equation 7 in Appendix B}$$

where:  $K$  = Boltzmann's Constant

$T_e$  = Effective temperature of the network referred to the input terminals

$B$  = Bandwidth

$G$  = Network Gain

The noise contributions of the three basic sources can be expressed in terms of this expression.

## 2.1 EXTERNAL NOISE

The component of noise introduced to the system through the antenna terminals is a function of antenna gain ( $G_a$ ) and the noise power density in space ( $\eta$ ). Since this noise is correlated, it is also dependent on the gain (or loss) of the black box when referred to the output terminals.

$$N_x = K B T_x G_r$$

$$\text{where } T_x = \frac{1}{K B} \int_{\Omega} G_a(u) \eta(u) d\Omega \quad (12)$$

$G_r$  = Effective gain of the black box network

$$G_r = \sum_n G_n$$

( $G_n$  is the incremental gain of the  $n^{\text{th}}$  element transferred to the output terminal.)

Since the antenna gain is proportional to the received signal power, the gain of a fixed beam broadside array, large enough to avoid edge effects, is of the form

$$G_a = \frac{4\pi |g_{en}(u)|^2 \left| \sum_n a_n e^{j\pi n u} \right|^2}{|Z_a|^2 \sum_n a_n^2} R_t \quad (13)$$

and the noise power density is related to space temperature by

$$\eta(u) = T_s(u) K B \quad (14)$$

Combining equations 12, 13, and 14, the external noise power present in the receiver is given by

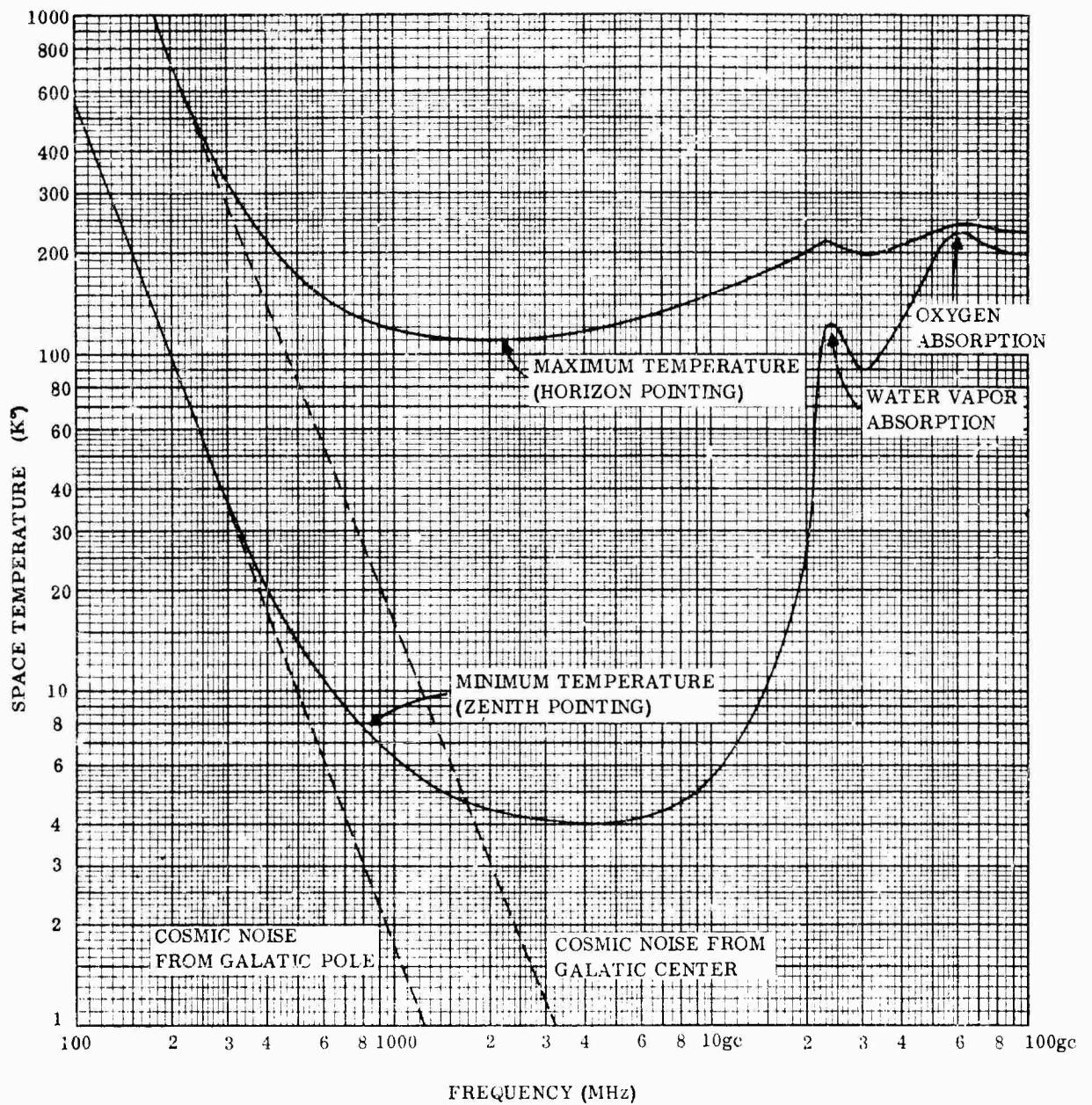
$$N_x = \frac{4\pi k B R_t G_r}{|Z_a|^2} \int_{\Omega} \frac{|g_{en}(u)|^2 T_s(u)}{\sum_n a_n^2} \left| \sum_n a_n e^{j\pi n u} \right|^2 d\Omega \quad (15)$$

The space temperature term [ $T_s(u)$ ] is a function of the antenna orientation and frequency. The magnitude of this term is affected by ground or sea temperature, noisy stars, the sun, the moon, atmospheric absorption, and general sky or galactic noise.

The range of space temperature is shown in Figure 12. The two solid curves represent the maximum and minimum noise temperature which will be present in the antenna. The shape of the curves indicate the "window" in the electro-magnetic spectrum (1 to 10 GHz) between cosmic noise and molecular absorption.

In order to completely specify the external noise conditions, the gain and noise temperature conditions must be known for the sector of space in which the system is





Note: Curves based on data of J. C. Green and M. T. Lehenbaum,  
 Letter in Microwave Journal, Vol. 2, pp. 13, 14  
 October 1959.

Figure 12. Noise Temperature vs. Frequency

to operate. Since this is likely to vary within a particular application, maximum and minimum limits can be established as an estimate of performance.

## 2.2 ANTENNA NOISE POWER ( $N_a$ )

Each antenna element is a source of noise with a related noise temperature  $T_{en}$ . The total effective noise temperature of the antenna is given by

$$T_a = \frac{\sum_n T_{en} G_n}{G_r}$$

where  $G_n$  is the gain of the network from the  $n^{th}$  terminal to the output

$$N_a = KBT_a G_r = KB \sum_n T_{en} G_n \quad (16)$$

## 2.3 NETWORK NOISE POWER ( $N_r$ )

The effective noise temperature of the black box network is  $T_r$ , therefore the internal noise present at the output terminal is

$$N_r = KBT_r G_r \quad (17)$$

The total noise power present at the output terminal is simply the sum of the three contributions and is given by

$$N_t = KBG_r \left[ \frac{4\pi R_t}{|Z_a|^2} \int_{\Omega} \frac{|g_{en}(u)|^2 T_s(u)}{\sum_n a_n^2} \left| \sum_n a_n e^{j\pi n u} \right|^2 d\Omega + \frac{\sum_n T_{en} G_n}{G_r} + T_r \right] \quad (18)$$

$$\text{or} \quad N_t = KBG_r (T_x + T_a + T_r). \quad (19)$$

Before taking the ratio of equations 10 and 18 to determine the signal-to-noise conditions in the array, some observations covering the noise expression in equations 18 and 19 are in order. The stated purpose of this study is to determine the effects of element spacing and weighting on the signal-to-noise ratio of the system. It is noted that if the array is comprised of a fixed number of elements, the only term in equation 19 which is affected by weighting and spacing is the first term  $T_x$ .

If the number of elements is not fixed, the  $T_a$  term may be affected but if the array elements are all assumed to be at the same temperature ( $T_e$ ), then  $T_a = T_e$  since  $\sum_n G_n = G_r$ .

A logical approach in improving the array signal-to-noise ratio is to consider the ratio of output signal to output noise resulting from the external noise power density ( $\eta$ ). Assuming the array beam is oriented to receive maximum signal, the signal-to-noise ratio which is affected by element spacing and weighting is given by taking the ratio of equations 10 and 15, keeping in mind that the signal at the output terminal is  $WG_r$ . After cancellation of common terms, this signal-to-noise ratio becomes

$$\frac{S}{N} = \frac{[g_e(u_o)]^2 \left| \sum_n a_n \right|^2}{4\pi KB \int_{\Omega} |g_{en}(u)|^2 T_s(u) \left| \sum_n a_n e^{jnu} \right|^2 d\Omega} \quad (20)$$

The significance of equation 20 can be generally stated in words. The numerator represents the maximum value of the antenna element gain function multiplied by the maximum value of the array function which is equivalent to the element gain times the number of elements in the array. The denominator is seen to be a constant times the integral (or summation) of the element gain function times the noise distribution times the array pattern function. It is this array pattern function which has been analyzed in Section III.

From equation 20, it can be seen that the signal-to-noise is dependent on a number of factors, including the following:

- a. Array gain
- b. Noise temperature distribution
- c. Antenna element pattern (as observed in the array, including coupling effects)
- d. Array pattern
- e. Beam pointing angle ( $u_o$ ).

In order to evaluate any array for  $S/N$ , these parameters must be known or assumed.

### 3. MAXIMIZATION OF SIGNAL-TO-NOISE RATIO

Considerable effort in the past has been devoted to the process of increasing the signal-to-noise ratio in array antenna systems. Neglecting the effect of external noise; i.e., assuming a uniform environment, these efforts have been directed toward (1) the minimization of uncorrelated noise and (2) the maximization of correlated signal.

The former approach has been pursued by Linder, Reference (11), and expanded by Cheng and Tseng, Reference (12). The process requires the representation of the array cross-correlation coefficients in a matrix which can be minimized by the application of Lagrange multipliers provided the quantity of array elements is small. This is equivalent to an inversion of the matrix which yields a solution in element weighting or amplifier gain. The results obtained by Linder indicate that a significant improvement in signal-to-noise ratio can be achieved with closely spaced elements (less than one-half wavelength) provided the severe amplitude weighting can be maintained.

The maximization of correlated signal is an attempt to increase the directive gain of the antenna array. This technique has been investigated extensively, References (13) thru (18). In a linear array, it has been shown by Tai, Reference (19), that the directivity can be

increased by close element spacing and a severe amplitude taper. The results of Tai and the mathematical formulation exactly parallels that of Linder even though the approach to the problem was based on different initial conditions.

The increase in array directivity or signal-to-noise ratio associated with close element spacing and severe amplitude tapering is commonly referred to as the "super-gain effect". Lo, et. al., Reference (20), relates the super-gain effect to a quality factor  $Q$ . For any set of conditions there is practical limit on the  $Q$ -factor which determines the degree of super-gain permissible. The  $Q$ -factor is essentially an expression of the bandwidth sensitivity and efficiency of the super-gain array.

The super-gain effect is illustrated in Figures 13 and 14. The curve in Figure 13 depicts the variation in array directivity, associated with a 10-element array, as a function of element spacing. It is noticed that for element spacing less than 0.5 wavelengths it is possible to achieve the super-gain condition through application of the prescribed optimum illumination function. The same information is shown in Figure 14 where the array length is fixed at five wavelengths while the number of elements comprising the array is allowed to vary.

Figure 13 shows that the highest directivity which can be achieved from a 10-element array is about 12 DB corresponding to element separation of about 0.9 wavelengths. Figure 14 shows that the highest directivity which can be obtained in a  $5\lambda$  aperture without super-gain is 10 DB and this is approached with a minimum of 6 elements also separated about 0.9 wavelengths.

A note concerning the practicality of the super-gain effect is in order. Although often stated, the limitations on achieving super-gain cannot be over emphasized. The super-gain condition is achieved by exciting the array elements with a severe amplitude taper which reverses phase on an element-to-element basis. This condition is extremely difficult to establish and maintain. The degree of super-directivity possible is dependent on the element spacing. As the elements are brought closer together, interelement coupling becomes stronger, making adjustment difficult. The excitation amplitudes become so critical that an error of one percent can completely destroy the super-gain effect. In application, therefore, super-directivity is limited to the narrow band situation where precise control is available to achieve a decrease in array beam width.

Although the terms super-gain and super-directivity are used interchangeably, the latter is correct. As the directivity is increased beyond that obtainable with uniform illumination, the efficiency is degraded accordingly, due to high currents (or gain requirements in amplification) required to produce the optimum illumination function.

Although the super-directive technique is not feasible as a means of achieving high gain from small apertures, some improvement in signal-to-noise ratio can be obtained if other aspects of system performance can be sacrificed. For example, low noise, variable-gain amplifiers might be used in a receiving array to produce an improved signal-to-noise ratio through gain adjustment. Improvement of this nature appears to be limited to about 10 percent under realistic conditions.

The study of signal-to-noise ratio by Cheng and Tseng, Reference (12), has provided a general formulation of the optimization process. It is noted that there are eight basic factors which affect the ultimate signal-to-noise ratio of a fixed array antenna system.

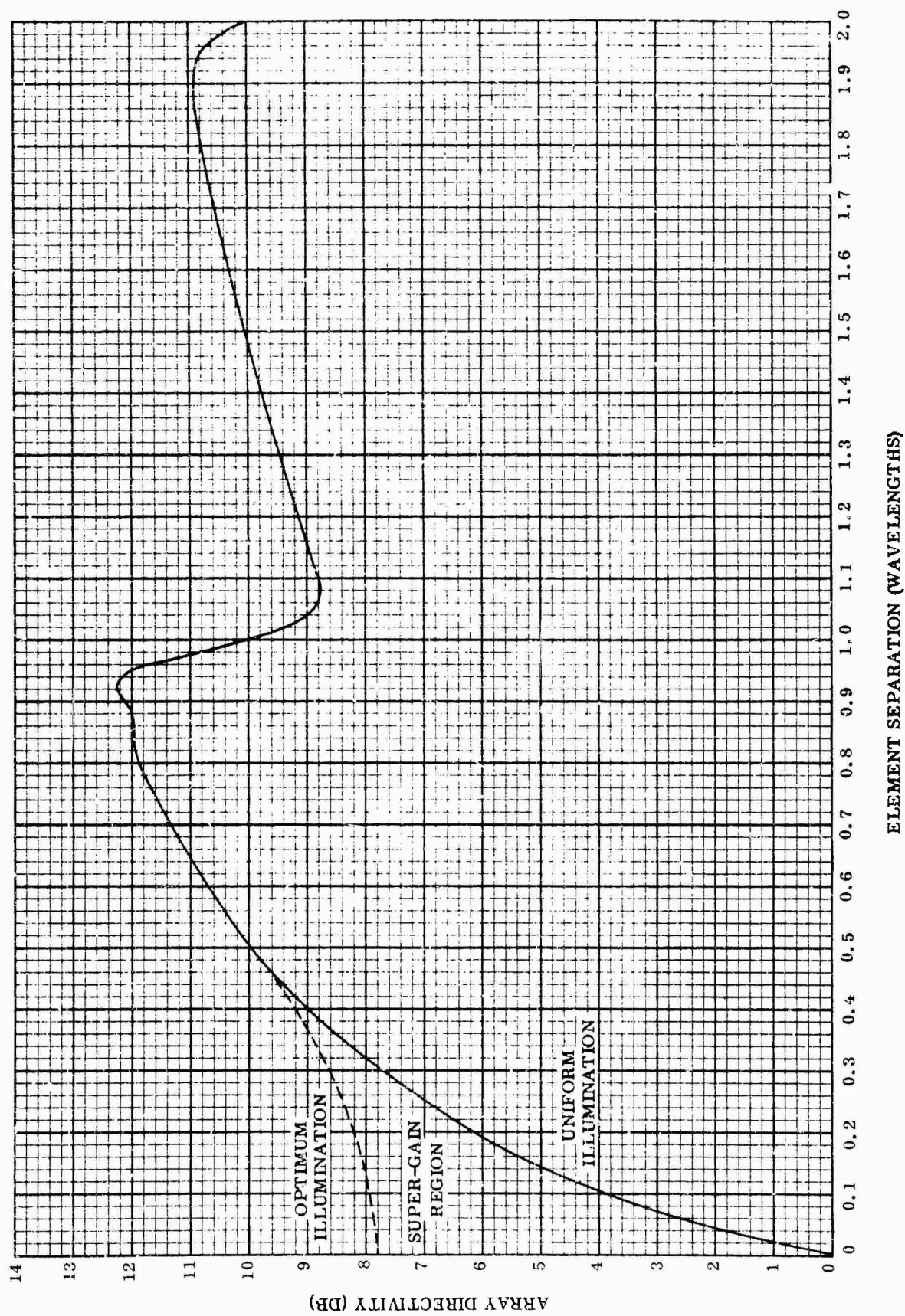


Figure 13. Array Directivity as a Function of Element Spacing;  $N = 10$  Elements



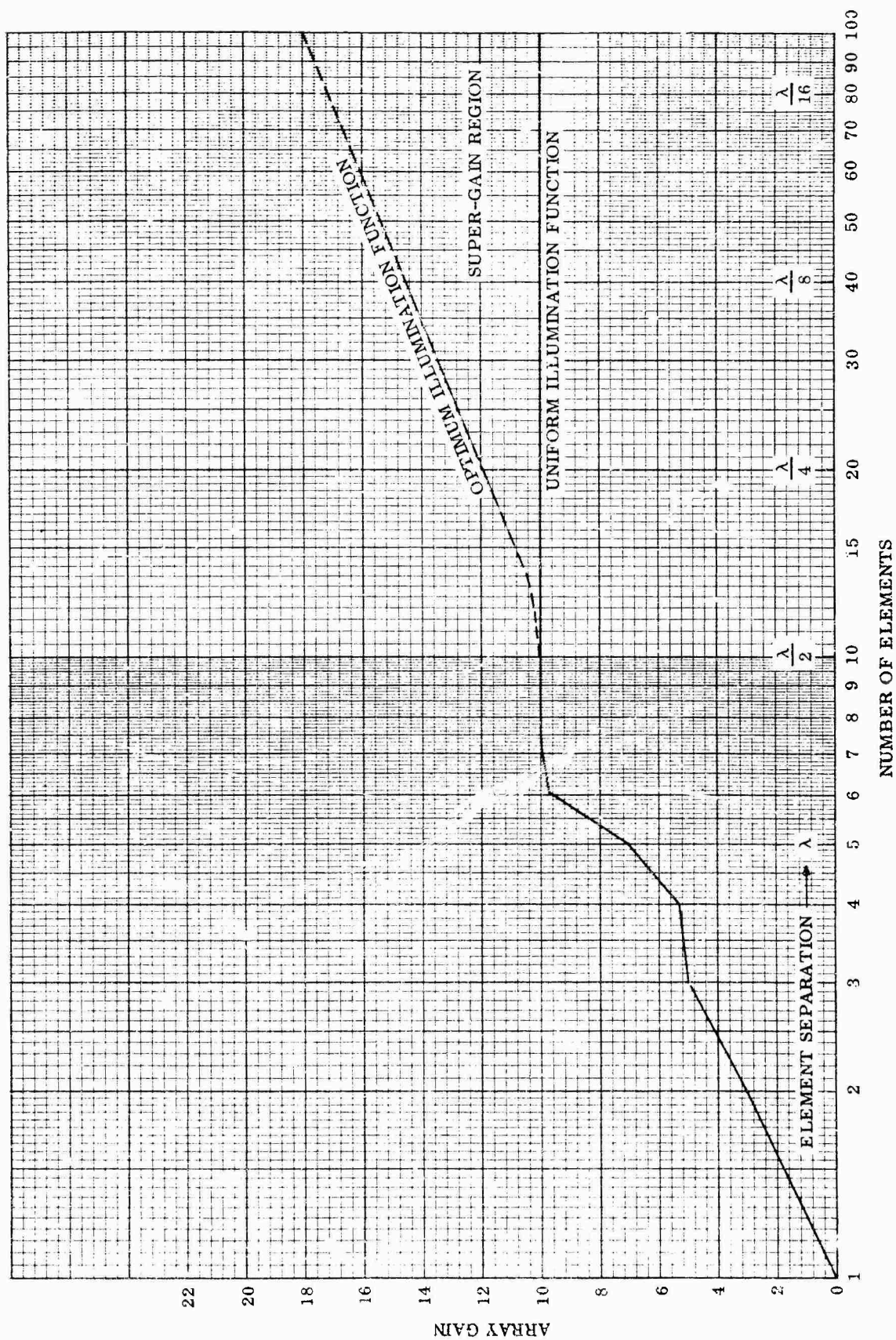


Figure 14. Linear Array of Isotropic Sources, Array Length =  $5\lambda$

- a. Antenna array configuration and element spacing
- b. Element radiation, impedance, and frequency characteristics (including coupling effects)
- c. Source direction relative to the array
- d. Receiver or filter response
- e. Signal spectrum
- f. Noise distribution in space and frequency
- g. Internal noise considerations
- h. Element weighting or amplification factors.

It has also been shown by Lo, et. al., Reference (20), that if the noise distribution in space and frequency is uniform, the conditions yielding maximum signal-to-noise ratio and maximum directivity are identical.

The directivity of any antenna is defined as the ratio of the peak radiated power per unit solid angle to the average radiated power per unit solid angle where the averaging process includes all space angles. Mathematically stated, using spherical coordinates, this is

$$D \triangleq \frac{\int_0^{2\pi} \int_0^{2\pi} P_{\max} \sin\theta \, d\theta \, d\phi}{\int_0^{2\pi} \int_0^{2\pi} P(\theta, \phi) \sin\theta \, d\theta \, d\phi} \quad (21)$$

which, since  $P_{\max}$  is constant, equation 21 is

$$D = \frac{4\pi P_{\max}}{\int_0^{2\pi} \int_0^{2\pi} P(\theta, \phi) \sin\theta \, d\theta \, d\phi} \quad (22)$$

For a broadside linear array of  $N$  discrete elements with feed coefficients,  $A_n$ , aligned on the  $z$ -axis,

$$P(\theta, \phi) = |E(\theta, \phi)|^2 \quad (23)$$

where

$$E(\theta, \phi) = G(\theta, \phi) \sum_{n=1}^N A_n e^{j \frac{2\pi n d}{\lambda} \cos \theta} \quad (24)$$

If the element pattern function is taken as unity so that  $G(\theta, \phi) = 1$ , the linear array consists of  $N$  isotropic radiators. Further, if the feed coefficients are cophasal, the beam maximum will occur at  $\theta = \pi/2$ . The radiation pattern can then be normalized to unity so that  $P_{\max} = 1$  and equation (24) becomes,

$$E(\theta) = \frac{\sum_{n=1}^N A_n e^{j \frac{2\pi nd}{\lambda} \cos \theta}}{\sum_{n=1}^N A_n} \quad (25)$$

Using equation (25) with equation (22) gives,

$$D = \frac{2}{\int_0^\pi |E(\theta)|^2 \sin \theta d\theta} = \frac{2}{I} \quad (26)$$

Maximizing the directivity amounts to minimizing the integral

$$I = \frac{1}{\left| \sum_{n=1}^N A_n \right|^2} \int_0^\pi \left| \sum_{n=1}^N A_n e^{j \frac{2\pi nd}{\lambda} \cos \theta} \right|^2 \sin \theta d\theta. \quad (27)$$

An alternate way of writing the factor which is the square of the absolute value in equation (27) is,

$$\sum_{n=1}^N A_n e^{j \frac{2\pi nd}{\lambda} \cos \theta} \sum_{m=1}^N A_m e^{-j \frac{2\pi md}{\lambda} \cos \theta}$$

Then,

$$I = \frac{1}{\left( \sum_{n=1}^N A_n \right)^2} \int_0^\pi \sum_{n=1}^N \sum_{m=1}^N A_n A_m e^{j \frac{2\pi d}{\lambda} (n-m) \cos \theta} \sin \theta d\theta \quad (28)$$

By letting  $x = \cos \theta$ , the integral is simplified to

$$I = \frac{1}{\left( \sum_{n=1}^N A_n \right)^2} \sum_n \sum_m A_n A_m \int_{-1}^1 e^{j \frac{2\pi d}{\lambda} (n-m) x} dx$$



Or, upon performing the indicated integration,

$$I = \frac{2}{\left(\sum_{n=1}^N A_n\right)^2} \sum_{n=1}^N \sum_{m=1}^N A_n A_m \frac{\sin \frac{2\pi d}{\lambda} (n-m)}{\frac{2\pi d}{\lambda} (n-m)} \quad (29)$$

In the general case the value of this term is dependent on the antenna element gain function ( $G(\theta, \phi)$  in equation 24), the element amplitudes ( $A_n$ ), the antenna element spacing ( $d$ ), the number of elements in the array ( $N$ ) and the operating frequency ( $f = c/\lambda$ ).

The expression "I" is defined for a uniform array of isotropic sources. The equation can be made general by replacing the  $\sin x/x$  term with the generalized cross correlation coefficient between the  $n^{\text{th}}$  and  $m^{\text{th}}$  elements ( $R_{n,m}$ ).

$$I = \frac{2}{\left(\sum_{n=1}^N A_n\right)^2} \sum_{n=1}^N \sum_{m=1}^N A_n A_m R_{n,m} \quad (30)$$

It is clear that  $R_{n,m}$  is dependent on the distance between the two elements as well as the applied frequency conditions.

The condition for maximum directivity is found by differentiating equation (30) with respect to each of the amplitude coefficients and setting the result equal to zero.

$$\frac{\partial I}{\partial A_k} = \frac{-2}{\left(\sum_n A_n\right)^3} \sum_n \sum_m R_{n,m} + \frac{2}{\left(\sum_n A_n\right)^2} \sum_n A_n R_{n,k} = 0$$

or

$$\left(\sum_{n=1}^N A_n R_{n,k}\right) \left(\sum_{n=1}^N A_n\right) = \sum_{n=1}^N \sum_{m=1}^N A_n A_m R_{n,m} \quad (31)$$

Equation 31 represents a set of  $N$  simultaneous equations where  $k = 1, 2, 3, \dots, N$ . Setting each of these equations to zero and solving for  $A_k$  yields the amplitude coefficients required to maximize the array directivity.

A matrix inversion method can be used to solve for the amplitude coefficients of equation 31. This expression can be rewritten in the form

$$\sum_{n=1}^N A_n R_{n,k} = \frac{\sum_{n=1}^N \sum_{m=1}^N A_n A_m R_{n,m}}{\sum_{n=1}^N A_n} \quad (32)$$

which can also be expressed in matrix form

$$[R]_{N,N} [A]_{N,1} = [K]_{N,1}$$

where  $[K]$  is a column vector of identical elements equal to the right hand side of equation 32. Premultiplying by the inverse matrix of  $[R]$  gives

$$[A]_{N,1} = [D]_{N,N} [K]_{N,1} \quad \text{where } [D] \triangleq [R]^{-1}$$

The amplitude coefficients are then proportional to the sum of the matrix elements

$$A_k \propto \sum_{j=1}^N D_{k,j} \quad K = 1, 2, 3, \dots, N$$

In a large array the matrix inversion required for solution becomes difficult. In a symmetrical array, the matrix inversion can be simplified by shifting the reference from the centerline of the array to the center of one side. This is accomplished by redefining the correlation coefficient

$$\beta_{n,m} \triangleq R_{n,m} + R_{n,N+1-m}$$

This transformation holds for both odd and even arrays. Making this substitution in equation 31 the new form is

$$\left( \sum_{n=1}^M A_n \beta_{n,k} \right) \left( \sum_{n=1}^N A_n \right) = \sum_{n=1}^M \sum_{m=1}^M A_n A_m \beta_{n,m} \quad (33)$$

The solution to equation 33 is identical with that described above for equation 31. The advantage is that the new matrix  $[\beta]$  is one half the order of the matrix  $[R]$  which simplifies the inversion required for solution.

For very large arrays ( $N > 100$ ) even the simplified form of equation 31 is difficult to solve by means of matrix inversion. For this reason an iterative technique has been developed which is described in Section VII. Four forms of the basic equation expression 31 are used to implement the iterative process

$$A_k = \frac{\sum_{n=1}^N \sum_{m=1}^M A_n A_m R_{n,m}}{\sum_{n=1}^N A_n} - \sum_{\substack{n=1 \\ (n \neq k)}}^N A_n R_{n,k} \quad (34)$$

$$A_k = \frac{\sum_{n=1}^N \sum_{\substack{m=1 \\ (n, m \neq k)}}^M A_n A_m R_{n,m} - \left( \sum_{n=1}^N A_n \right) \left( \sum_{n=1}^N A_n R_{n,k} \right)}{\sum_{\substack{n=1 \\ (n \neq k)}}^N A_n - \sum_{n=1}^N A_n R_{n,k}} \quad (35)$$

$$A_k = \frac{\sum_{n=1}^M \sum_{m=1}^M A_n A_m \beta_{n,m}}{\beta_{k,k} \sum_{n=1}^N A_n} - \frac{1}{\beta_{k,k}} \sum_{\substack{n=1 \\ (n \neq k)}}^M A_n \beta_{n,k} \quad (36)$$

$$A_k = \frac{\sum_{n=1}^M \sum_{\substack{m=1 \\ (n, m \neq 1)}}^M A_n A_m \beta_{n,m} - \left( \sum_{n=1}^M A_n \right) \left( \sum_{\substack{n=1 \\ (n \neq k)}}^M A_n \beta_{n,k} \right)}{\beta_{k,k} \sum_{n=1}^M A_n - \sum_{\substack{n=1 \\ (n \neq k)}}^M A_n \beta_{n,k}} \quad (37)$$

Equations 34 and 35 are based directly on equation 31 while 36 and 37 are derived from its counterpart, equation 33. The equation to be used depends on the nature of the array. Equations 36 and 37 apply only to symmetrical arrays but, in general, produce a higher rate of convergence.

The iterative process begins by assuming values for the excitation coefficients such as  $A_n = 1$  for all  $n$ . After the  $A_k$  terms have been computed, these terms are used to replace the  $A_n$  terms and the process is repeated until the change is negligible. The rate of convergence is somewhat dependent on which elements are computed first.

Even though the iterative process does converge, there is no assurance that the values obtained are optimum. It is usually desirable to use more than one of the above expressions as a final check on the solution.

#### 4. MAXIMIZATION OF ARRAY DIRECTIVITY THROUGH ELEMENT SPACING

The process of optimizing array directivity through control of the antenna element location is directly analogous to the process described above where the amplitude of excitation was used as the controlling factor. The basic equation 30 is again differentiated, but this time with respect to  $d_k$  rather than  $A_k$ .

Before differentiating it is convenient to rewrite equation 30 for symmetric array with the center of the array used as a reference. Under these conditions the denominator of equation 30 becomes

$$\sum_{n=1}^N A_n = A_o + 2 \sum_{n=1}^P A_n, \quad P = \frac{N-1}{2} \quad \text{for } N \text{ odd}$$

$$\sum_{n=1}^N A_n = 2 \sum_{n=1}^P A_n, \quad P = \frac{N}{2} \quad \text{for } N \text{ even} \quad (38)$$

for an even array, the numerator of equation 30 is

$$\sum_{n=1}^N \sum_{m=1}^N A_n A_m R_{n,m} = 2 \sum_{n=1}^P \sum_{m=1}^P A_n A_m [R_{n,m} + R_{n,-m}]$$

For an array having an odd number of elements, the double sum is

$$A_o^2 + 2A_o \sum_{n=1}^P A_n (R_{o,n} + R_{o,-n}) + 2 \sum_{n=1}^P \sum_{m=1}^P A_n A_m [R_{n,m} + R_{n,-m}] \quad (39)$$

or

$$A_o^2 + 2A_o \sum_{n=1}^P A_n R_{o,n} + 2 \sum_{n=1}^P \sum_{m=1}^P A_n A_m [R_{n,m} + R_{n,-m}]$$

It is noted that the summations for the odd array reduce to the even array formulation by simply letting  $A_o$  equal zero. Thus, a solution of the odd array case can be applied to an array having an even number of elements quite simply. The derivation is performed for the odd array for this reason.

Substituting equations 38 and 39 into equation 30 for the odd element condition

$$I = \frac{A_o^2 + 4A_o \sum_{n=1}^P A_n R_{o,n} + 2 \sum_{n=1}^P \sum_{m=1}^P A_n A_m [R_{n,m} + R_{n,-m}]}{\left( A_o + 2 \sum_{n=1}^P A_n \right)^2} \quad (40)$$

In this form differentiation with respect to  $d_x$  is straightforward.

$$\begin{aligned} \frac{\partial I}{\partial d_k} = & \frac{2}{A_o + 2 \sum_{n=1}^P A_n} \left[ 2A_o A_k \frac{\partial (R_{o,k})}{\partial d_k} + A_k^2 \frac{\partial (R_{k,k} + R_{k,-k})}{\partial d_k} \right. \\ & \left. + \sum_{\substack{n=1 \\ n \neq k}}^P A_k A_n \frac{\partial (R_{n,k} + R_{n,-k})}{\partial d_k} + \sum_{\substack{m=1 \\ m \neq k}}^P A_k A_m \frac{\partial (R_{k,m} + R_{k,-m})}{\partial d_k} \right] \quad (41) \end{aligned}$$

This expression can be simplified considerably. Let  $R'(d)$  be the first derivative of the correlation coefficient with respect to the distance between two elements. Then, since  $R'(d)$  is an odd function,

$$R'(-d) = -R'(d),$$

and it becomes apparent that the order of the subscripts is significant. The convention adopted here is

$$R'(d) = R'(d_n - d_k) = R'_{n,k}$$

Using this convention and notation, the derivatives indicated in equation 41 are

$$\begin{aligned} \frac{\partial R_{n,k}}{\partial d_k} &= R'_{n,k} & \frac{\partial R_{n,-k}}{\partial d_k} &= R'_{n,-k} \\ \frac{\partial R_{k,n}}{\partial d_k} &= R'_{k,n} = R'_{n,k} & \frac{\partial R_{k,-n}}{\partial d_k} &= R'_{k,-n} = R'_{n,-k} \\ \frac{\partial R_{k,k}}{\partial d_k} &= 0 & \frac{\partial R_{k,-k}}{\partial d_k} &= 2R'_{k,-k} \\ \frac{\partial R_{o,k}}{\partial d_k} &= -R'_{o,k} = R'_{k,o} \end{aligned}$$

Applying these simplifications, equation 41 becomes

$$\frac{\partial I}{\partial d_k} = \frac{4A_k}{A_o + 2 \sum_{n=1}^P A_n} \left[ A_o R'_{k,o} + \sum_{n=1}^P A_n (R'_{k,n} + R'_{k,-n}) \right] \quad (42)$$

where the  $n \neq k$  restriction of equation 41 has been removed. Equating this derivative to zero and dividing through by the constants gives the condition of maximizing array directivity through element position control.

$$\sum_{n=1}^P A_n (R'_{k,n} + R'_{k,-n}) = A_o R'_{k,o} \quad (43)$$

The appearance of equation 43 is less formidable if a new variable is defined. Let

$$\gamma_{k,n} \triangleq -R'(d_k - d_n) - R'(d_k + d_n) \quad (44)$$

Then equation 43 becomes

$$\sum_{n=1}^P \gamma_{k,n} A_n = A_o R'_{k,o} \quad (45)$$

where  $k = 1, 2, \dots, P$ , since there are  $P$  possible element pair locations. Fixing some of these element pairs amounts to imposing a constraint on some of the pair positions. Where  $d_k$  is constrained to a specified fixed position,  $\gamma_{k,n} = 0$  and  $R'_{k,o} = 0$ . Thus,  $k = 1, 2, \dots, L$ , where  $L$  is the number of degrees of freedom in the system of equations. A good example of the practicality of fixing an element pair position is to specify the position of the end element pair, thereby limiting the overall aperture. Equation 45 written in matrix form is

$$[\gamma]_{L,P} [A]_{P,1} = A_o [R']_{L,1} \quad (46)$$

Although the form of equation 46 is identical with the amplitude weighting solution, the problem of determining the actual element pair positions from the equation presents some difficulty. This arises from the fact that a solution is not generally unique. This non-uniqueness may result in many minor maximum values of array directivity. Since the absolute maximum directivity is normally desired, it is apparent that equation 46 is a necessary but not a sufficient condition.

The solution to equation 43 might be identified as an experimental process similar to one which could be encountered on an antenna test range. The first step in experimental solution would be to determine the spacing required to obtain the maximum directivity for an equally spaced array. However, the maximum directivity for an array of unequally spaced elements must be higher than that of the optimum array using equal element spacing. Thus, the equally spaced array serves as a starting point. The next step is an attempt to increase the directivity by adjusting the positions of each pair of elements, one pair at a time. The process can be repeated until there is no perceptible movement of the element positions. This procedure can be applied mathematically using the appropriate equations.

For a given set of amplitude coefficients, the array directivity can be determined for equal element spacing by applying equation 26. Then the necessary condition, represented by equation 43, can be applied. For computation purposes, equation 43 can be written in the form,

$$F(d_k) = A_0 R'_{k,0} + A_k R'_{k,-k} + \sum_{\substack{n=1 \\ n \neq k}}^P A_n (R'_{k,n} + R'_{k,-n}) \quad (47)$$

where the solution for  $d_k$  is such that  $F(d_k) = 0$ . To obtain this solution, a modification of Newton's method for finding roots can be applied. The solution, according to Newton's method is

$$d'_k = d_k - F(d_k) / F'(d_k) \quad (48)$$

Since the correction on  $d_k - F(d_k)$ , can be quite large, some upper limit on the correction should be imposed. The derivative of equation 47 is

$$F'(d_k) = A_0 R''_{k,0} + 2A_k R''_{k,-k} + \sum_{n=1}^P A_n (R''_{k,n} + R''_{k,-n}) \quad (49)$$

After using the modification of Newton's method for finding the  $k^{\text{th}}$  element pair locations, the  $(k \pm 1)$ -th pair can be determined. By going through the array several times in this manner, any possible improvement in the array directivity can be found. A difficulty with this approach is that there is no guarantee that the directivity will be the absolute maximum, although it will be higher than the equally spaced array.

As an example of the results which can be obtained through element control, two array conditions are presented in Table 3. The relative element spacing is compared with that of a comparable uniform array, and the directivity values are presented indicating the degree of improvement available.

TABLE 3. RESULTS OF ELEMENT SPACING COMPUTATIONS

6 Elements — Uniform Amplitudes		
Element Number	Element Spacing for single frequency	
	UNIFORM	OPTIMUM DIRECTIVITY
1	157.8	161.7
2	473.4	482.3
3	788.9	778.8
S/N	9.788 DB	9.844 DB
20 Elements — Uniform Amplitudes		
Element Number	Element Spacing for single frequency	
	UNIFORM	OPTIMUM DIRECTIVITY
1	165.0	173.4
2	495.0	520.0
3	824.9	866.2
4	1154.9	1212.0
5	1484.9	1556.9
6	1814.9	1900.4
7	2144.9	2241.9
8	2474.8	2580.0
9	2804.8	2911.8
10	3134.8	3217.2
S/N	15.410 DB	15.623 DB



## SECTION V

### WIDEBAND EFFECTS

The array design considerations and the signal, noise, and directivity analysis presented in Sections III and IV were limited to the single frequency condition. Most systems do not operate at precisely a single frequency, i.e. with a continuous wave input, but rather operate over a range of frequencies defined by input waveform, noise conditions, tunability of equipment or other component characteristics. Unless the bandwidth is very wide, the single frequency assumption provides an acceptable base from which to determine approximate system performance.

In this section, the narrow band assumption is removed and the effect of wide-band signals on array performance is determined in terms of aperture effects and signal-to-noise ratio effects. A possibility of utilizing the wideband condition as a means of improving array performance is also presented.

#### 1. APERTURE EFFECTS

The general expression for the radiation pattern of an array of  $N$  elements is given by

$$E(u, t) = e^{j2\pi ft} \sum_{n=1}^N A_n e^{j(\pi n \frac{f}{f_0})u} \quad (50)$$

where

- $f$  = the frequency of the incoming wave
- $f_0$  = an arbitrary "center" frequency
- $u = \frac{2d}{\lambda_0} \sin \theta$ ,  $d$  is the element spacing
- $\lambda_0$  = the wavelength of the center frequency
- $\theta$  = the observation angle relative to boresight
- $A_n$  = the array element amplitude coefficients

In the analysis of narrow band arrays, it is often convenient to neglect the  $e^{j2\pi ft}$  term with a statement that it is "understood" to be a multiplier of all expressions. This is valid only if the applied signal is independent of time, i.e. a CW signal. If more than one frequency is applied to the array simultaneously, a component of  $E(u, t)$  will result for each frequency, so that equation 50 becomes

$$E(u, t) = \sum_{k=1}^K \left( \sum_{n=1}^N F_k A_n e^{j2\pi f_k t} e^{j(\pi n \frac{f_k}{f_0})u} \right) \quad (51)$$

where  $F_k$  is the amplitude weighting of the  $k^{\text{th}}$  frequency. If the frequencies are related so that

$$f_k = f_0 + k\Delta f \quad k = 0, \pm 1, \pm 2, \pm 3, \dots, \pm \frac{k-1}{2} \quad (52)$$

( $\Delta f$  is a small difference frequency), equation 52 can then be rewritten

$$E(u, t) = \sum_{k=-1}^K \sum_{n=1}^N F_k A_n e^{j2\pi(f_0 + k\Delta f)t} e^{j\pi n(1 + k\frac{\Delta f}{f_0})u} \quad (53)$$

Equation 53 represents a repeating waveform with a period  $T = \frac{1}{\Delta f}$ . The spectral lines comprising the waveform are characterized by the phase and amplitude of the complex form  $F_k e^{j2\pi(f_0 + k\Delta f)t}$ .

In application, it is common to separate signal information from its RF carrier by means of detection. The detection circuit provides the means by which the  $e^{j2\pi f_0 t}$  term in equation 53 is removed. Since this carrier is a time varying signal, the time constant of the detector circuit is extremely important. The requirements for good detection are: the detector time constant must be long, as compared with the RF cycle, and short as compared with the desired video waveform. These two requirements may not be compatible where extremely large bandwidths are involved but, for purposes of analysis, perfect detection is assumed.

Removing the RF component from equation 53 yields the detected output.

$$E(u, t) = \left( \sum_{n=1}^N A_n e^{j\pi n u} \right) \left( \sum_{k=1}^K F_k e^{j\pi k (2\Delta f t + n \frac{\Delta f}{f_0} u)} \right) \quad (54)$$

Equation 54 is based on the excitation of an array containing a fixed number of elements  $N$ , with a fixed number of spectral components  $K$ . It is possible to establish a comparable expression wherein the illumination function and the frequency spectrum are continuous. The video response corresponding to the continuous function is

$$E(z, t) = \int_{f_0 - \delta}^{f_0 + \delta} \int_{-\frac{1}{z}}^{\frac{1}{z}} F(f) G(x) e^{j2\pi \frac{f}{f_0} z x} e^{j2\pi(f - f_0)t} dx df \quad (55)$$

where

$$z = \frac{A}{\lambda_0} \sin \Theta, \quad A = \text{the aperture in wavelengths (center frequency)}$$

$$2\delta = \text{the bandwidth}$$

$$G(x) = \text{the aperture amplitude distribution}$$

$$F(f) = \text{the frequency amplitude distribution}$$

In the manner of equations 54 and 55 the combination of continuous and discrete functions can be expressed.

### Discrete aperture with continuous spectrum

$$E(u, t) = \int_{f_0 - \delta}^{f_0 + \delta} F(f) e^{j2\pi(f - f_0)t} \sum_{n=1}^N A_n e^{j\pi n u} df \quad (56)$$

### Continuous aperture with discrete spectrum

$$E(z, t) = \int_{-\frac{1}{z}}^{\frac{1}{z}} G(x) e^{j2\pi \frac{f}{f_0} z x} \left[ \sum_{k=1}^K F_k e^{j\pi k (2\Delta f t + n \frac{\Delta f}{f_0} u)} \right] dx \quad (57)$$

Each of the above expressions represents a radiation function which is variable in both space and time. This means that a true representation of the wideband array can only be observed in the time-space coordinate system. An example of the power response observed in the time-space domain for a uniform discrete array, illuminated with a uniform discrete frequency function, is shown in Figure 15.

The three dimensional model of Figure 15 is used to illustrate the distribution of energy as specified by equation 54. There are several characteristics of this distribution which are significant:

- The principal plane pattern along the time axis ( $u = 0$ ), follows the  $\frac{\sin x}{x}$  variation, but along the angular axis ( $tf_0 = 0$ ) decays rapidly to an insignificant level.
- A peak off-axis response occurs along straight lines displaced in both time and space.
- The far out sidelobe response along these displaced lines is 6 DB below the peak sidelobe response of the same array excited with a CW signal.

An explanation of these observations can be gleaned from a close examination of an ideal time waveform defined by the Fourier integral

$$E_i(t) = \frac{1}{2\delta} \int_{-\delta}^{\delta} A(f) e^{j2\pi f t} df \quad (58)$$

where:

$2\delta$  = the frequency range

$A(f)$  = the spectral density

defined so that a peak value is obtained at  $t = t_0$ .

In the wideband antenna array, the ideal waveform is modified by the antenna function  $G(f)$ .

$$E(t) = \frac{1}{2\delta} \int_{-\delta}^{\delta} G(f) A(f) e^{j2\pi f t} df \quad (59)$$

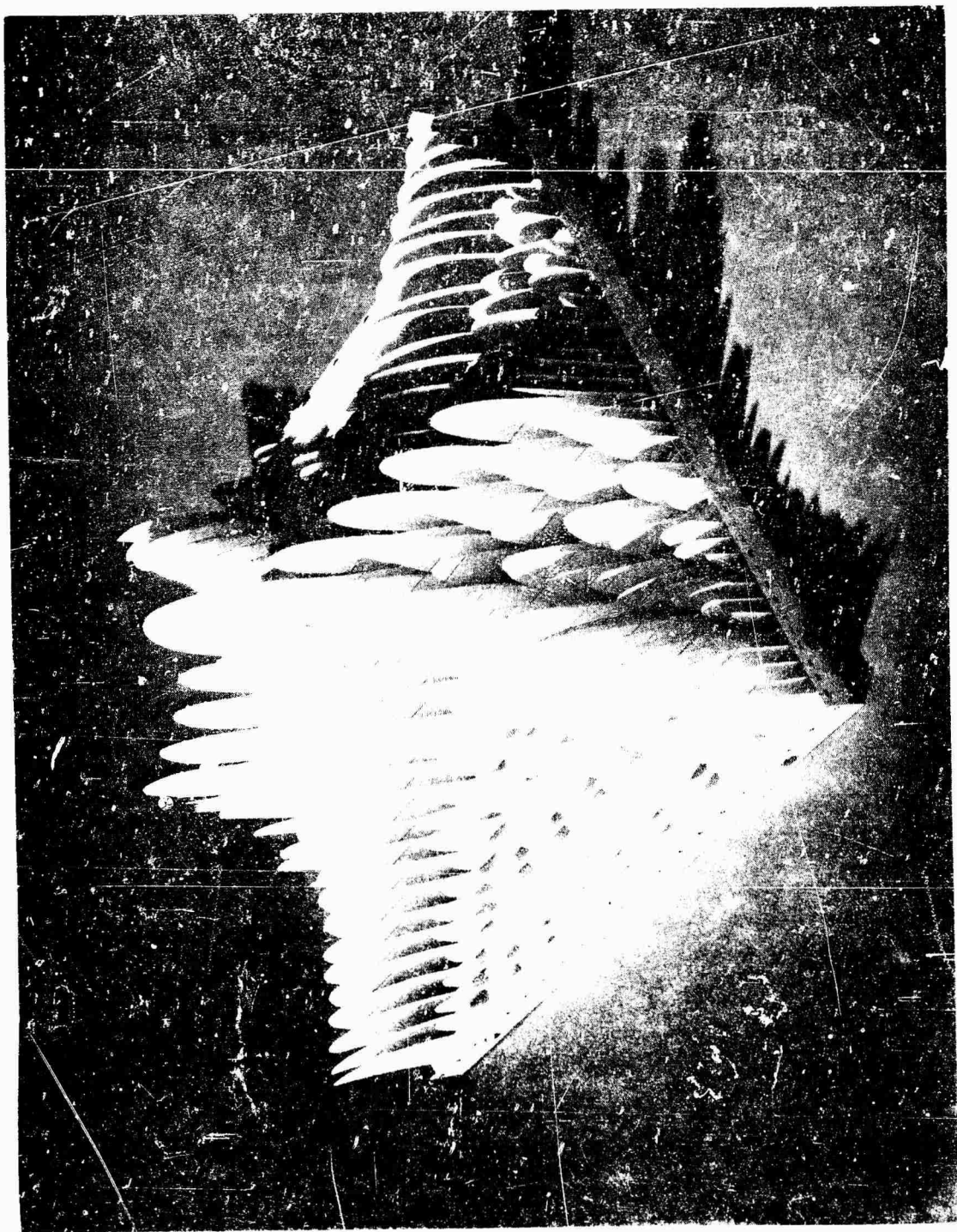


Figure 15. Time-Space Response of Wideband Array

The antenna array sidelobe behavior is defined in terms of  $G(i)$ , but for many linear arrays the peak value is essentially constant over a limited range and can be approximated by

$$G(f) = \cos \left( \frac{\pi N u}{2} \cdot \frac{f_0 + f}{f_0} \right) \quad (59)$$

where:

- $N$  = the number of array elements
- $f_0$  = the center frequency
- $f$  = the deviation from  $f_0$
- $u$  = the far-field space coordinate

Since equation 59 represents only the sidelobe structure of the array pattern,  $u$  must be limited to large values. Incorporating the cosine identity

$$\cos x \equiv \frac{e^{jx}}{2} + \frac{e^{-jx}}{2}$$

into equation 60 and substituting into equation 59 a sum in the form of equation 58 is obtained. Utilizing the general form of equation 58 the result can be written

$$E(t) = \frac{1}{2} e^{j \frac{\pi N u}{2}} E_i \left( t + \frac{N u}{4 f_0} \right) + \frac{1}{2} e^{-j \frac{\pi N u}{2}} E_i \left( t - \frac{N u}{4 f_0} \right) \quad (61)$$

An understanding of the sidelobe behavior in the far-out pattern can be obtained by considering the narrow band and wideband response. In the narrow band case  $f = 0$ , and the sidelobe pattern is given by equation 60 as  $\cos \pi N u / 2$ . When the bandwidth becomes large, the response is given by equation 61 which consists of two separate terms. The sidelobe region can then be considered as the sum of two ideal waveforms. In the far-out region, the interaction between these waveforms is very slight and the response contains a double peak in time appearing at

$$t = t_0 \pm \frac{N u}{4 f_0} \quad \text{or} \quad t = t_0 \pm \frac{N d}{2 c} \sin \theta \quad (62)$$

where:

- $d$  = element separation
- $c$  = velocity of light
- $\theta$  = angular displacement

This double peak response is observed in Figure 15 for any value of  $t f_0$  displaced from zero. Since the response is symmetrical about  $t = 0$ , there are four equal lobes appearing in the time-space pattern.

The amplitude of the sidelobe function in the region of slight interaction is given by

$$E \left( t_0 \pm \frac{N u}{4 f_0} \right) = 1/2 E_i(t_0) \quad (63)$$

which occurs at the peak of the waveform. The  $1/2$  in equation 63 represents the nominal 6-DB reduction observed in the time-space domain over that appearing in the CW case.

The above discussion is limited to the behavior of the array in the time-space domain, removed from the area of the major lobe. In the area of the major lobe, the response is not so well defined. The response of the uniform-array (Figure 15) in the area of the major lobe is shown, expanded, in Figure 16. It is noted, in following the response along the  $u$  axis, that the major lobe broadens and smooths out prior to splitting into the double peak indicated by equation 61. This effect is caused by severe interaction of the two terms. The effect of interaction can be seen in Figure 17 which is a contour diagram of the response depicted in Figures 15 and 16. The peak response is shown as a dashed line which is seen to meander about the line predicted by equation 62, for small values of  $u$ . The actual response along this predicted line is shown in Figure 18, compared with peak response at  $t = 0$ . The difference between these two curves is shown to be, on the average, about 6 DB corresponding to the prediction of equation 63. The variation in amplitude, as a function of  $u$ , represents the degree of interaction between the terms of equation 61.

The time-space response of an array is dependent on the frequency and amplitude weighting functions. The response for various functions is shown in contour form in Figures 17 through 28. The excitation conditions are indicated in Table 4.

TABLE 4 . ILLUSTRATED TIME-SPACE RESPONSE FUNCTIONS

Contour Diagram Figure No.	Illumination Function	Frequency Function	$u_0 = \left(\frac{N}{4}\right)u$ Response Figure No.
17	Uniform	Uniform	18
19	Uniform	Cosine	20
21	Cosine	Uniform	22
23	Cosine	Cosine	24
25	Uniform	Square Pulse	--
26	Cosine	Square Pulse	--
27	Uniform	Trapezoidal Pulse	--
28	Cosine	Trapezoidal Pulse	--

## 2. SIGNAL-TO-NOISE RATIO EFFECTS

In Section IV the signal-to-noise ratio of an array system is defined in terms of a number of interdependent factors which represent variables in the signal power and noise power present at the terminals of the array.

Linder, Reference (11), has shown that the signal-to-noise ratio in a linear array can be expressed as

$$S/N = \frac{\left( \sum_{n=1}^N A_n \right)^2}{\sum_{n=1}^N \sum_{m=1}^N A_n A_m R_{n,m}} \quad (64)$$

where:

$A_n$  = the amplitude of the  $n$ th element

$A_m$  = the amplitude of the  $m$ th element

$R_{n,m}$  = the cross-correlation coefficient between the  $n$ th and  $m$ th elements.



Figure 16. Near Boresight Response (Expanded) Wideband Array



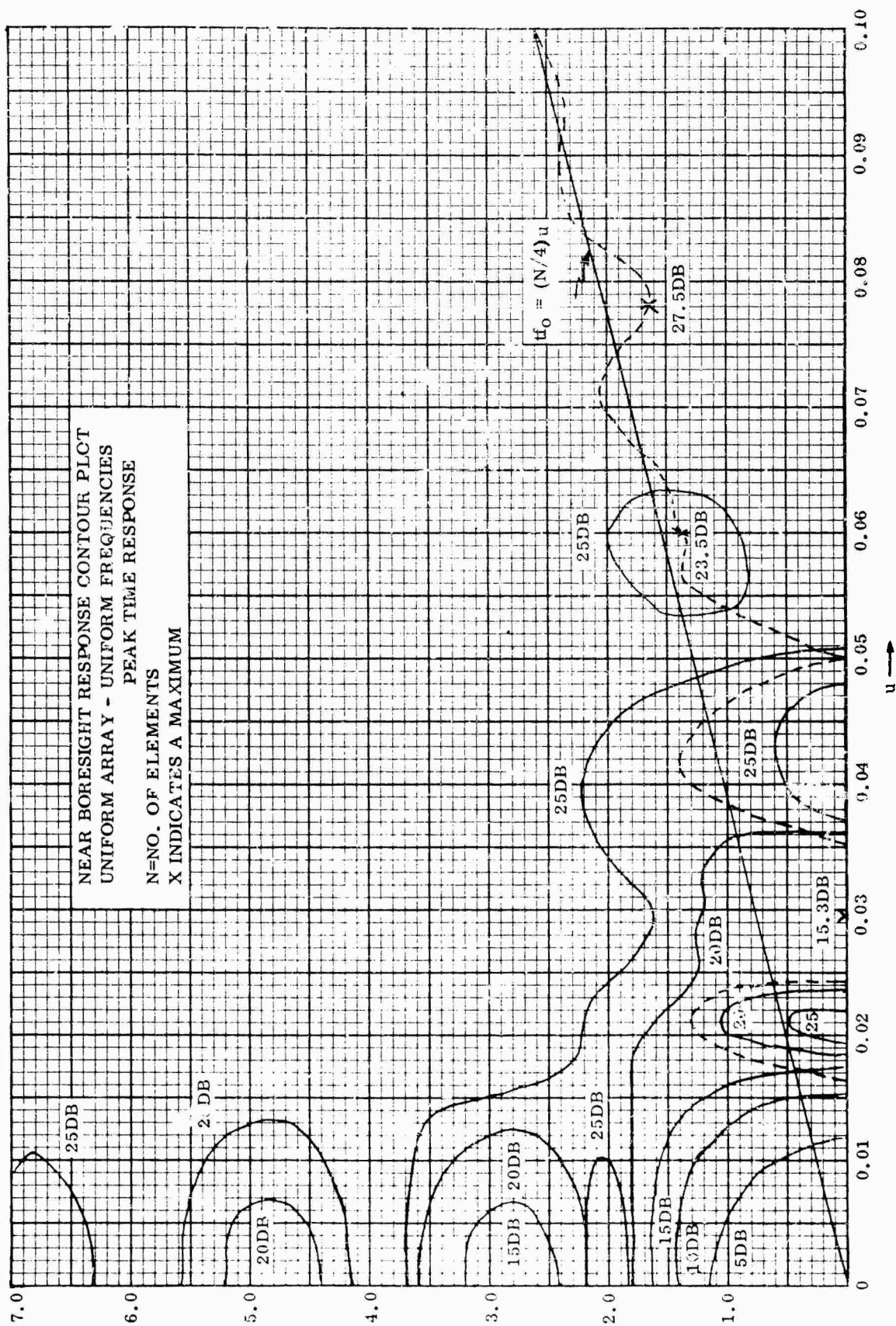


Figure 17. Near Boresight Response Contour Plot-Uniform Frequency



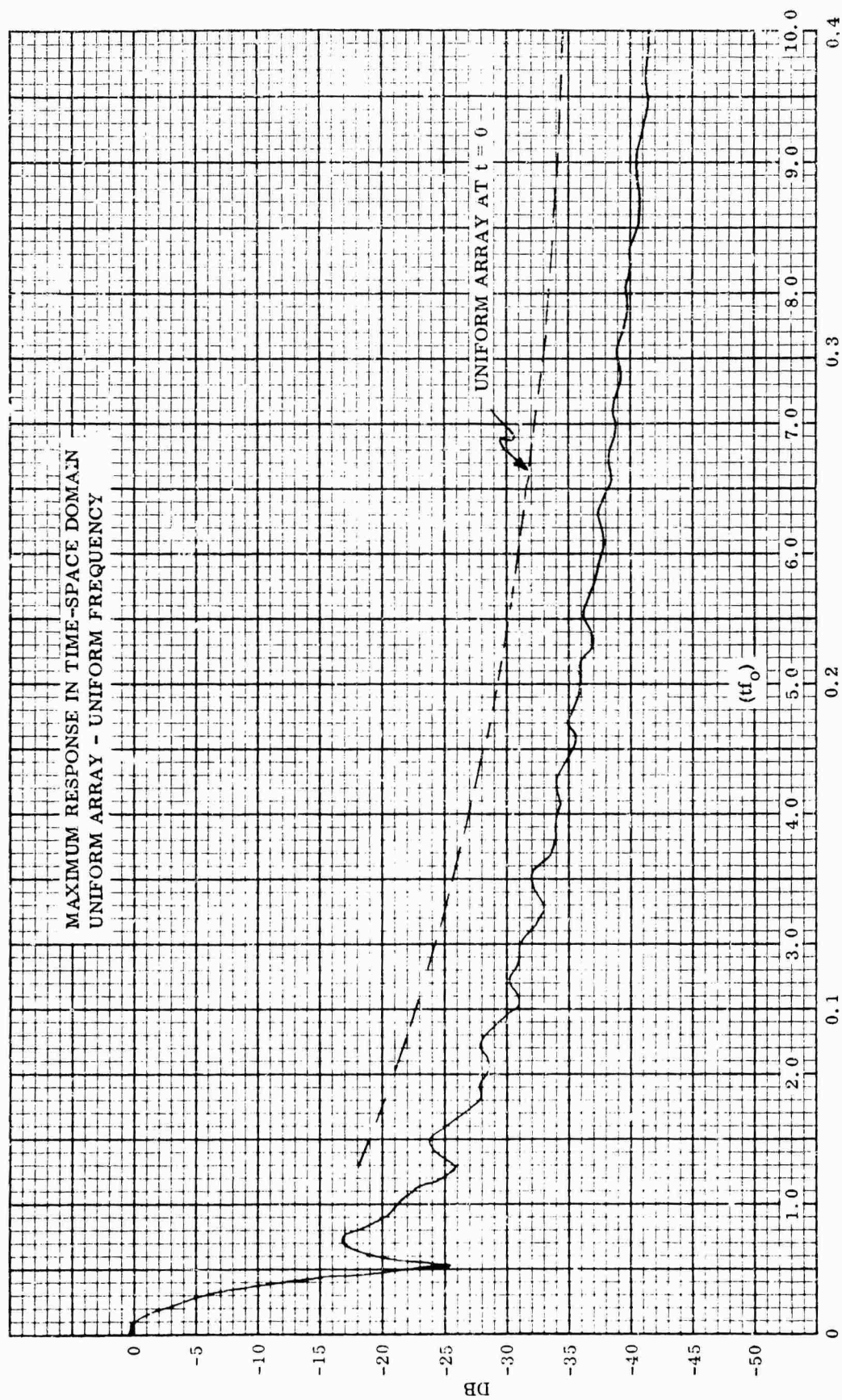


Figure 18. Maximum Response in Time-Space Domain

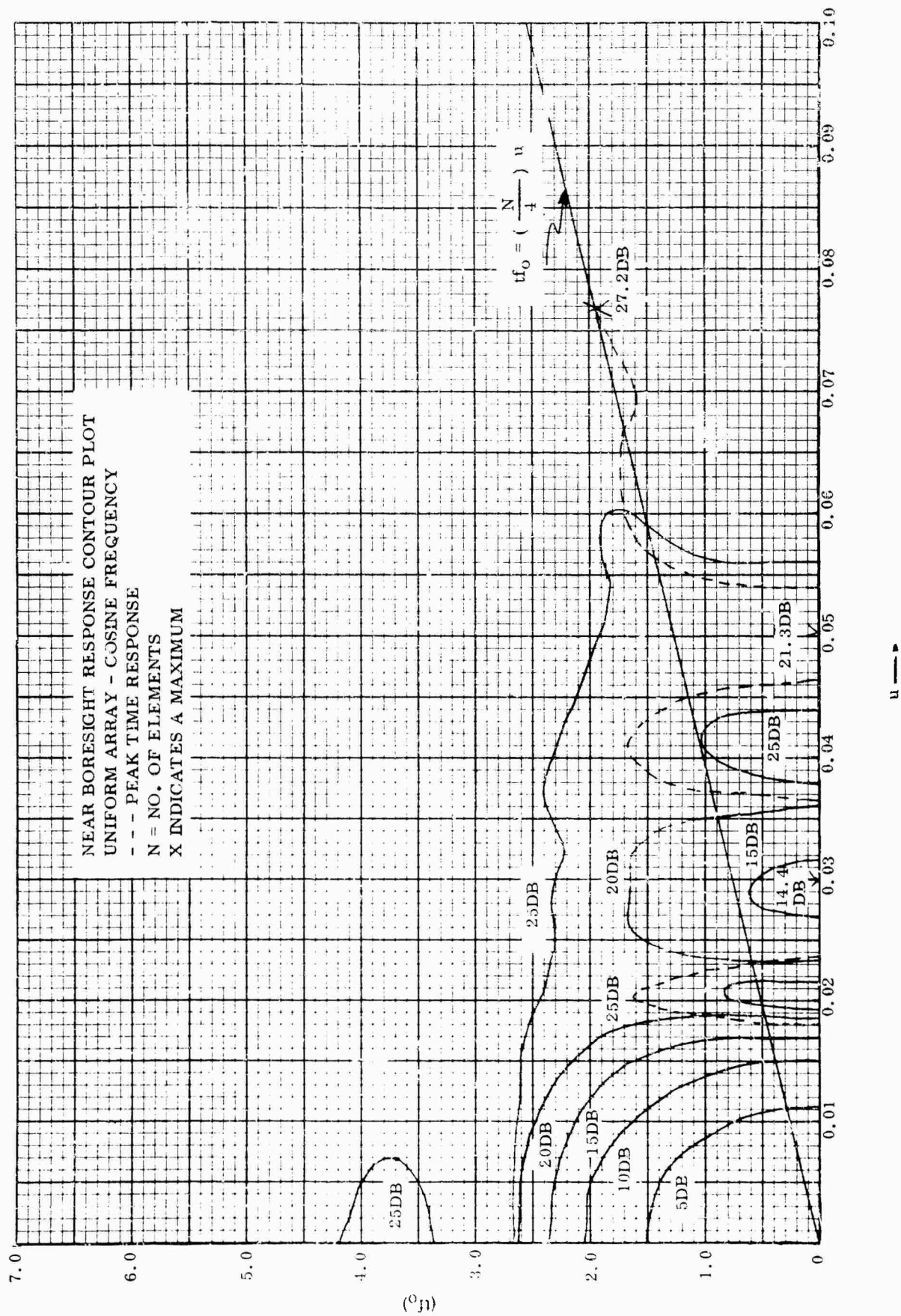


Figure 19. Near Bore-sight Response Contour Plot-Cosine Frequency

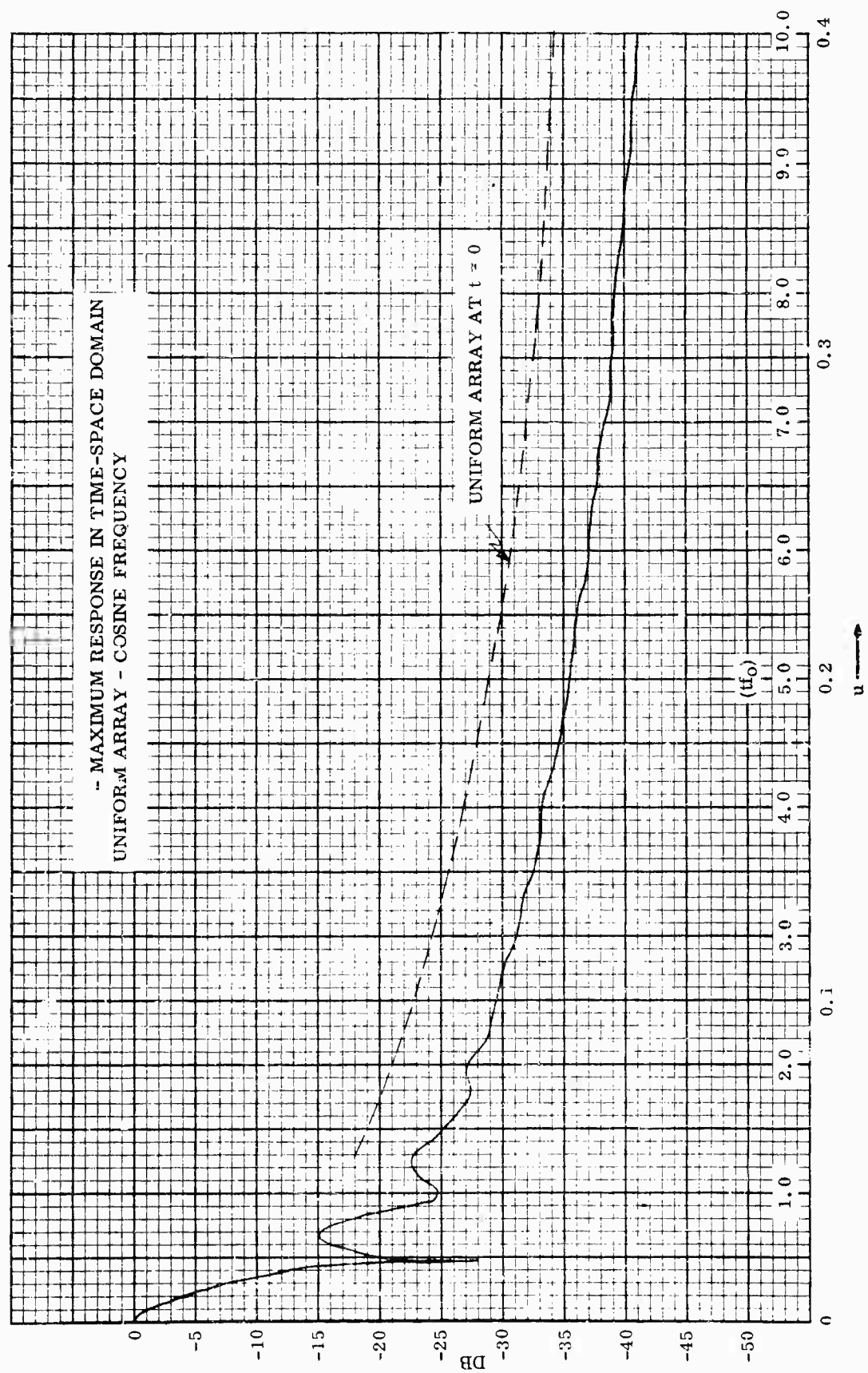


Figure 20. Maximum Response in Time-Space Domain-Cosine Frequency

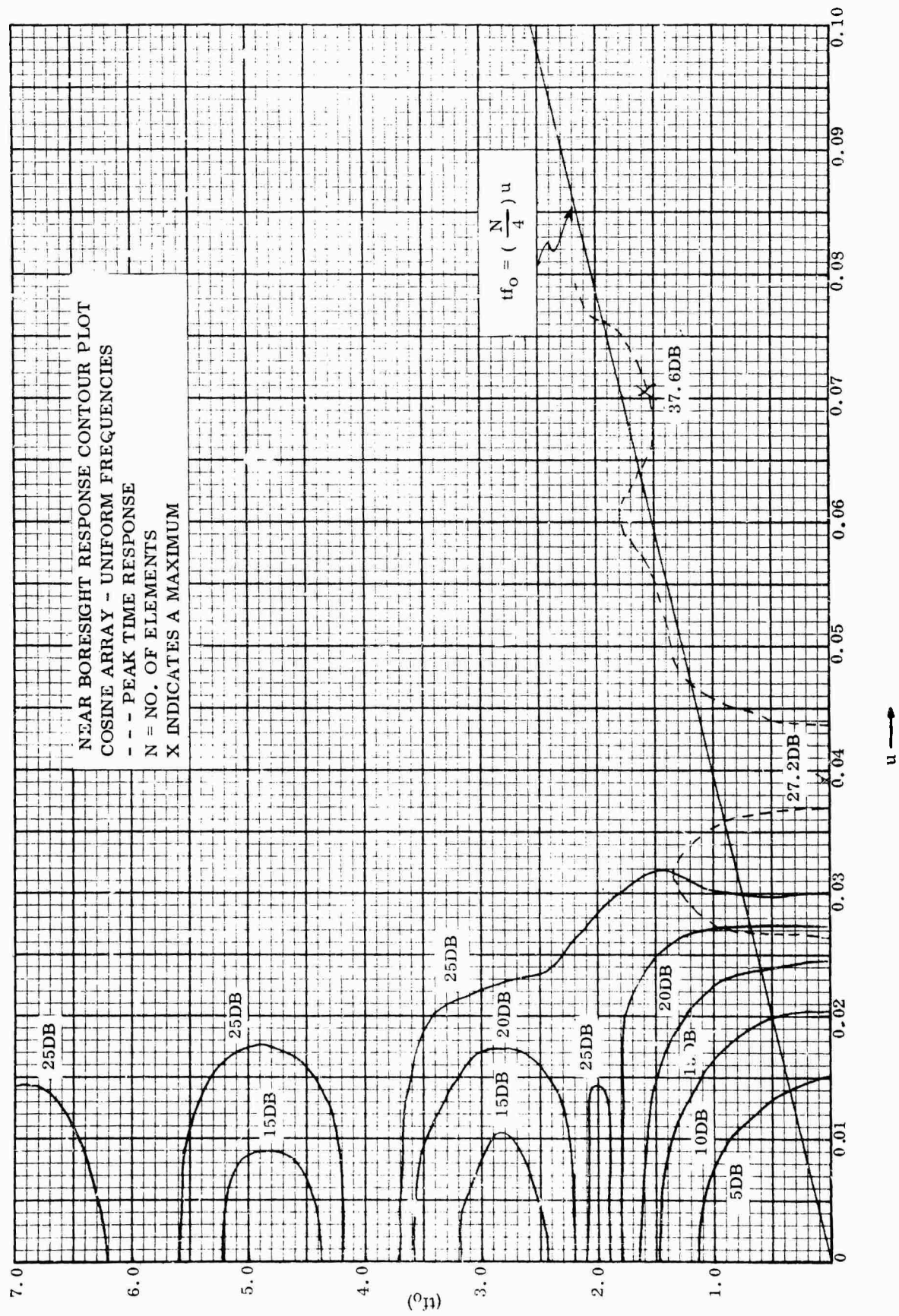


Figure 21. Near Bore-sight Response Contour Plot



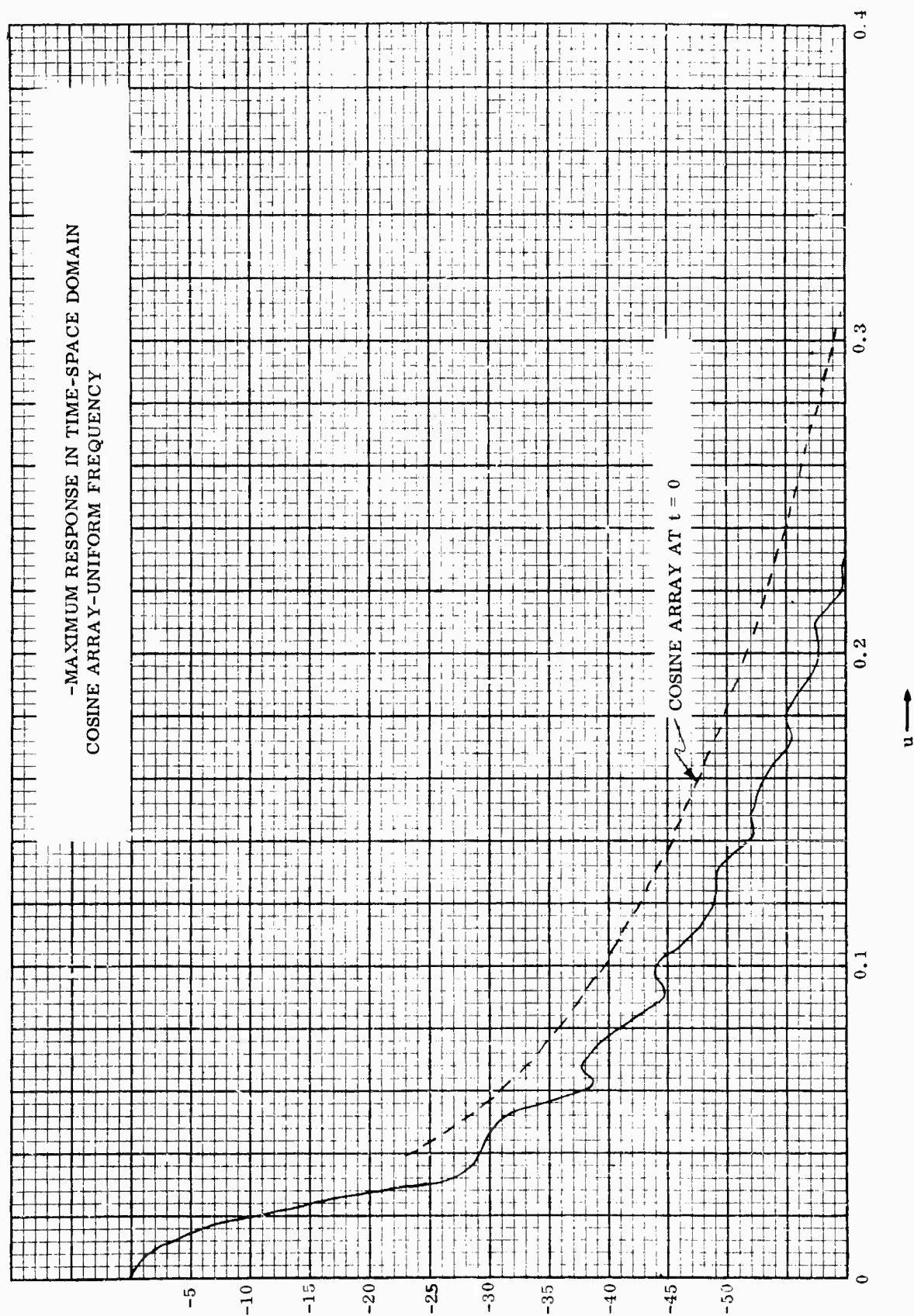


Figure 22. Maximum Response in Time-Space Domain

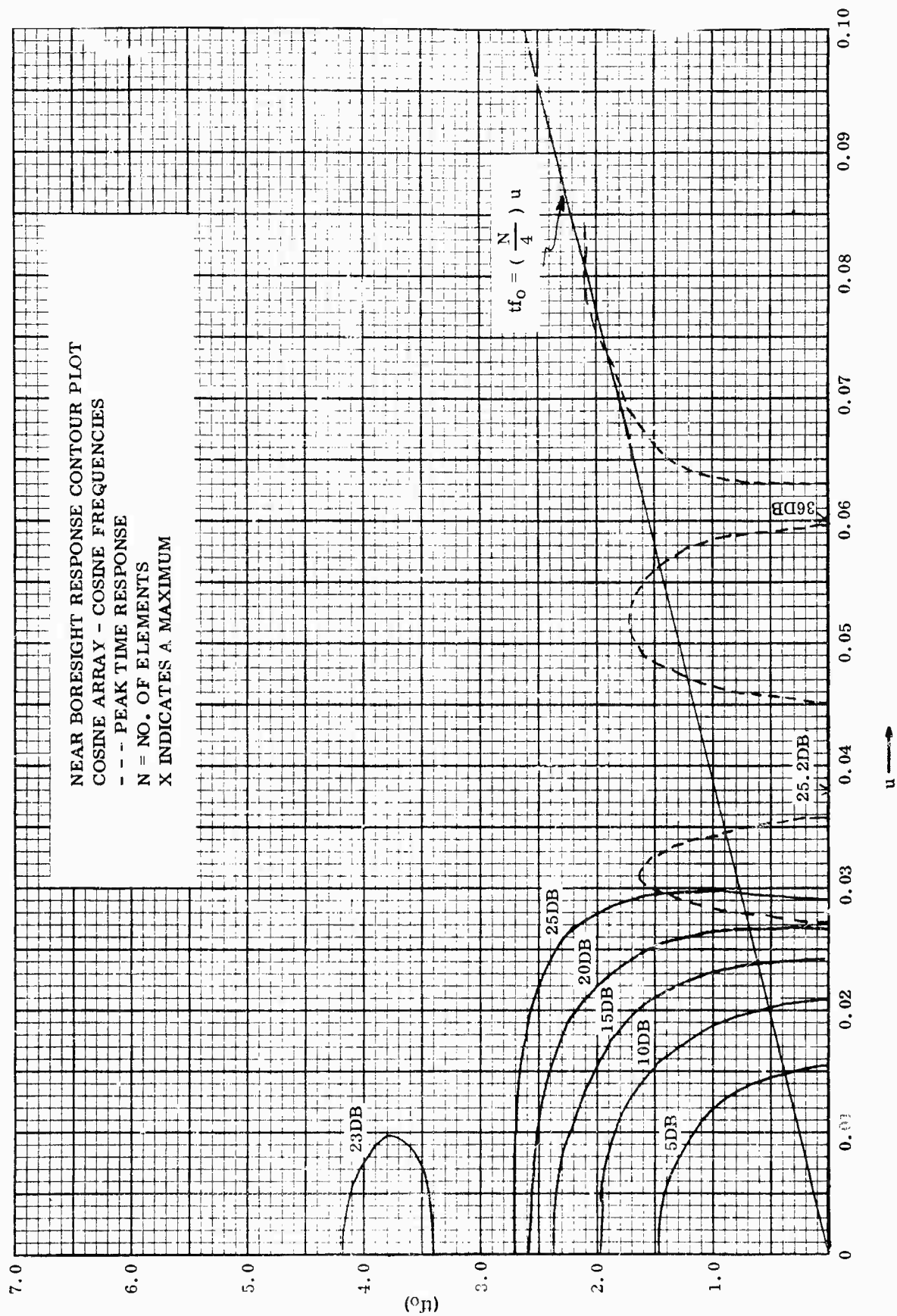


Figure 23. Near Boresight Response Contour Plot

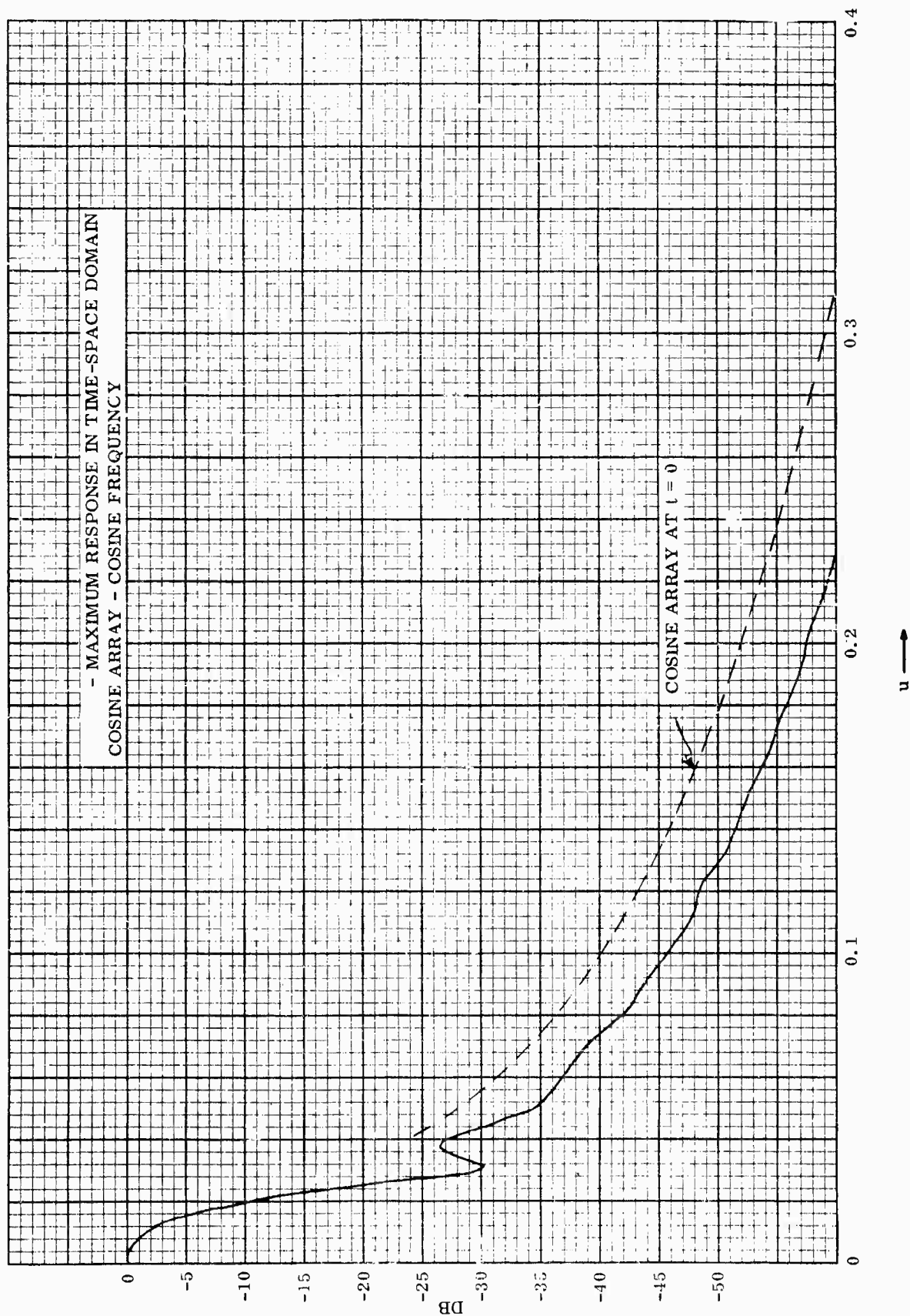


Figure 24. Maximum Response in Time-Space Domain

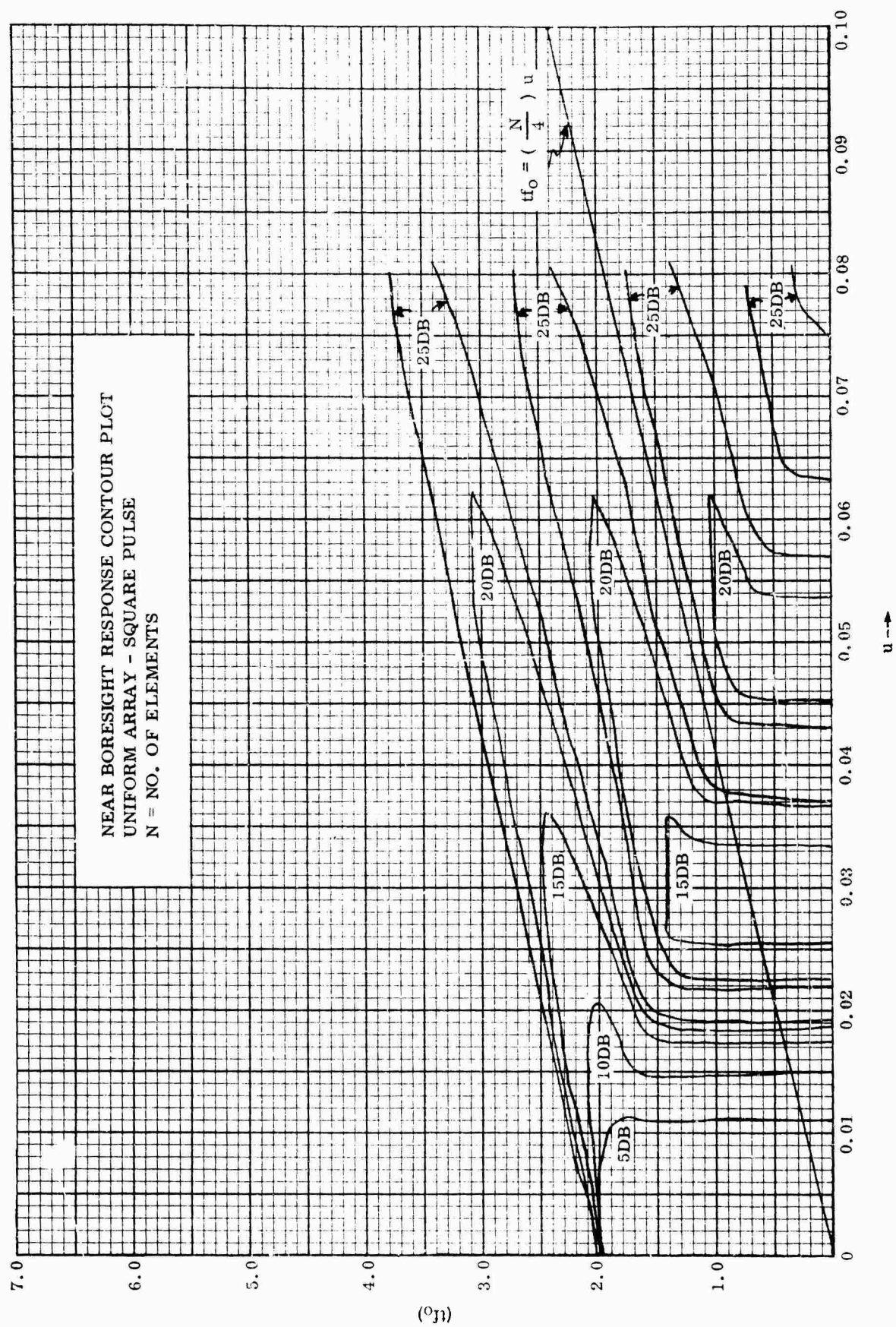


Figure 25. Near Bore-sight Response Contour Plot



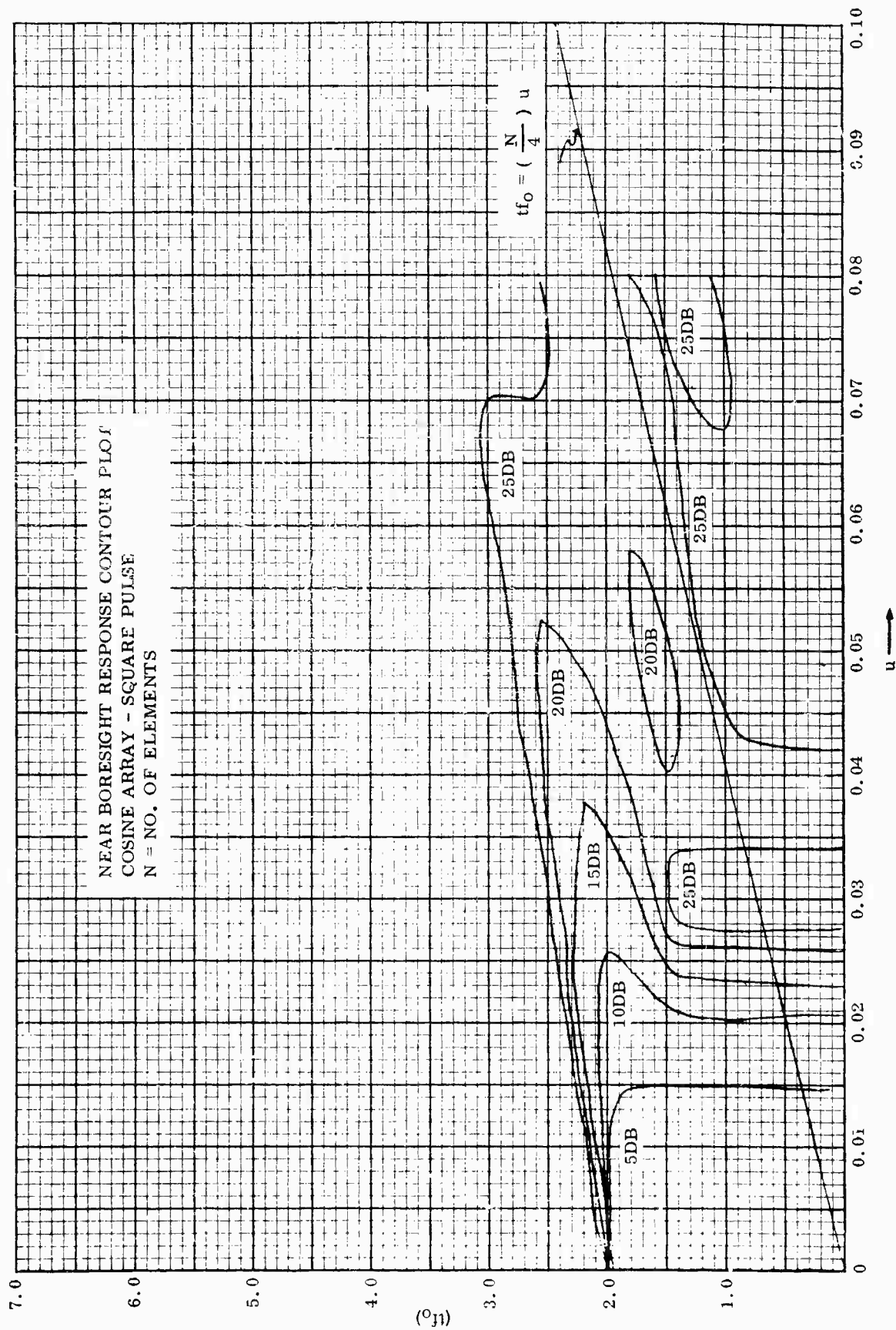


Figure 26. Near Boresight Response Contour Plot

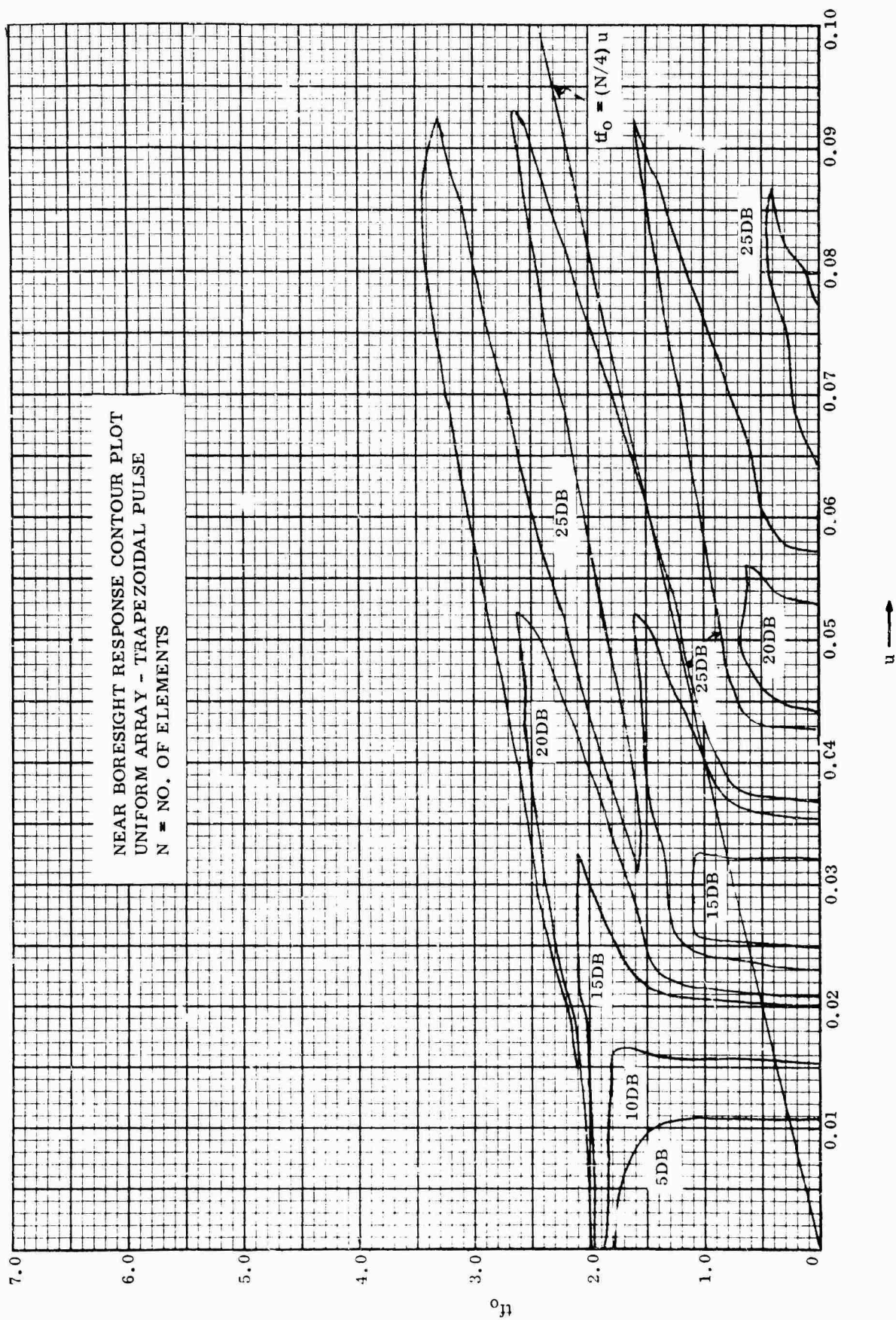


Figure 27. Near Boresight Response Contour Plot

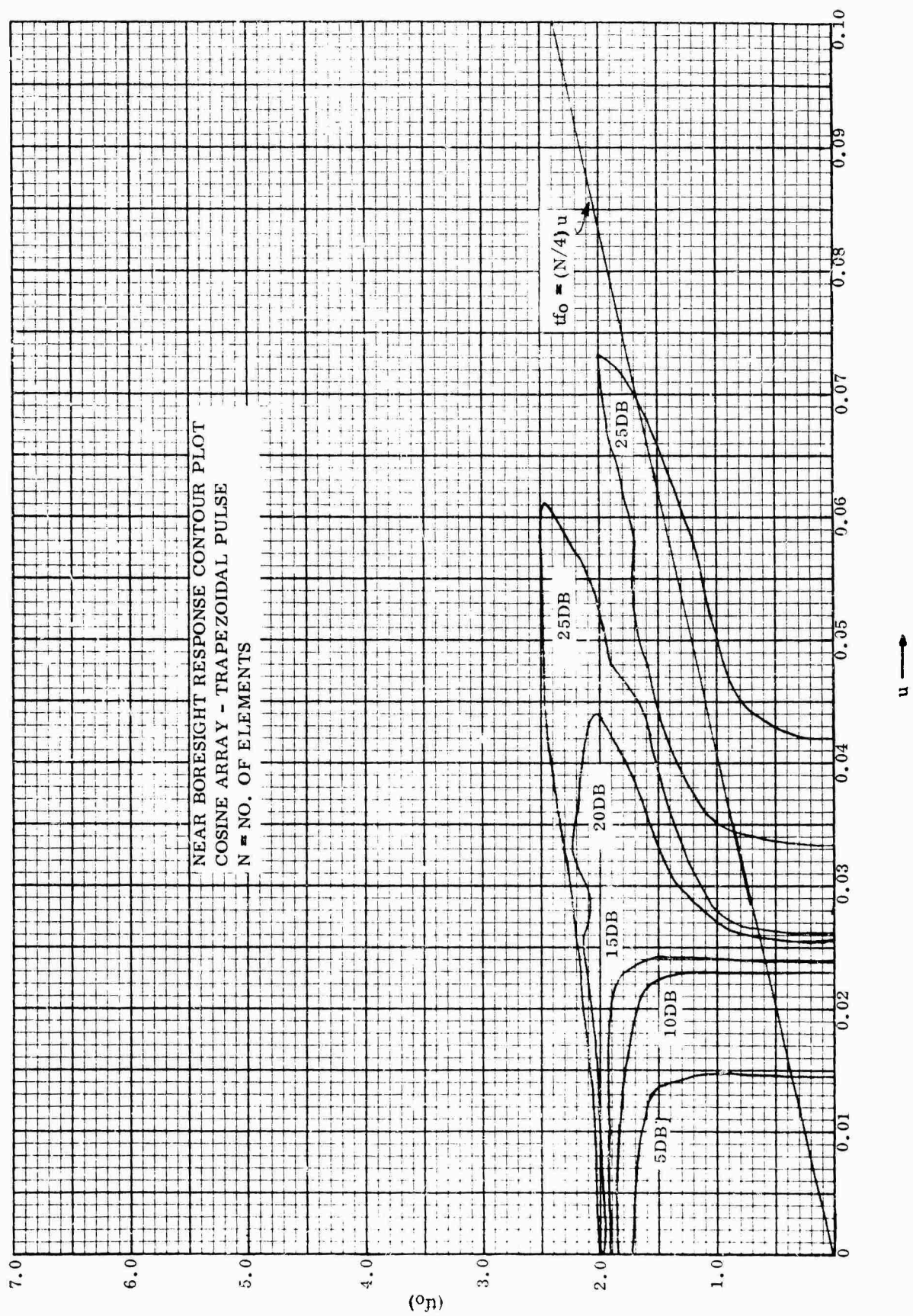


Figure 28. Near Boresight Response Contour Plot

In its general form, the cross-correlation coefficient is a function of

- a. Separation between antenna elements
- b. Antenna element pattern function
- c. Noise power distribution in space
- d. Signal power spectral density.

A discussion of the cross-correlation coefficient is contained in Appendix C. Graphical representation of the correlation coefficient is used to illustrate the effect of antenna element type, frequency bandwidth, and spatial noise distribution.

The effect of bandwidth on the array signal-to-noise ratio can be observed from its effect on the correlation coefficients. In the linear array of isotropic source elements, operating in a uniform noise environment at a single frequency, the correlation coefficient is given by

$$R(d) = \frac{\sin \frac{2\pi d}{\lambda}}{\frac{2\pi d}{\lambda}} \quad (65)$$

where  $d$  is the separation between elements.

If the single frequency restriction is removed, the correlation coefficient becomes

$$R(d) = \frac{f_o}{\frac{2\pi d \Delta f}{\lambda_o}} \left\{ S_i \left[ \frac{2\pi d}{\lambda_o} \left( 1 + \frac{\Delta f}{2f_o} \right) \right] - S_i \left[ \frac{2\pi d}{\lambda_o} \left( 1 - \frac{\Delta f}{2f_o} \right) \right] \right\} \quad (66)$$

where:

$\lambda_o$  = wavelength corresponding to the center frequency

$\Delta f$  = flat bandwidth

The effect of bandwidth on the correlation coefficient can be observed in Figure 29 where bandwidths of 25% and 50% are compared with the single frequency case (zero bandwidth).

It is shown in Section IV that, for a uniform distribution of spatial noise, optimization of the signal-to-noise ratio is synonymous with the maximization of array directivity. If the noise power is uniformly distributed over the frequency band of interest, this corollary holds for the wideband array. Therefore, the effect of bandwidth on signal-to-noise ratio can be determined by applying the correlation coefficients given by equation 66 to the conditions of maximum directivity presented in Section IV. The identity equation (Equation 29 in Section IV) which is to be minimized for maximum directivity is expressed as follows for the linear wideband array of isotropic elements with uniform noise.

$$I = \frac{f_o}{\frac{\pi \Delta f d}{\lambda_o} \left( \sum_{n=1}^N A_n \right)^2} \sum_{n=1}^N \sum_{m=1}^N \frac{A_n A_m}{(n-m)} \left\{ S_i \left[ \frac{2\pi d}{\lambda_o} \left( 1 + \frac{\Delta f}{2f_o} \right) (n-m) \right] - S_i \left[ \frac{2\pi d}{\lambda_o} \left( 1 - \frac{\Delta f}{2f_o} \right) (n-m) \right] \right\} \quad (67)$$



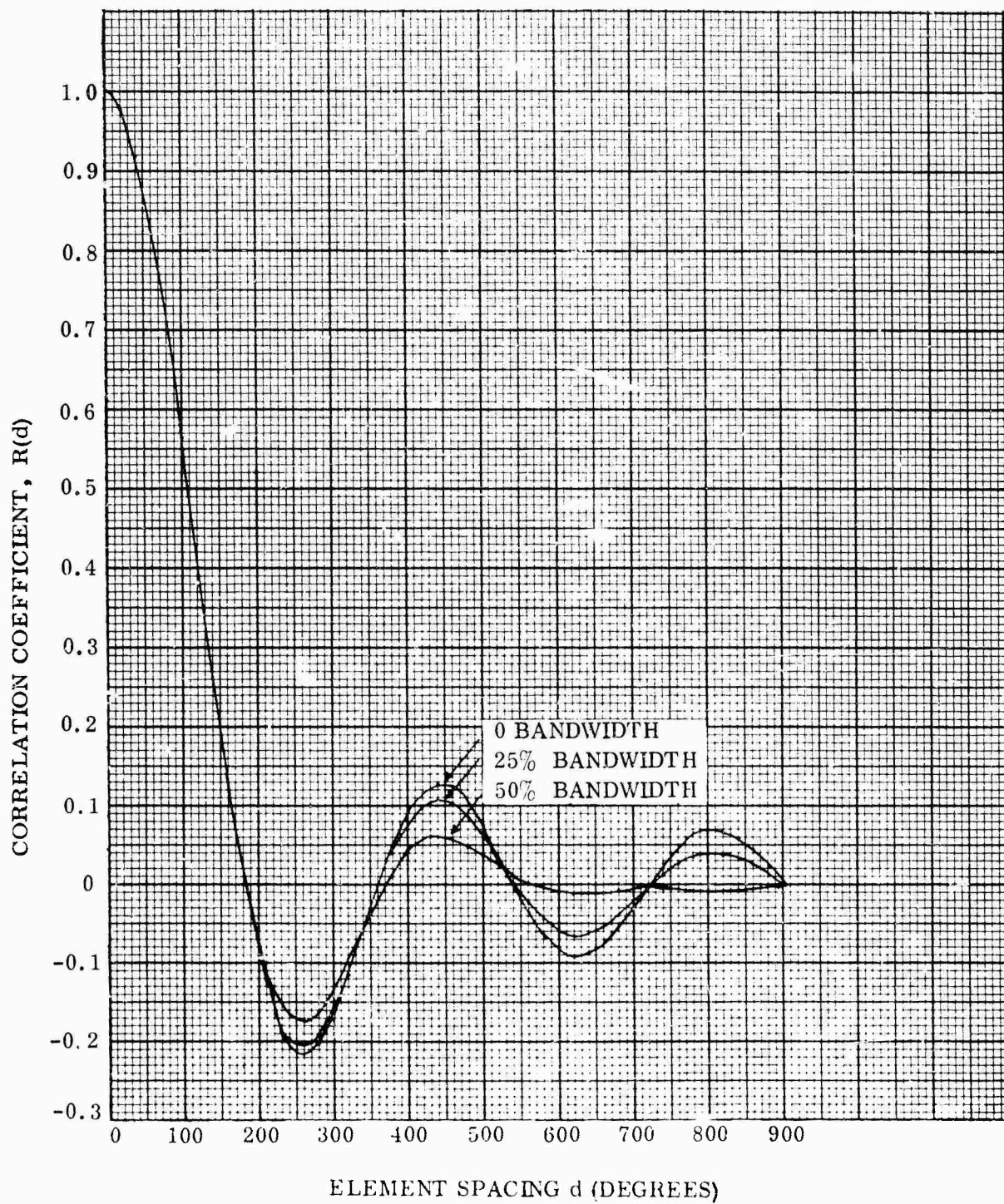


Figure 29. The Correlation Coefficient for Band-Limited White Noise

Equation 67 can be minimized by solving for the amplitude coefficients (amplitude weighting) or the spacing coefficients (density weighting) as in Section IV.

The effect of bandwidth on array directivity is illustrated in Figures 30 and 31. Figure 30 shows the optimized directivity as a function of amplitude control for bandwidths of 0, 25%, and 50%. The array consists of five elements and the equal amplitude cases are shown as dashed lines for comparison. The five element array is optimized as a function of element spacing in Figure 31 with the equal spacing case added for comparison.

The optimized directivity response curves in Figures 30 and 31 reveal several significant characteristics. It is noted that the maximum directivity is reduced as the bandwidth is increased, and the maximum directivity occurs at closer element spacing as the bandwidth is increased. The increase in array directivity available through amplitude control (Figure 30) is very slight regardless of element spacing, while the optimized element spacing (Figure 31) provides a considerable increase for large element spacing. This effect is the result of spurious lobe suppression which is obtained as a by-product in the optimized element spacing case.

Since amplitude weighting and element spacing are variables in the optimization of array directivity in the wideband case, it is conceivable to utilize both variables simultaneously. An example of this condition is presented in Table 5. The conditions for this computation are:

- a. Five element array
- b. Broad side fixed beam
- c. Isotropic antenna elements
- d. No mutual coupling between elements
- e. Uniform noise over bandwidth and space
- f. No internal uncorrelated noise
- g. Conjugate matched flat receiver response

Corresponding to Figures 30 and 31, it is noted that as the bandwidth is increased the total length of the optimized array is significantly reduced. While the element spacing varies considerably, the amplitude weighting is very nearly uniform. From the above examples, it can be concluded that

- a. Increased bandwidth decreases the maximum signal-to-noise ratio in an array.
- b. Optimum performance exceeds the uniform amplitude and uniform spacing case only slightly, except at large element spacing.
- c. Optimized performance is achieved with less aperture as the frequency band increases.

### 3. SPACE - FREQUENCY EQUIVALENCE

In the wideband array, a relationship exists between element spacing and bandwidth which can be used as a design parameter. This concept was originally proposed by Kock and Stone, Reference (21), and later adapted to wideband arrays by Dausin, et.al, Reference (22). The application of space frequency equivalence is illustrated in Figure 32.

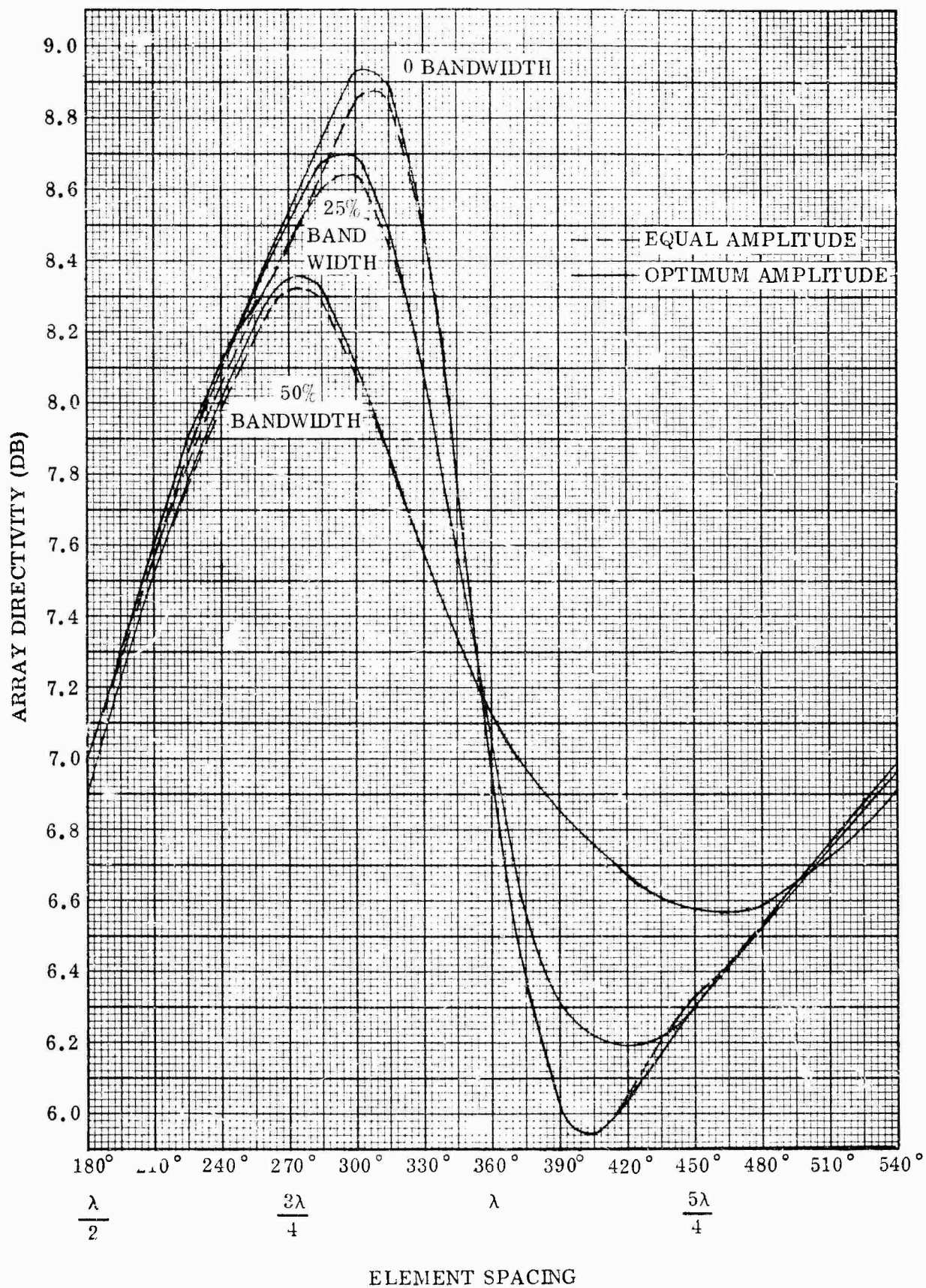


Figure 30. Maximized Antenna Directivity by Amplitude Control

TABLE 5 . MAXIMUM ANTENNA DIRECTIVITY BY AMPLITUDE CONTROL, ELEMENT SPACING, AND ARRAY LENGTH

Noise Bandwidth (%)	0		10		25		50	
Maximum Directivity (DB)	8 967		8.917		8.730		8.366	
Optimum Array Length (DEG)	1214		1206		1168		1096	
Element No. 1 Element No. 2 Element No. 3 Element No. 4 Element No. 5	Spacing	Amplitude	Spacing	Amplitude	Spacing	Amplitude	Spacing	Amplitude
	-607.0	.9042	-603.0	.9015	-584.0	.8980	-548.0	.9111
	-311.8	1.0558	-310.1	1.0572	-300.7	1.0593	-278.0	1.0595
	0	1.0808	0	1.0834	0	1.0862	0	1.0604
	311.8	1.0558	310.1	1.0572	300.7	1.0593	278.0	1.0595
	607.0	.9042	603.0	.9015	584.0	.8980	548.0	.9111



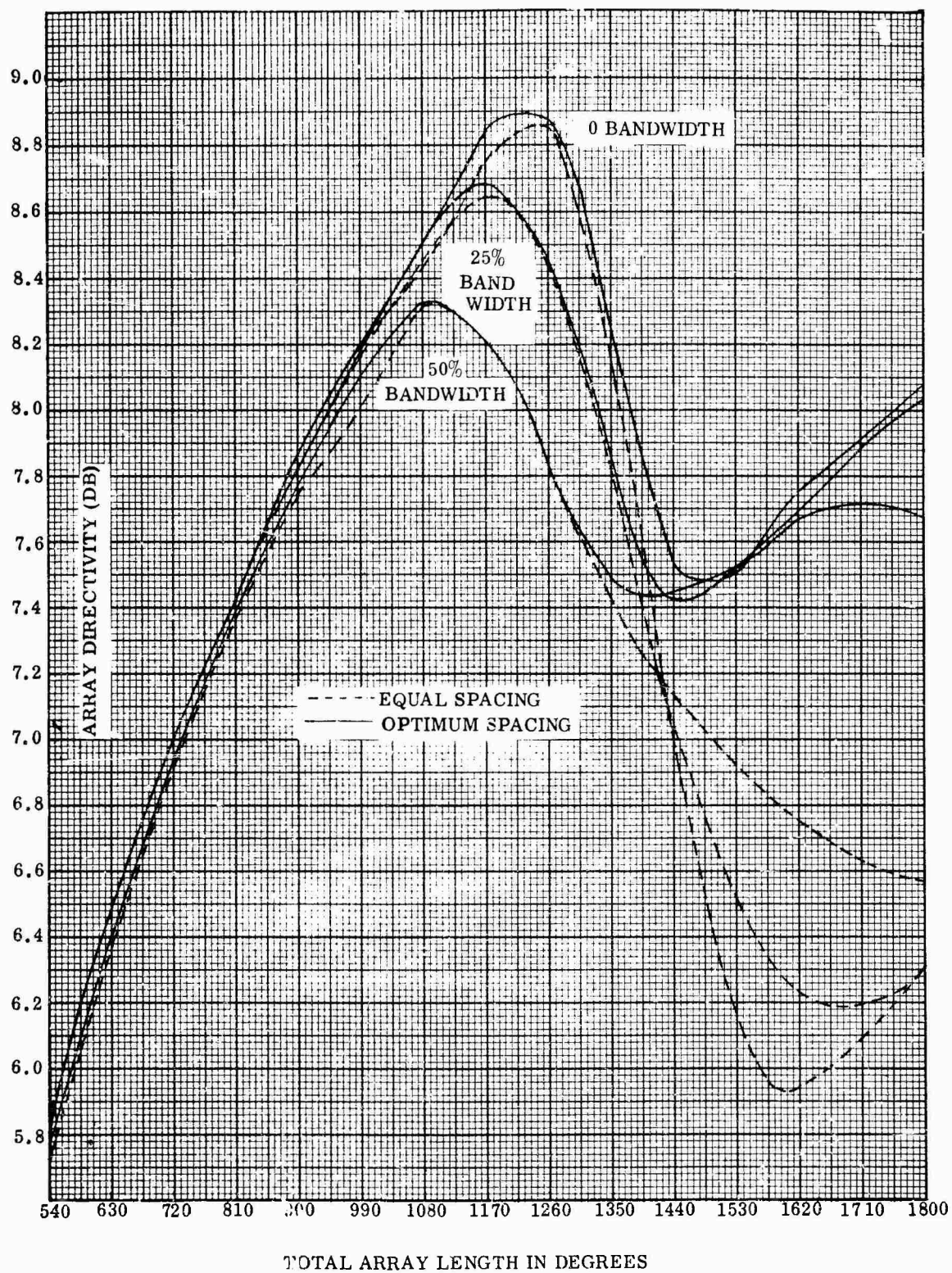


Figure 31. Maximized Antenna Directivity by Element Spacing

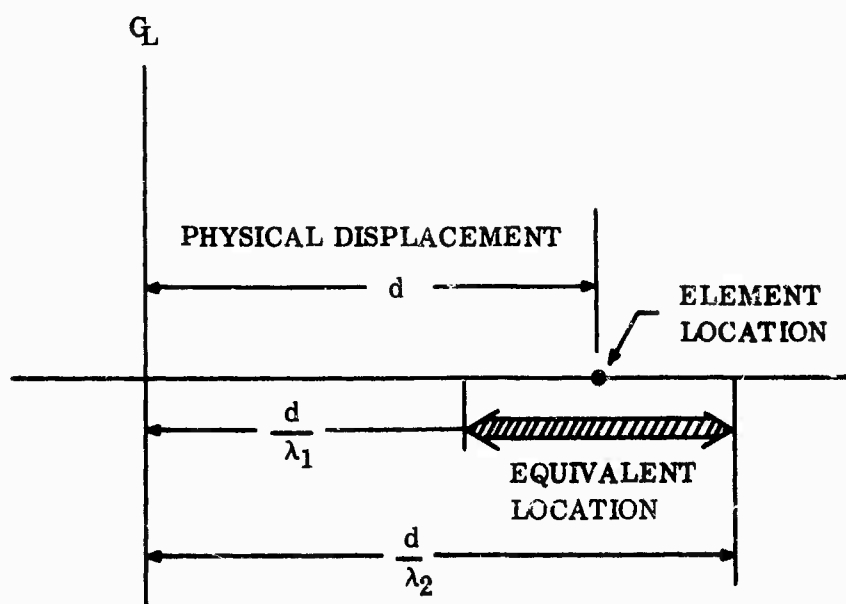


Figure 32. Space-Frequency Equivalence

The location of any array element, relative to the center line of the array, when measured in wavelengths, is a function of frequency. For a given physical location, the element is a greater number of wavelengths removed at a higher frequency ( $\lambda_2$  in Figure 32) than at a lower frequency ( $\lambda_1$ ). In the wideband array, this variation in effective displacement is referred to as the equivalent location. It is noted that as the physical displacement of the element increases, with respect to the array centerline, the equivalent location also increases.

The utilization of this concept in the design of wideband arrays is dependent on the ultimate array application. To illustrate the design procedure, consider an array with an overall aperture of approximately  $50\lambda_0$ , which is to be excited with 25 spectral frequency components separated by  $0.01 f_0$  for a total bandwidth of 25 percent.

As a first attempt at evaluating the space-frequency equivalent array, the elements are arranged so that the equivalent locations just touch but do not overlap. For the elements near the array center, the equivalent locations cannot touch, therefore these elements are left in their  $\lambda_0/2$  locations. The resulting array contains a total of thirty elements. The computed radiation pattern (at  $t = 0$ ) is shown in Figure 33 along with the pattern of the same array operating at a single frequency  $f_0$ . Since complete evaluation of any wideband array must include time as well as space variations, the time response for several values of  $u$  is shown in Figure 34.

Although the space-frequency equivalence has the effect of lowering the sidelobes in the far-out region, the smearing effect shown in Figure 33 is not desirable for the purpose of producing a well-defined major lobe.

It is noted that in the thirty element array, the first six elements on either side of the center line remain on the nominal  $\lambda_0/2$  spacing. In Section III, a space taper procedure is described wherein the sidelobes near the major lobe can be reduced through incremental element spacing. Applying this principle to the center twelve elements of the thirty element array produces the patterns shown in Figures 35 and 36. It is noticed that a relatively uniform sidelobe level is maintained over the entire range of angle shown.

The purpose of the above example is to illustrate the combination of array design techniques and the latitude of control available where the variables are not confined. Confinement of these variables is dependent on application, but it is felt that the combination of design techniques can be effectively used in many practical applications.

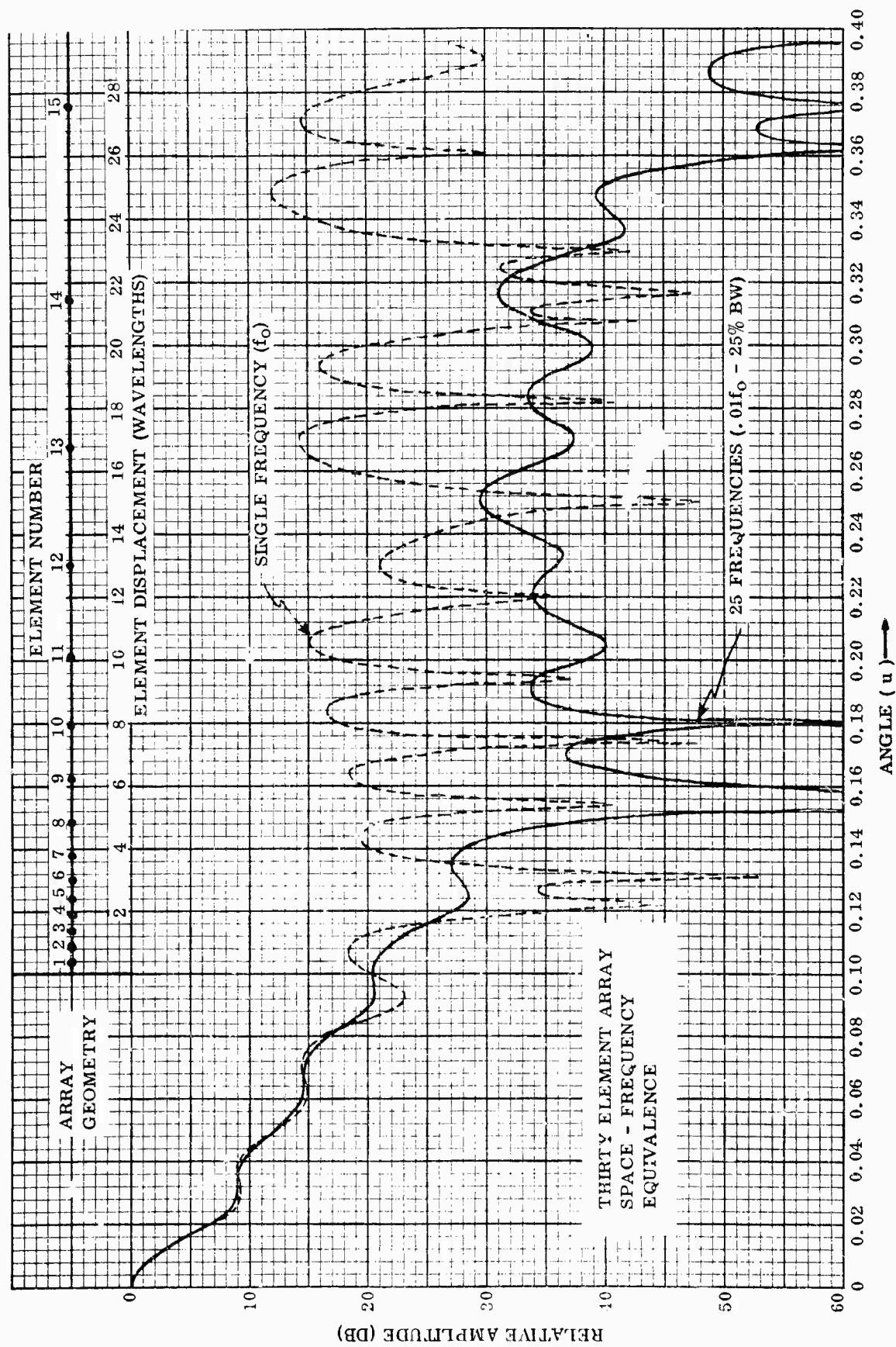


Figure 33. Thirty Element Array Space-Frequency Equivalence

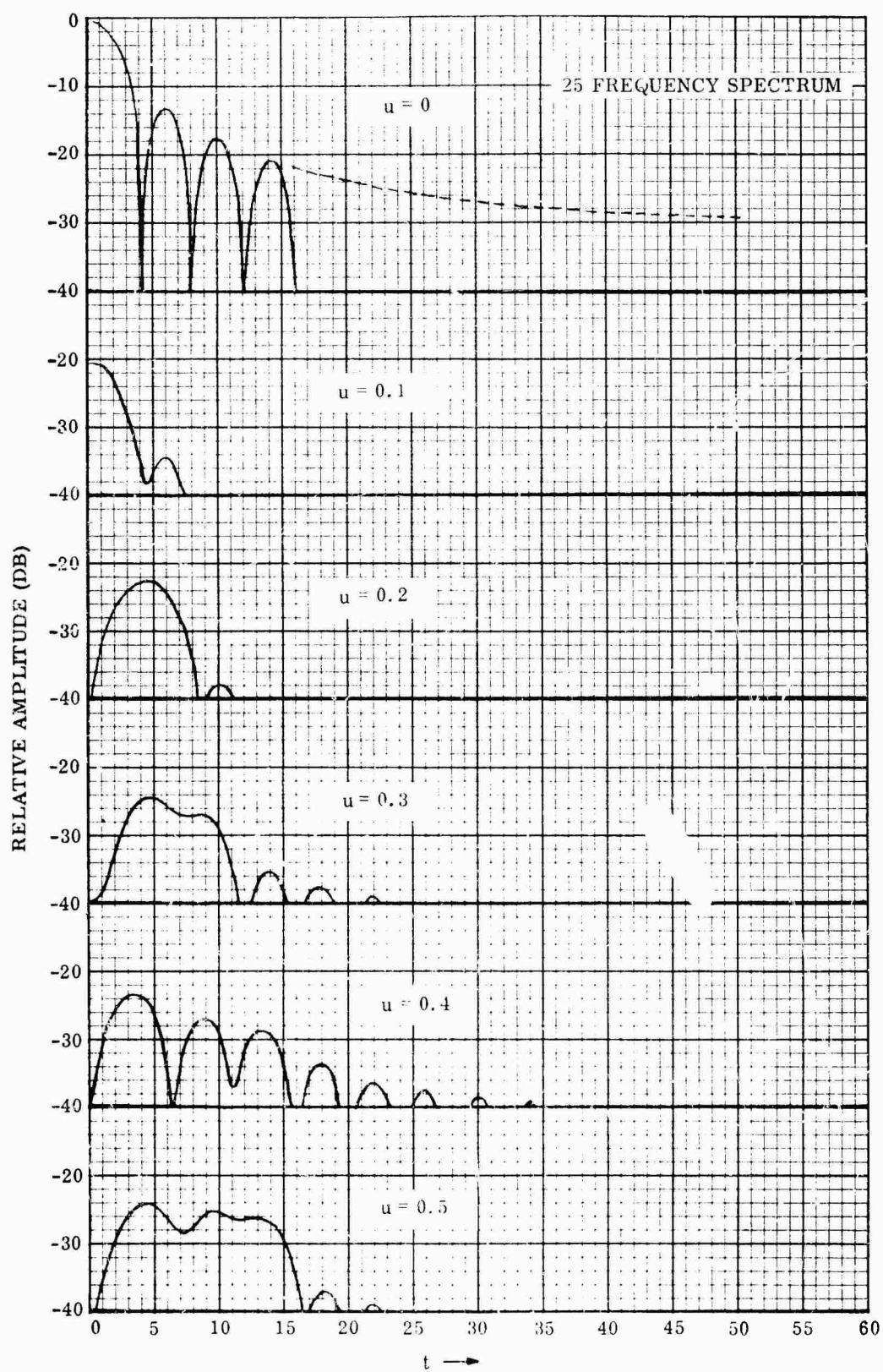


Figure 34. Time Response of Thirty Element Array



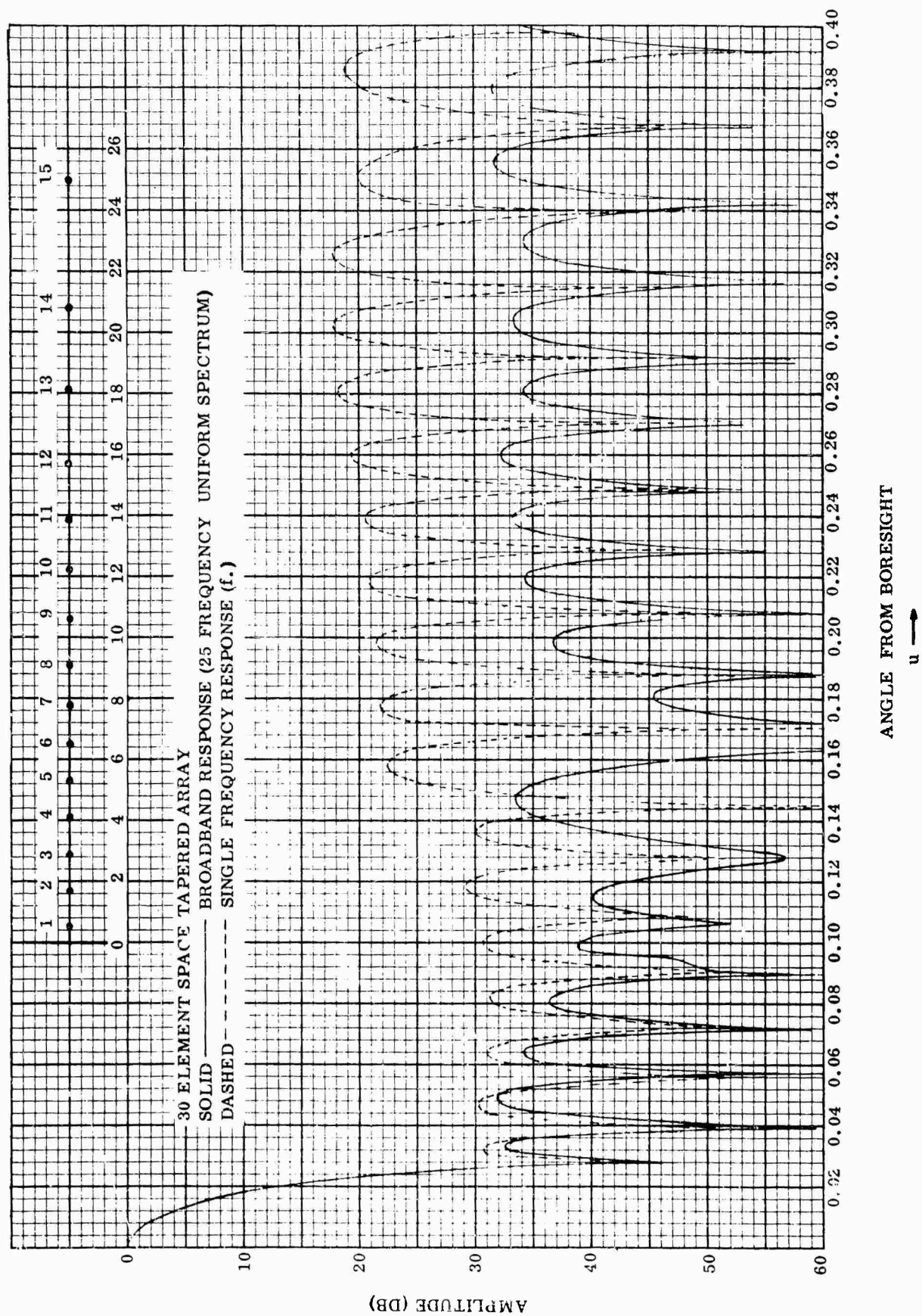


Figure 35. Thirty Element Space Tapered Array



## SECTION VI

### APPLICATIONS

In the preceding sections, the effects of array geometry, signal allocation, frequency bandwidth, and noise distribution on the response of a linear array are discussed in detail. This investigation has revealed several array characteristics which could be applied to enhance the performance of particular systems utilizing array antennas. Several design and functional concepts of application are discussed in this section. These are not intended to be complete, but rather indicative of the manner in which the observed effects may be used to complement other system requirements. In addition to the applications relating to linear arrays, examples are provided which illustrate the effect, on signal-to-noise ratio, of applying the principals to two dimensional planar arrays.

#### 1. SIGNAL-TO-NOISE RATIO IN DIRECTIVE ARRAYS

In Section IV it is shown that the signal-to-noise ratio is directly related to array directivity in a uniform noise environment. It is further shown (see Figure 42) that the array directivity is a function of the number of elements employed and the spacing between them. As the elements become closely spaced (less than  $\lambda/2$ ) an increase in directivity (super-gain) is possible through critical control of the element amplitudes. Although this does not represent a true increase in array gain, it can represent an increase in signal-to-noise ratio since the array is more directive, thereby discriminating against its noise environment.

If a particular application can utilize the increased directivity in the array pattern, and the demand for additional elements can be tolerated, then an increase in signal-to-noise ratio can be obtained which is consistent with the stability, noise figure, and bandwidth of the weighting components. For example, a super directive array could be considered in a radio astronomy application where the array is required to receive only, and noise and directivity are of paramount importance. Low noise amplifiers in a controlled environment would be required to establish the critical weighting function.

#### 2. SPECTRAL OR WAVEFORM DETECTION

It is shown in Section IV that the time response of a wideband array is a function of the angle of observation with respect to the beam maximum. It follows therefore, that the observed waveform and its associated spectral content are also dependent on the observation angle. The only angle at which the impressed spectrum or waveform can be observed is boresight, since the angular position of the beam maximum is not a function of frequency.

The spectral response which is observed at any angle other than boresight is simply the antenna response to each of the spectral components. This can be computed for any regular array by considering the spectral components of the impressed signal separately in determining the array response as a function of the angle. The angular spectrum is then constructed by picking the response at a particular angle for each of the components comprising the total spectrum.



Since the impressed waveform and its associated spectrum are accurately reproduced only in the major lobe, it appears that using the impressed waveform as a reference, a means of major lobe identification can be established. As an example, consider the pulsed transmitter excitation of a uniform array depicted in Figure 37. The boresight response is shown to be a replica of the impressed signal while the sidelobe response is distorted. To be exact, it must be stated that the input is accurately reproduced only in the center of the major lobe, but for practical purposes, the shape is well maintained within the half-power angle.

In a one-way propagation path the transmitted signal would be collected by a receiving antenna and processed in a receiver circuit to yield the desired output. This processing might take the form illustrated in Figure 38 wherein the received signal is amplified and passed through a filter of special design. If the filter is a matched filter, Reference (23) i.e. a conjugate network, maximum output can only be obtained in the boresight region. The filter will discriminate against the distorted waveform in the sidelobe region thereby reducing the effect of sidelobe radiation. The filter can be matched to the total waveform, or discrimination can be achieved on a spectral basis, by matching to the specific frequency components.

An alternate form of the detection technique is shown in Figure 39. A sample of the received signal is processed on a parallel basis and used to control a switch which completely isolates the receiver when the incoming wave does not match the known transmitter function. There are two characteristics of parallel signal processing which may be advantageous to some systems. When the switch is activated to the off position, complete suppression of the undesired radiation is obtained rather than a reduction resulting from the filtering action. The parallel processing also permits the received signal to be transferred directly to the receiver without modification by the filter which may be desirable in some applications.

The spectral detection technique, as herein described, presupposes that, (1) the spectrum of the transmitted waveform is known, and (2) that it does not vary. If the former is true but not the latter, an adaptive filter could be employed which is adjusted to variations in the transmitter spectrum.

In application, the two way path of a radar system might be considered. A replica of the transmitted spectrum is always available. If the radar utilizes a pulsed transmitter, the spectrum of the output is essentially constant being determined by the pulse characteristics and system bandwidth. If the target is assumed to approximate a point target, the received signal spectrum will be essentially that transmitted with reduced amplitude. The spectral detection technique could then be employed to reduce the spurious response of sidelobe and gating lobe radiation.

In essence, the processing of the signal spectrum in this manner is a self referencing sidelobe cancellation technique. The assumption which would limit its usefulness in a practical radar application is the point target requirement. Most radar targets are not point targets or even symmetrical targets, therefore, the observed spectrum of the returned signal is not identical to that transmitted. A probability criterion could be established for specific targets but the effectiveness of the detection scheme would be reduced with the possibility of lost targets.

### 3. SECURE COMMUNICATIONS

An adaptation of the spectral detection technique might be employed to secure a communications link in which coded information is to be relayed. This application,

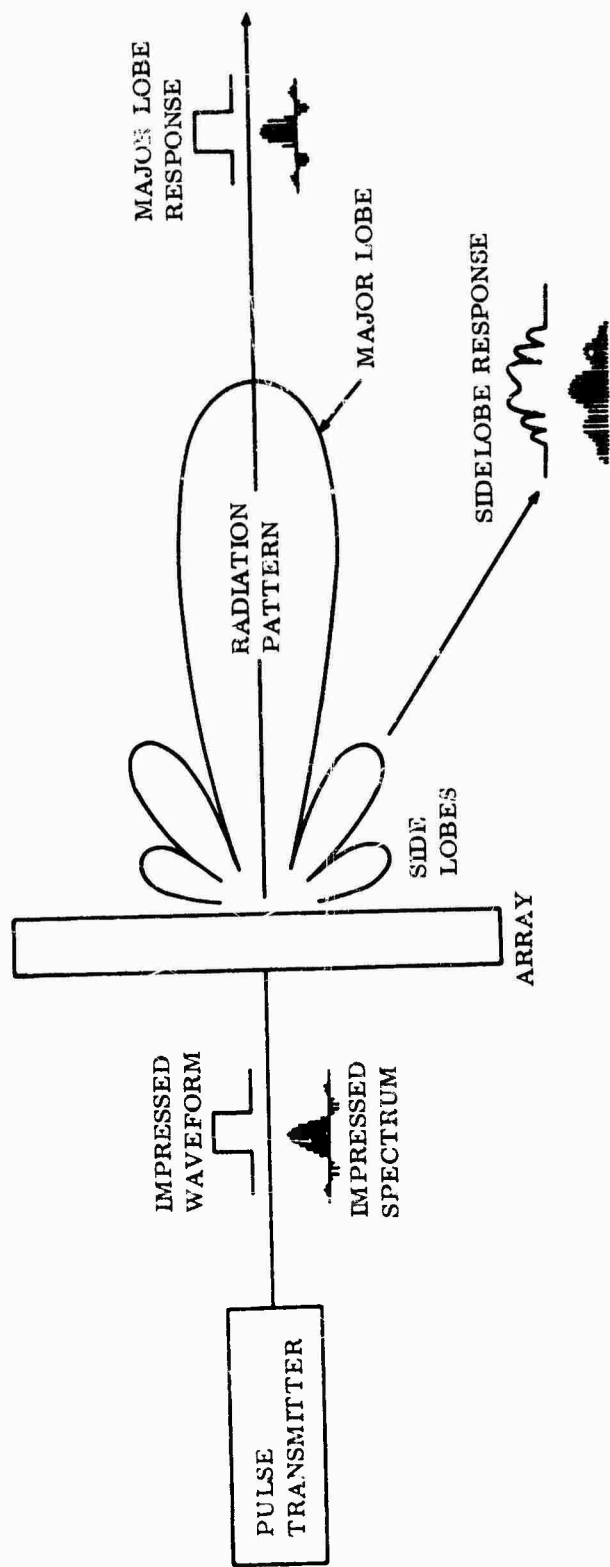


Figure 37. Transmitted Waveform and Spectrum

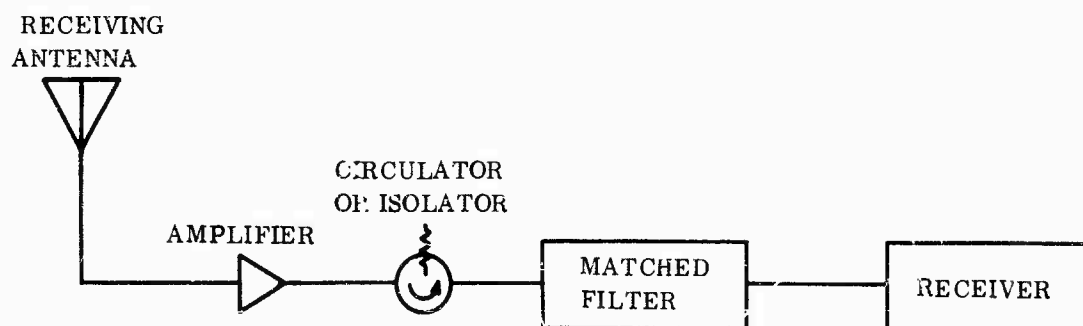


Figure 38. Direct Signal Processing

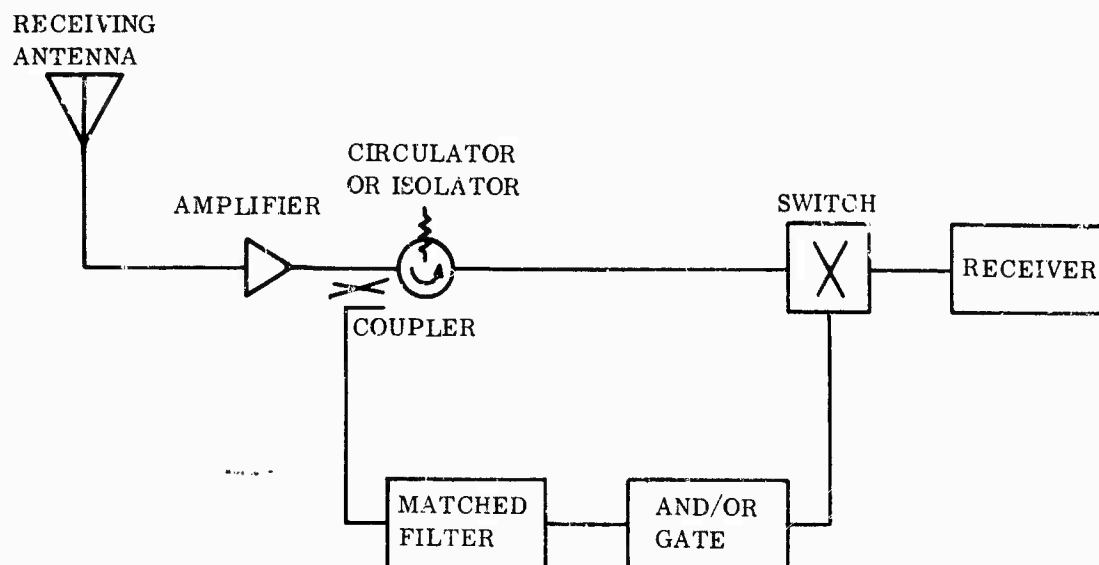


Figure 39. Parallel Signal Processing

like the detection concept, is based on the fact that waveform distortion occurs in the far field of the array for all angles displaced from the major lobe.

Assuming, for example, that the information to be transmitted is in the form of short pulses, the pulse train could be developed to produce a highly distorted response in the sidelobe region. The degree of distortion is dependent on the total bandwidth required for transmission, the shape of the pulses, the separation between pulses, and the characteristics of the array.

#### 4. ADAPTATION IN A NON-UNIFORM NOISE ENVIRONMENT

One of the conditions assumed in the study of signal-to-noise optimization is uniform noise distribution over all space. It has been shown that with this confinement, optimum signal-to-noise ratio occurs for near uniform weighting and equal element spacing of approximately 300 degrees in the narrow band case. It is well known that uniform noise is not a practical noise model, even in the "window" which occurs between cosmic noise and molecular absorption (1 GHz to 10 GHz).

Although the definition of a practical noise model is beyond the scope of this project, it is of interest to determine the behavior of the optimization process in a specified non-uniform environment. To illustrate a possible adaptive control technique, three non-uniform noise models are considered as examples.

- a. Uniform noise with a 20 DB increase in the overall sidelobe region.
- b. Uniform noise with a 20 DB increase applied only in the far out sidelobe region.
- c. Uniform noise with a 10 DB increase in the major lobe and near sidelobe region.

The signal-to-noise ratio is optimized for each of the assumed models through amplitude control. The resulting radiation patterns are shown in Figures 40 through 42. It is noted that the optimized radiation pattern is severely modified by the noise environment. The signal-to-noise ratio with increased sidelobe noise is optimized by maintaining a low sidelobe level (Figure 40). When the increase in noise is confined to the far out sidelobes (Figure 41), the close in lobes rise. When the noise is increased in the region of the major lobe (Figure 42), high uniform sidelobes are characteristic of the optimized pattern.

This variation in radiation pattern, as a given array is optimized for maximum signal-to-noise ratio in different noise environments, suggests the possibility of adapting an array to its noise environment by amplitude weighting of the antenna elements.

The concept of noise adaptation could be implemented in a number of ways. Consider, for example, a scanning receiver array (mechanical, or electronic) with a variable gain amplifier on each antenna element. With the gain of each amplifier constant (uniform illumination) the array could be scanned to determine the local noise environment. The gain of the element amplifiers could then be adjusted for maximum signal-to-noise ratio as described above. This process could be up-dated at any time to account for changes in the environment such as, antenna orientation, atmospheric changes, or the presence of ECM equipment.

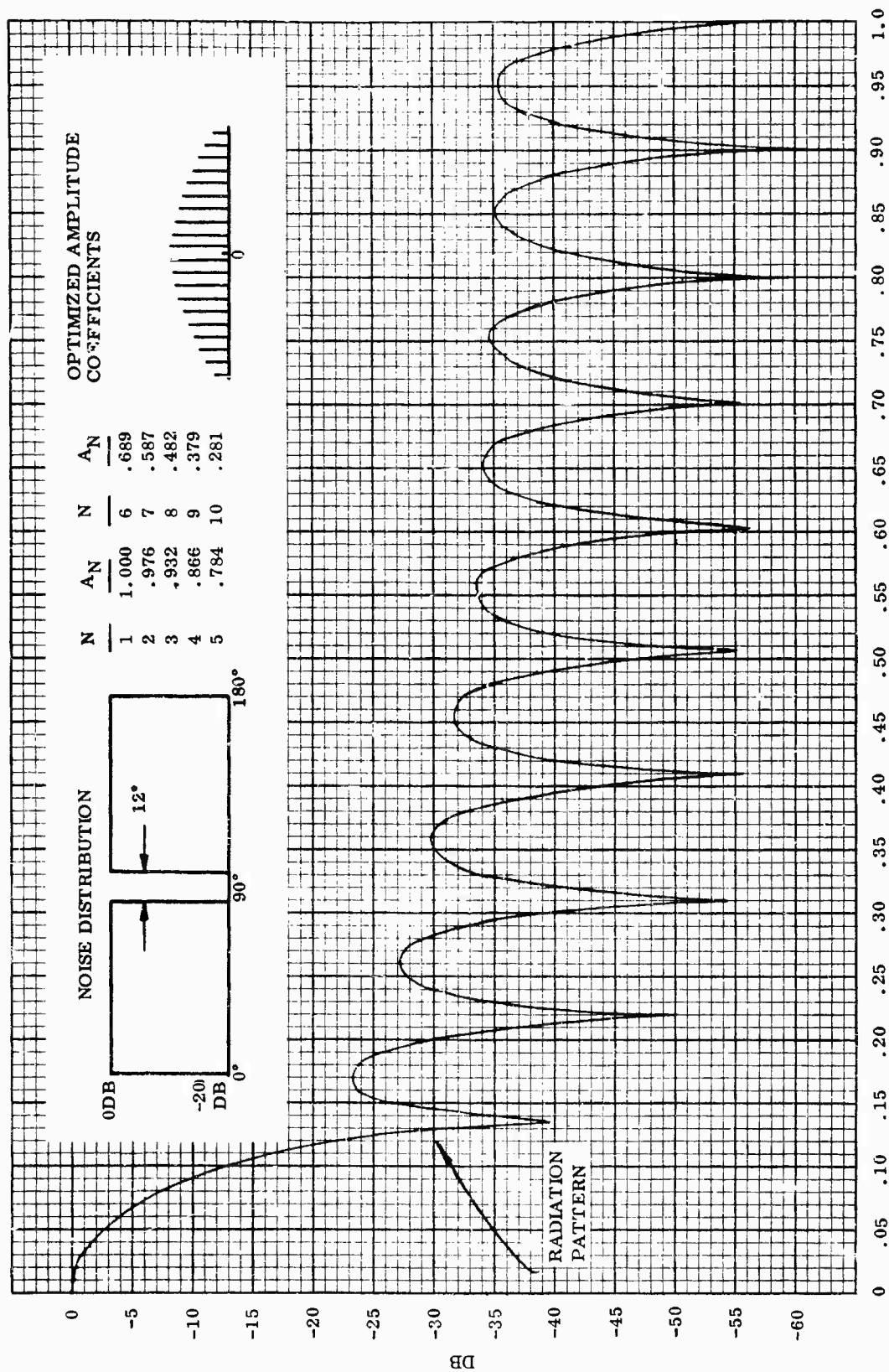


Figure 40. Optimized

Figure 40. Optimized S/N for a 20 DB Noise Increase in the Sidelobe Region

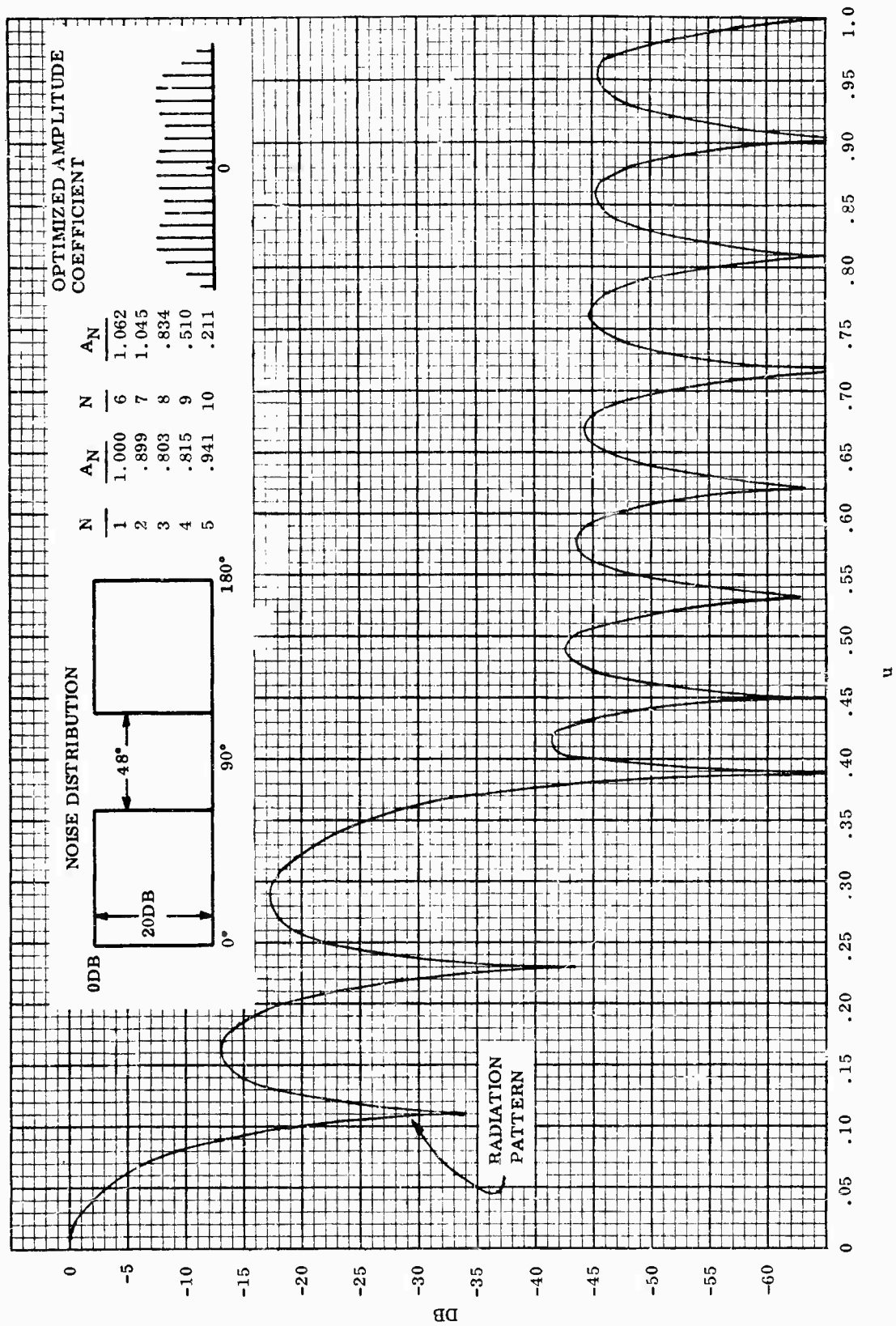


Figure 41. Optimized S/N for a 20 DB Noise Increase in the Far-out Sidelobe Region

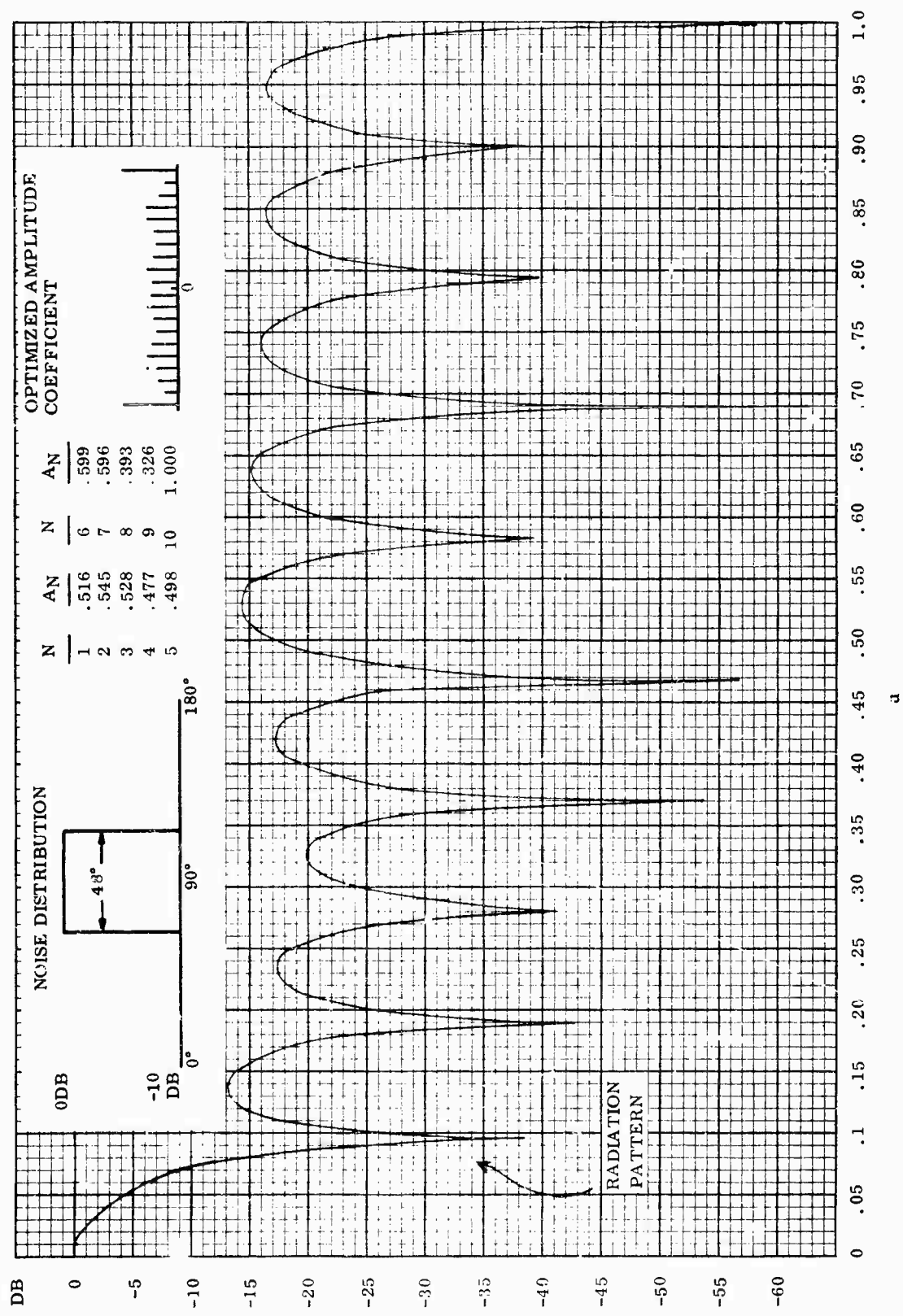


Figure 42. Optimized S/N for a 10 DB Noise Increase Near Boresight

## 5. APPLICATION TO PLANAR ARRAYS

The primary area of investigation in this study is the linear array. A two dimensional extension of the generalized cross-correlation coefficient (Appendix C) indicates that the conditions for optimizing the planar are of the same form as those encountered in the analysis of the linear array. The complicating factor in the planar array analysis, is the two dimensional element spacing factor which permits the array to assume an unconfined geometrical form. For comparison, two common element arrangements are considered: (1) square spacing and (2) triangular spacing. The optimized directivity (S/N in the uniform noise environment) is shown in Figure 43 for the narrow frequency band and in Figure 44 for a 50 percent bandwidth. In each case, the planar array is comprised of 25 equal amplitude elements.

The results of the planar array closely parallel those obtained for the linear array (See Figures 30 and 31). It is noted that while maximum directivity is obtained with square element spacing, the triangular spacing produces higher directivity for closely spaced elements. This brief investigation illustrates that the techniques developed for the optimization of signal-to-noise ratio in linear arrays apply also to the planar array although the computational procedure is more complex.



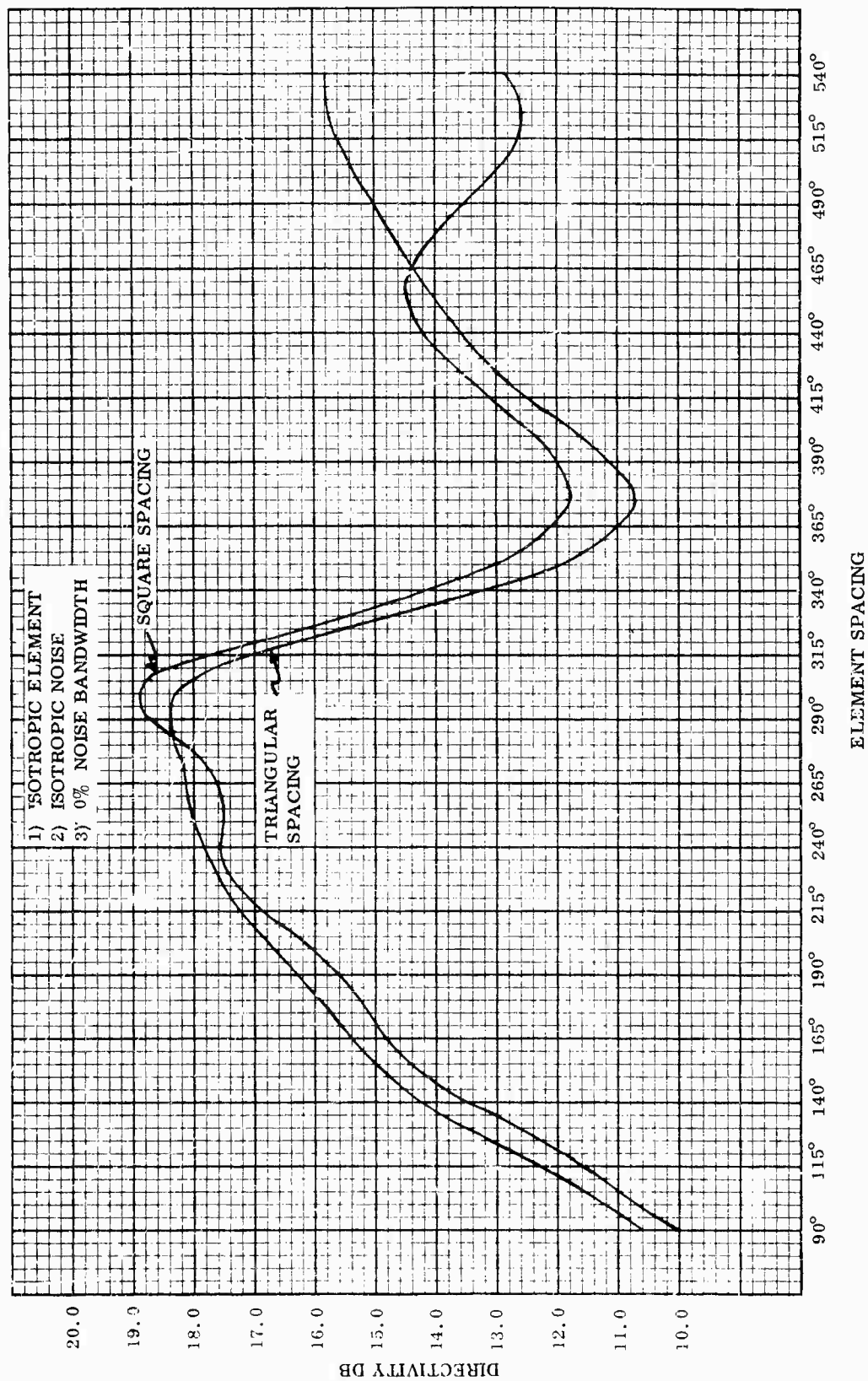


Figure 43. Optimized Planar Array -- Narrow Band

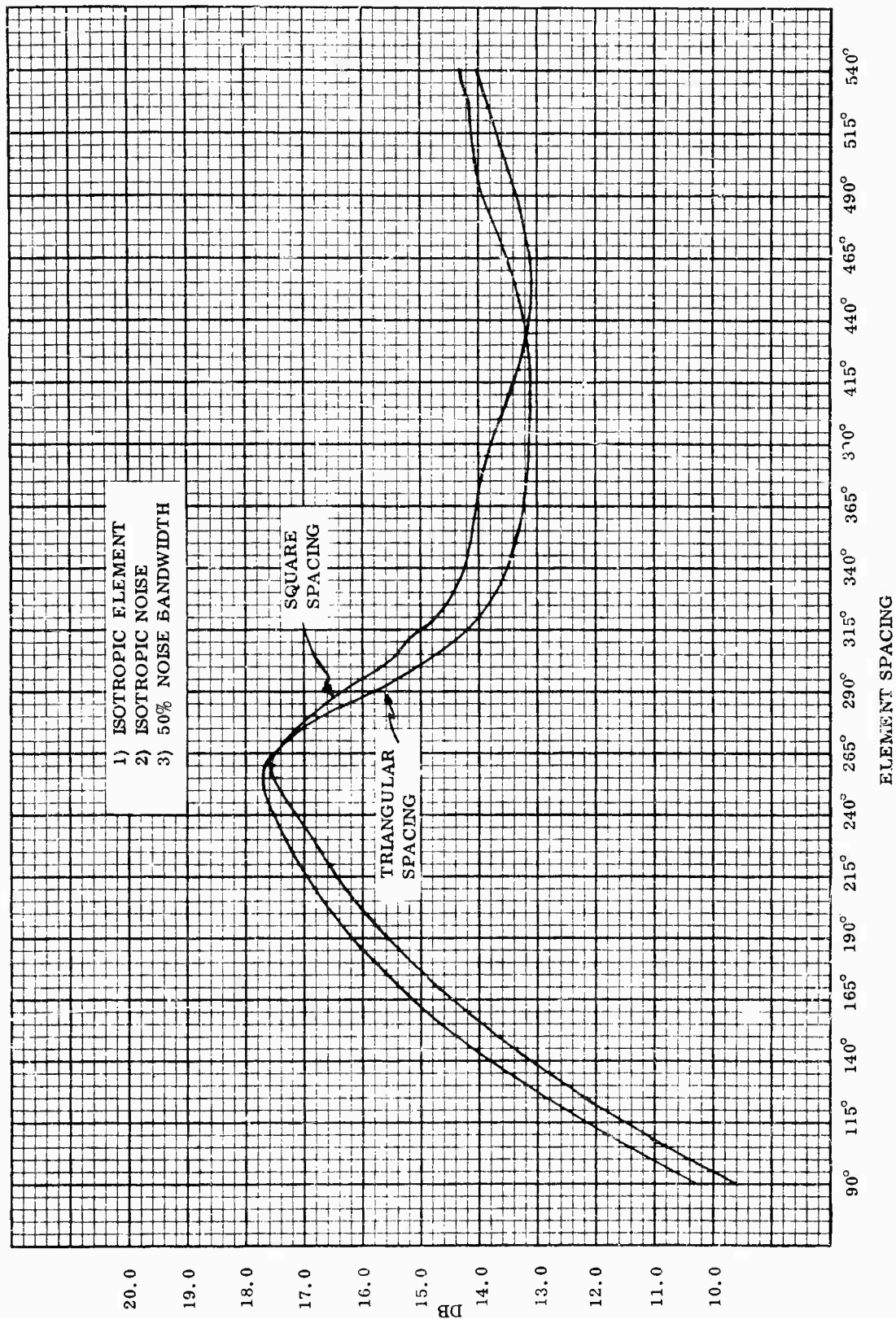


Figure 44. Optimized Planar Array - Wideband

## SECTION VII

### COMPUTATIONAL TECHNIQUES

During the course of investigation covered by this report, several significant mathematical techniques evolved, which are described in this section. Each technique is described qualitatively; the details of analysis of the various methods appear in the appendix. Examples are included where appropriate.

#### 1. A METHOD FOR CONTROLLING PATTERN SIDELobe LEVEL THROUGH SPACE AND AMPLITUDE TAPERING

This method evolved from a method by Harrington, Reference (24). Basically, the method is an iterative technique using the finite difference approach. It was originally intended to be applied to space tapered arrays, but during the development of the method, it became clear that the technique is general and therefore is applicable to amplitude tapered arrays.

The normalized far field pattern, for an array of  $2N$  elements equally spaced is given by,

$$E(u) = \frac{1}{N} \sum_{n=1}^N A_n \cos [(n-0.5)\pi u] \quad (68)$$

where

$$u = \frac{2d}{\lambda} (\sin \theta - \sin \theta_o)$$

$d$  = is the element spacing

$\lambda$  = is the wavelength at the operating frequency

$\theta$  = is the observation angle from boresight

$\theta_c$  = is the array steering angle

$A_n$  = is the amplitude of the  $n^{\text{th}}$  element

Applying finite differences to both sides of equation 68

$$\Delta E = \frac{1}{N} \sum_{n=1}^N \Delta A_n \cos [(n-0.5)\pi u] \quad (69)$$

The far field pattern is then described by,

$$E_d(u) = E(u) + \Delta E \quad (70)$$

Implementation of this method consists of introducing small changes in the amplitude coefficients of the normalized far-field pattern equation which are proportional to the sum of the amplitudes of an arbitrary number of impulse functions, each of which is multiplied by a cosine function whose argument involves the points at which the impulse functions are applied.

The impulse functions are applied at the sidelobe maximum of the power pattern and the number of such functions used depends upon how many sidelobes require reduction. The degree of reduction is determined by the absolute difference in the desired and actual sidelobe peaks. Reasonable sidelobe control can be obtained by reducing only one sidelobe at a time, although some reduction in computation time can be achieved by applying impulses at all of the sidelobe maxima for the range  $0^\circ \leq \theta \leq 90^\circ$ . These amplitude deviations are then added algebraically to the original amplitude coefficients, which can be arbitrary. The resulting voltage pattern is computed using these new coefficients and the cycle is repeated. This iteration is continued until the resultant pattern approximates the desired pattern within a prescribed error.

Application of the iterative technique is simplified through the application of a side lobe deviation function

$$\Delta A_n = -F \sum_{k=1}^K a_k \cos [(n-.5) \pi u_k] \quad (71)$$

where

$$a_k = E(u_k) - E_d(u_k) \quad (72)$$

and  $F$  is a convergence factor,  $u_k$  is the point at which the impulse function is applied, and  $K$  is the number of sidelobes to be reduced.

Equations 71 and 72 can be directly applied to a computer program for solution. The programming procedure described in the algorithm of Table 6.

To ensure convergence, it may be necessary to modify the amplitude deviations by a scaling factor. This scaling factor can be determined by trial and error until convergence of the method is obtained.

The derivation of equations 71 and 72 appears in Appendix A.

## 2. AN EXACT METHOD OF DETERMINING THE ARRAY OUTPUT WAVEFORM FOR ANY SPECIFIED INPUT WAVEFORM

This technique is based on the application of the array impulse response to the far-field pattern equation containing the frequency characteristics of the antenna for a given observation angle. The inverse Fourier Transform is then applied to the product of the array input spectral density function and the far field pattern function. The result is the impulse response of the array if the array input spectral density function is considered to be a constant. Simplification of the impulse response can be effected by sampling the function at specific times. The convolution integral is then applied to the array impulse response and the specified input time waveform, determining the output time waveform. The waveform thus obtained is described by

TABLE 6 . ALGORITHM FOR ITERATIVE PATTERN SYNTHESIS

1. Initiate the iterative program with arbitrary array coefficients.
2. Compute the normalized voltage pattern.
3. Tabulate the sidelobe peaks, location of the peaks, and number of sidelobes within the desired control region.
4. Compute the impulse magnitudes,  $a_k$ , at the sidelobe peaks,  $u_k$ .
5. Compute the amplitude (or spacing) correction for each element using equations 71 and 72.
6. Apply the correction to each of the amplitudes (or spacing).
7. Go to step 2 if last pattern computed is not sufficiently approximated by the desired pattern, otherwise proceed to the next step.
8. List the element amplitudes (or spacing).
9. Compute the resulting pattern.

$$V(u, t) = \sum_n A_n e^{-j\pi n u \phi} T(t - t_n) \quad (73)$$

where

$$t_n = \frac{n}{2f_0} (u_t - u)$$

$A_n$  is the amplitude of the  $n$ th element

$T(t - t_n)$  is the specified input time waveform

$t_n$  is the  $n$ th sampling time

$u_\phi$  is the phase steering angle

$u_t$  is the real-time steering angle

The above equation is a simple finite summation which is easily applied. This method is applicable to any discrete array.

As an example of the application of this method, consider a simple CW signal expressed as,

$$T(t) = e^{j2\pi f_0 t} \quad (74)$$

From equation 73 the waveform is described by

$$V(u, t) = e^{j2\pi f_0 t} \sum_n A_n e^{j\pi n (u - u_t - u_\phi)} \quad (75)$$

Equation 75 is the general time, space antenna pattern of an array, subject to both phase and real-time steering. The time variation,

$$e^{j2\pi f_0 t},$$

represents the carrier frequency.

As another example, consider a single linear FM pulse defined by

$$T(t) = \text{RECT.} \left( \frac{t}{T_1} \right) e^{j(2\pi f_0 t + \frac{nt^2}{2})} \quad -\frac{T_1}{2} \leq t \leq \frac{T_1}{2} \quad (76)$$

The array response to this signal is

$$V(u, t) = e^{j(2\pi f_0 t + \frac{n}{2} t^2)} \sum_n A_n \text{RECT.} \left( \frac{t + \frac{nu}{2f_0}}{T_1} \right) e^{j\pi n u V} \quad (77)$$

where

$$V = \pi + \frac{nt}{2f_o} + \frac{Mnu}{8f_o^2}$$

and  $u_\psi = u_t = 0$ .

### 3. MAXIMIZATION TECHNIQUES

Several methods of mathematical processing are available to the problem of maximizing array directivity or signal-to-noise ratio with respect to element amplitude control or element spacing. All of these methods can be generally categorized as either an iteration process or a matrix inversion technique. The choice of method is entirely dependent on the parameters of the problem. The iterative technique is often more accurate and can be applied to large arrays, but for some conditions fails to converge. The matrix inversion method, on the other hand, is difficult to implement for large arrays and is subject to round off errors. A combination of these techniques can be used to advantage in some specialized cases, but in general the combination incurs some of the disadvantages of each method.

#### a. Iterative Processes

The iterative technique of maximizing a function follows the process described in Table 7. In general this process is applied to the first or second derivative of the function to be maximized. An example of this process is described in Section IV.4 for determining the maximum array directivity from control of the applied amplitude coefficients.

The primary advantage of the iterative process is the simplicity of form. A large number of terms can be handled in computation with minimum capacity. The computer time required to reach a solution may be considerable if the solution does not converge rapidly, but for a function with many terms this may be the only form of solution. The major disadvantage of the iterative technique is the fact that optimum performance is not assured. The calculation may converge about any maximum value, not necessarily the optimum one. Parallel computation can be used as a check on optimization.

#### b. Matrix Inversion

The problem of matrix inversion has been investigated for many years and several excellent forms of solution have been obtained, Reference (25). Since the problems encountered in this study are specific rather than general, only a form utilizing Gaussian elimination has been applied.

The matrix inversion technique described has proven effective in obtaining the inverse of a non-singular matrix. The only prerequisite for the matrix is that none of its diagonal elements be zero.

TABLE 7 . MAXIMIZATION ALGORITHM

1. Assume an arbitrary set of amplitude coefficients;  $A_1, A_2, \dots, A_N$ .
2. Solve the iteration equation  $A_k = QA_n + R$  for all values of  $k$ :  
 $k = 1, 2, \dots, N$ . In general, the factors  $Q$  and  $R$  are functions of  $n$  and  $A_n$ .  
 (See Section IV.4 of this report.)
3. If the new coefficients agree within a prescribed error with the old coefficients terminate the iteration. Otherwise, go to the next step.
4. Replace the old set of amplitude coefficients with the new set.
5. Go to step 2.



Let the nxn matrix [A] be denoted

$$[A] = \begin{bmatrix} a_{11} & a_{12} & a_{13} & \dots & a_{1n} \\ a_{21} & a_{22} & & & \\ a_{31} & & & & \\ \vdots & & & & \\ \vdots & & & & \\ \vdots & & & & \\ a_{n1} & \dots & \dots & \dots & a_{nn} \end{bmatrix} \quad (78)$$

The basic matrix is then augmented with an nxn identity matrix [I] to obtain a modified matrix, [A/I]

$$[A/I] = \left[ \begin{array}{cccc|cccc} a_{11} & a_{12} & \dots & a_{1n} & 1 & 0 & 0 & \dots & 0 \\ a_{21} & a_{22} & & & 0 & 1 & 0 & \dots & 0 \\ \vdots & & \ddots & & \vdots & & \ddots & & \vdots \\ \vdots & & & & \vdots & & & & \vdots \\ \vdots & & & & \vdots & & & & \vdots \\ a_{n1} & \dots & \dots & a_{nn} & 0 & \dots & \dots & \dots & 1 \end{array} \right] \quad (79)$$

By a sequence of elementary row operations upon A/I, an attempt is made to transform the left-half of [A/I] into an identity matrix. If this is possible then it can be shown that the right half of 79 is then  $[A]^{-1}$ .

The first portion of the procedure is to obtain zeros in the off-diagonal terms of A and unity along the diagonal. This procedure is best illustrated by means of an arbitrary example. Consider the following 3 x 3 matrix.

$$[A] = \begin{bmatrix} 1 & -2 & 3 \\ -3 & 7 & 12 \\ 4 & -4 & -2 \end{bmatrix} \quad (80)$$

Augmenting this matrix with the identity matrix [I]

$$[A/I] = \left[ \begin{array}{ccc|ccc} 1 & -2 & 3 & 1 & 0 & 0 \\ -3 & 7 & 12 & 0 & 1 & 0 \\ 4 & -4 & -2 & 0 & 0 & 1 \end{array} \right] \quad (81)$$

It can be shown that a valid operation on 81 is to add to any row (column) any multiple of another row (column). Thus in 81, to obtain a zero in row 2 and column 1, we can add row 1 multiplied by 3 to obtain:

$$[A/I]' = \begin{bmatrix} 1 & -2 & 3 & 1 & 0 & 0 \\ 0 & 1 & 21 & 3 & 1 & 0 \\ 4 & -4 & -2 & 0 & 0 & 1 \end{bmatrix} \quad (82)$$

The next step is to add the first row multiplied by a negative 4 to row 3; which yields:

$$[A/I]'' = \begin{bmatrix} 1 & -2 & 3 & 1 & 0 & 0 \\ 0 & 1 & 21 & 3 & 1 & 0 \\ 0 & 4 & -14 & -4 & 0 & 1 \end{bmatrix} \quad (83)$$

The elimination of the element in the third row and second column is achieved by adding row 2 multiplied by -4 to row 3;

$$[A/I]''' = \begin{bmatrix} 1 & -2 & 3 & 1 & 0 & 0 \\ 0 & 1 & 21 & 3 & 1 & 0 \\ 0 & 0 & -98 & -16 & -4 & 1 \end{bmatrix} \quad (84)$$

Repeating this procedure on the upper triangular part of [A] yields,

$$[I/A^{-1}] = \begin{bmatrix} 1 & 0 & 0 & -0.349 & 0.163 & 0.459 \\ 0 & 1 & 0 & -0.43 & 0.143 & 0.214 \\ 0 & 0 & 1 & 0.163 & 0.0408 & -0.0102 \end{bmatrix} \quad (85)$$

which is the desired inverted matrix. A problem consisting of a set of simultaneous equations can be solved by using the above method or a partial Gaussian elimination procedure may be incorporated.

The partial procedure may be applied to an nxn matrix (real) and  $\vec{X}$  and  $\vec{Y}$  which are two nx1 column matrices

$$[A] \vec{X} = \vec{Y} \quad (86)$$

The procedure is to obtain the form of equation 86 above. If the left-half of the matrix in 84 is identified by  $A^*$  and the right half as  $I^*$  then equation becomes

$$[A]^* \vec{X} = [I]^* \quad (87)$$

In the example cited previously, this expression becomes,

$$\begin{aligned} X_3 &= -\frac{1}{98} (-16Y_1 - 4Y_2 + Y_3) \\ X_2 &= 3Y_1 + Y_2 - 21X_3 \\ X_1 &= Y_1 + 2X_2 - 3X_3 \end{aligned} \quad (88)$$

Thus, the solution is apparent since  $\vec{Y}$  is specified and  $X^* = [X_1, X_2, X_3]$ .

The solution vector of a set of linear equations is obtained faster on a digital computer by this method of partial elimination than by calculating the inverse using full Gaussian elimination.

### c. Combination

A combination of techniques may be applicable in the solution of specific problems. Since there is an infinite number of combinations possible, the technique is described as an example wherein the gain of an antenna array is to be optimized. A form of the gain function can be expressed as the ratio of two bilinear forms,

$$G(\vec{A}) = \frac{\sum_n \sum_m A_n^* \alpha_{n,m} A_m}{\sum_n \sum_m A_n^* \beta_{n,m} A_m} \quad (89)$$

and

$$\beta_{n,m} = \frac{\sin \left[ \frac{2\pi d}{\lambda} (n-m) \right]}{\frac{\pi d}{\lambda} (n-m)} \quad (90)$$

$$\alpha_{ij} = 1 \quad i, j = 1, 2, 3, \dots, N$$

Obviously,  $[\alpha]$  is a singular matrix but this does not present a problem in the development.

Applying a theorem of Gantmacher, Reference (26), the condition for which  $G(\vec{A})$  is maximum is given by,

$$[\alpha] \vec{A} = \lambda_{\max} [\beta] \vec{A} \quad (91)$$

$\vec{A}$  is a  $n \times 1$  column vector

$$\vec{A} = \begin{bmatrix} a_1 \\ a_2 \\ a_3 \\ \vdots \\ a_n \end{bmatrix} \quad (92)$$

Substituting equation 92 into the vector form of equation 89

$$G(\vec{A}) = \lambda_{\max} \quad (93)$$

The characteristic equation corresponding to 91 can be shown to be

$$\left| [\alpha] - \lambda_{\max} [\beta] \right| = 0 \quad (94)$$

where the bars denote the determinant of the enclosed expression.

Premultiplying both sides of 91 by the inverse of  $[\beta]$  and transposing terms

$$\left\{ [\beta]^{-1} [\alpha] - \lambda_{\max} [I] \right\} \vec{A} = 0 \quad (95)$$

Defining a new matrix  $[\gamma]$ ,

$$\left\{ [\gamma] - \lambda_{\max} [I] \right\} \vec{A} = 0 \quad (96)$$

where  $\gamma_{ij} = \sum_j \beta_{ij}^{-1}$ . It is important that  $[\alpha]$  be premultiplied on the left by

$[\beta]^{-1}$  and not on the right. Thus all columns of  $[\gamma]$  are identical. This matrix  $[\gamma]$  is valid only for the single frequency case, but with a modification, a similar matrix can be constructed that accounts for the wideband case. In either case, the computational procedure is the same.

In computation the inverse of  $[\beta]$  is premultiplied by  $[\alpha]$  to obtain  $[\gamma]$ . The coefficients of  $[\gamma]$  are then obtained by an iterative process.

Starting with an initial vector  $\vec{X}^{(0)}$  the components of which are arbitrary, the iteration is performed according to the following algorithm.

- (1) Let  $n = 0$
- (2) Compute a new vector  $\vec{X}^{(n+1)} = [\gamma] \vec{X}^{(n)}$
- (3) Determine the value of the element of  $\vec{X}^{(n+1)}$  that has the largest absolute value; call this value  $\lambda_n$ .
- (4) Increment  $n$  by one.
- (5) If  $\lambda_n - \lambda_{n-1} \leq \epsilon$  or  $\vec{X}^{(n)} - \vec{X}^{(n-1)} \leq \delta$  exit from algorithm, otherwise go to step 2 above.

Normally only two or three iterations are needed before convergence is obtained.

## SECTION VIII

### REFERENCES

1. R.S. Elliott, "The Theory of Antenna Arrays" Chapter 1, Microwave Scanning Antennas, Vol. II, Edited by R.C. Hansen, Academic Press, New York, 1966.
2. J.D. Kraus, Antennas, Appendix 17, pp 519-534, McGraw-Hill Book Company Inc. New York, 1950.
3. R.B. Blackman, J.W. Tukey, "The Measurement of Power Spectra from the Point of View of Communications Engineering, Part II", Bell System Technical Journal, Vol. XXXVII, No. 2, p502, March, 1958.
4. T.T. Taylor "One Parameter Family of Line Source Producing Modified  $(\sin \pi \eta)/\pi \eta$  Patterns," Hughes Aircraft Co. Tech. Mem. 324, Culver City, Calif. September, 1953.
5. C.L. Dolph, "A Current Distribution for Broadside Arrays Which Optimizes the Relationship between Beamwidth and Sidelobe Level", Proc IRE, 34, No. 6 pp 335-348, June, 1946.
6. T.T. Taylor, "Design of Line-Source Antennas for Narrow Beamwidth and Low Sidelobes", IRE Trans. on Antennas and Propagation, Vol. AP-3, pp 16-28, Jan., 1955.
7. J.D. Kraus, "Antennas", McGraw-Hill Book Co., Inc. New York, 1950, pp 52-54.
8. W.E. Rupp, "Impedance Variation in Scanning Arrays" THE MICROWAVE JOURNAL, Vol. VIII, No. 12, December, 1965, pp 52-57.
9. J.L. Allen, "Gain and Impedance Variations in Scanned Dipole Arrays", IRE Transactions, AP-10, No. 5, September, 1962, pp 566-572.
10. A. Waldman and G.J. Wooley, "Noise Temperature of a Phased Array Receiver", THE MICROWAVE JOURNAL, Vol. IX, No. 9, September, 1966, p 91.
11. I.W. Linder, "Application of Correlation Techniques to Antenna Systems", U of Calif., Dept. of Elec. Engr. Series No. 60, Issue No. 267, Jan. 11, 1960.
12. D.K. Cheng and F.I. Tseng, "Signal-to-Noise Ratio Maximization for Receiving Arrays" Transactions IEEE, Antennas and Propagation, Vol. AP-14, No. 6, pp 792-794, November, 1966 (Correspondence).
13. Winston E. Kock, "Related Experiments with Sound Waves and Electromagnetic Waves", Proceedings of the IRE, Vol. 47, July, 1959, pp 1192-1201.
14. H.J. Riblet, "A Note on the Maximum Directivity of an Antenna", Proc. IRE, Vol. 36, p 620, 1948.
15. L. Solymar, "Maximum Gain of a Line Source Antenna if the Distribution Function is a Finite Fourier Series", Transactions IRE on Antennas and Propagation, AP-6, p 215, 1958.
16. N. Yaru, "A Note on Super-Gain Antenna Arrays", Proceedings IRE, Vol. 39, p 1081, 1951.

17. L.J. Chu, "Physical Limitations of Omni-Directional Antennas", Journal of Applied Physics, Vol. 19, p 1163, 1948.
18. A. Bloch, R.D. Medhurst, and S.D. Pool, "A New Approach to the Design of Superdirective Aerial Arrays" Proc. IEEE (London), Pt. III, Vol. 100, pp 303-314, September, 1953.
19. C.T. Tai, "The Optimum Directivity of Uniformly Spaced Broadside Arrays of Dipoles", IEEE Transactions on Antennas and Propagation, Vol. AP-12, pp 447-454, July, 1964.
20. Y.T. Lo, S.W. Lee, and Q.H. Lee, "Optimization of Directivity and Signal-to-Noise Ratio of an Arbitrary Antenna Array", PROCEEDINGS OF THE IEEE, Vol. 54, No. 8, August 1966, pp 1033-1045.
21. W.E. Kock and J.L. Stone, "Space Frequency Equivalence", Proc. IRE Vol. 46, pp 499-500, February, 1958 (correspondence).
22. L.R. Dausin, K.E. Niebuhr, and N.J. Nilsson, "The Effects of Wide Band Signals on Radar Antenna Design, IRE Wescon Conv. Record, Vol. 3, Pt. 1, pp 40-48, 1959.
23. D.O. North, "An Analysis of the Factors which Determine Signal/Noise Discrimination in Pulsed-Carrier Systems", RCA Technical Report PTR-6C, June 25, 1943.
24. R.F. Harrington, "Sidelobe Reduction by Nonuniform Element Spacing" IRE Trans. on Antennas and Propagation, Vol. AP-9, pp 187-192; March, 1961.
25. M.H. Kietzke, R.W. Stoughton and Marjorie P. Lietzke, "A Comparison of Several Methods for Inverting Large Symmetric Positive Definite Matrices", Mathematics of Computation, Vol. 18, July 1964, pp 449-456.
26. F.R. Gantmacher, The Theory of Matrices, Translated by K.A. Hirsch, Vol. 1, New York, Chelsea Publishing Company, 1959.

## BIBLIOGRAPHY

- W.B. Adams, "The Broad-Band-Signal Response of a Phased-Steered Linear Receiving Array, Proc. IEEE, p. 406, January, 1963.
- D.K. Cheng, and F.I. Tseng, "Transient and Steady-State Antenna Pattern Characteristics for Arbitrary Time Signals", IEEE Transactions on Antennas and Propagation, July, 1964.
- K.M. Chen, "FM Effect on the Radiation Patterns of High-Gain Antenna Arrays", IEEE Trans. on Antennas and Propagation (Correspondence), Vol. AP-12, November, 1964.
- J. DiFranco and W. Rubin, "Distortion Analysis of Radar Systems", Proc. Seventh Ann. East Coast Conf; PGANE, Baltimore, Md., October 24-26, 1960, pp. 2.1.3-(1-5).
- J.V. DiFranco and W.L. Rubin, "Transient Performance of Array Antennas", IEEE Internat'l Conv. Rec., Pt. 1, pp. 93-97, March, 1963.
- J.V. DiFranco and W.L. Rubin, "Analysis of Signal Processing Distortion in Radar Systems", IRE Transactions on Military Electronics, pp. 219-227; April, 1962.
- N.H. Enestein, "Transient Build-up of the Antenna Pattern in End-fed Linear Arrays", E Conv. Rec., Pt. 2, pp. 49-55, March, 1953.
- J. Galejs, "Minimization of Sidelobes in Space Tapered Linear Arrays" IEEE Trans. on Antennas and Propagation, Vol. AP-12, pp. 497-498, July, 1964.
- C.S. Gardner and J.B. Keller, "The Field of a Pulsed Dipole in an Interface", presented at the URSI Symp. on Electromagnetic Theory, Toronto, Canada; June 15-20, 1959.
- R.F. Harrington, "Antenna Excitation for Maximum Gain" Transactions of IEEE, Antennas and Propagation, AP-13, No. 6, pp. 896-903, November, 1965.
- D.L. Huffman, "Short Pulse-Fresnel Radiation Patterns of Traveling-Wave Antennas", presented at the 1962 12th Annual Symp. on USAF Antenna Research and Development at University of Illinois, Monticello, Ill.
- A. Ishimaru, "Theory of Unequally-Spaced Arrays", IRE Trans. on Antennas and Propagation, Vol. AP-10, pp. 691-702, November, 1962.
- D.D. King, R.F. Packard, and R.K. Thomas, "Unequally Spaced, Broad-band Antenna Arrays", IRE Trans. on Antennas and Propagation, Vol. AP-8, pp. 380-385; July, 1960.
- R.M. Lerner, "A Matched Filter Detection System for Complicated Doppler Shifted Signals", IRE Transactions on Information Theory, Vol. IT-6, No. 3; June, 1960.
- I.W. Linder, "Correlation Processes in Antenna Arrays" University of California, Berkeley, Serial 60, Issue 371, Contract AF49(638)-1043, June 13, 1961.
- B. Mayo, "Transient Behavior of Aperture Antennas", Letter to the Editor, Proc. IRE, Vol. 49, No. 4, April, 1961, pp. 817-819.
- B.R. Mayo, P.W. Howels, and W.B. Adams, "Generalized Linear Radar Analysis", Microwave Journal, Vol. 4, No. 8; August, 1961.

C. Polk, "Transient Behavior of Aperture Antennas", Proc. IRE, Vol. 48, pp. 1281-1288, July, 1960.

J. Reed, "Long Line Effect in Pulse Compression Radar", Microwave J., Vol. 4, pp. 99-100; September, 1961.

H. Rosenblatt, "Short Pulse Radiation Effect of a Long Array Utilizing Series and Corporate-Series Feed", IEEE Internat'l Conv. Rec., Pt. 2, pp. 179-184, March, 1964.

W.L. Rubin and J.V. DiFranco, "Spatial Ambiguity and Resolution for Array Antennas with Wide-Band Phase Coded Signals", Proceedings of Pulse Compression Techniques and Applications Symposium, Rome, New York; October, 1962.

H.J. Schmitt, "Transients in Cylindrical Antenna", Cruft Lab., Harvard University, Cambridge, Mass., Technical Report No. 296; January 5, 1959.

C. B. Sharpe and R. B. Crane, "Optimization of Linear Arrays for Broadband Signals", IEEE Transactions on Antennas and Propagation, Vol. AP-14, No. 4, July, 1966.

C. B. Sharpe and R. B. Crane, "A Broadband Theory for Linear Arrays", Willow Run Labs., Institute of Science and Technology, The University of Michigan, Ann Arbor, Report 6400-49-T, December, 1965 (unclassified).

S. Silver, "Microwave Antenna Theory and Design", McGraw-Hill Book Co., Inc., New York, 1949, pp. 270-273.

I. Skolnick, "Detection of Radar Signals in Noise", in Introduction to Radar Systems, McGraw-Hill Book Company, New York, 1962.

F. I. Tseng and D. K. Cheng, "Antenna Pattern Response to Arbitrary Time Signals", Can. J. Phys., Vol. 42, pp. 1358-1368, July, 1964.

F. I. Tseng and D. K. Cheng, "Gain Optimization for Arbitrary Antenna Arrays", IEEE Transactions on Antennas and Propagation (Communications), Vol. AP-13, pp. 973-974, November, 1965.

A. J. Villeneuve, "Optimization of Gain of Arbitrary Array Antennas" Hughes Aircraft Company, Scientific Report No. 5, Contract AF19(628)4349.

G. G. Weill, "Transients on a Linear Antenna", California Institute of Technology, Pasadena, Antenna Lab., Technical Report No. 20; August, 1959.

M. S. Wheeler and D. K. Alexander, "Short Pulse Effects in Traveling-Wave Antennas (U)", (Confidential Paper), 1962 8th Annual Radar Symp. Record (U), Institute of Science and Technology, The University of Michigan, Ann Arbor, Report 2900-367-X, August, 1962 (secret).

A. White and Robert R. Brown, "A Comparison of Methods for Computing the Eigenvalues and Eigenvectors of a Real Symmetric Matrix", Mathematics of Computation, Vol. 18, July, 1964, pp. 457-463.



# APPENDIX A

## DERIVATION OF THE PATTERN SYNTHESIS TECHNIQUE

This appendix derives the appropriate equations and describes the iterative synthesis technique for an amplitude tapered array. The procedure for space-tapered arrays is similar but more involved.

Equations 68, 69, and 70 in Section VII form the starting point for the development of the method. Equation 70 can also be written in another form.

$$E_d(u) \equiv \frac{1}{\sum_{n=1}^N A_n} \sum_{n=1}^N (A_n + \Delta A_n) \cos [(n-.5)\pi u] \quad (A-1)$$

The problem is to determine  $\Delta E$  so that the desired pattern can be achieved. Some consideration must be given as to how the desired pattern should be specified. The antenna properties of beamwidth and illumination efficiency are primarily a matter of a tradeoff with the desired sidelobe level and number of elements, but are not important here. The important feature of an antenna pattern is the envelope of the sidelobe peaks. It is natural, then, to define the desired pattern,  $E_d(u)$ , in terms of the sidelobe level envelope. The phase of a given sidelobe is not important insofar as the sidelobe peak envelope is concerned but must be considered when used with equation (A-1). This amounts to assigning a positive or negative sign to  $E_d(u)$ , depending upon the sign of  $E(u) + \Delta E$ , and presents no practical difficulty.

Using equations 69 and 70 from Section VII and rearranging terms:

$$\sum_{n=1}^N \Delta A_n \cos [(n-.5)\pi u] = \left( \sum_{n=1}^N A_n \right) (E_d(u) - E(u)) \quad (A-2)$$

The left hand term of (A-2) is recognized as a finite Fourier series which has a period of  $-1 < u < 1$ . Since it is a cosine series which indicates that it is an even function, and the right hand term is also an even function, the coefficients,  $\Delta A_n$ , can be found from the half-range expansion

$$\Delta A_n = 2 \left( \sum_{n=1}^N A_n \right) \int_0^1 [E_d(u) - E(u)] \cos [(n-.5)\pi u] du \quad (A-3)$$

$n=1, 2, \dots, N$

The value of this integral is highly dependant upon the assumed behavior of the desired pattern,  $E_d(u)$ . Since the only feature of interest in the patterns is the peak sidelobe level, the exact behavior of  $E_d(u)$  can be quite arbitrary. The integral can be evaluated at the points of concern—namely, the sidelobe peaks—by using the Dirac delta function. Thus,

$$\Delta A_n = 2 \left( \sum_{n=1}^N A_n \right) \int_0^1 [E_d(u) - E(u)] \delta(u-u_k) \cos [(n-.5)\pi u] du \quad (A-4)$$

where  $u_k$  are the locations of the sidelobe peaks which are to be altered. Performing the indicated integration of (A-4) yields

$$\Delta A_n = 2 \left( \sum_{n=1}^N A_n \right) \sum_{k=1}^K a_k \cos [ (n-.5) \pi u_k ] \quad (A-5)$$

where

$$a_k = E(u_k) - E_d(u_k) \quad (A-6)$$

Equation (A-5) may be written in the form

$$\Delta A_n = F \sum_{k=1}^K a_k \cos [ (n-.5) \pi u_k ] \quad (A-7)$$

which is identical to equation 71 in Section VII.

The only restraint on equation (A-7) is concerned with the F factor. For a specified voltage pattern, it is only required that F be small enough so that the iteration process converges.

## APPENDIX B

### NOISE ANALYSIS

The noise power which appears at the terminals of a circuit is a function of the circuit parameters and environment. Noise, and its effect on the performance of a system, is specified in a variety of terms. The purpose of this appendix is to define the terms and to provide the relationships which can be used in circuit analysis. Active and passive circuits are included with examples to illustrate the significance of component placement.

#### 1. DEFINITIONS AND NOMENCLATURE

The following terms are defined and assigned symbols for future reference.

- a. Noise Power (N) - The maximum power which can be transferred from a resistor of value R, operating at temperature T, to a resistive load of value R.

$$N = kTB \quad (B-1)$$

where k = Boltzmann's Constant

$$(1.38 \times 10^{-25} \text{ joule/degree K})$$

T = Noise Temperature - °K

B = Bandwidth

- b. Bandwidth (B) - The frequency band over which noise is considered.

$$B = \frac{1}{|H(f_0)|^2} \int_{-\infty}^{\infty} |H(f)|^2 df \quad (B-2)$$

where: H(f) = frequency response

H(f<sub>0</sub>) = maximum response

(usually center of band)

- c. Signal-to-Noise Ratio (S/N) - The usable power of a signal divided by the noise power (N)

$$S/N = \frac{S}{kTB} \quad (B-3)$$

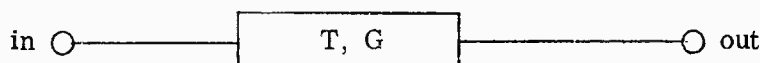
- d. Noise Figure (F) - The ratio of the signal-to-noise ratio at the input of a circuit to that appearing at the output of the circuit.

$$F = \frac{(S/N)_{in}}{(S/N)_{out}} \quad (B-4)$$

#### 2. DERIVATION

Using the noise figure (F) as a basic quality factor, and noise temperature (T) as a basic circuit parameter, the following relationships can be established.

Consider a basic network with gain  $G$  and operating at the input noise temperature  $T$ .



$$(S/N)_{in} = \frac{S_{in}}{kTB}$$

$$(S/N)_{out} = \frac{GS_{in}}{kTBG + \Delta N}$$

$\Delta N$  = noise power introduced by the circuit

From equation (B-4)

$$F = \frac{kTBG + \Delta N}{kTBG} = 1 + \frac{\Delta N}{kTBG} \quad (B-5)$$

The noise temperature ( $T$ ) has been standardized<sup>1</sup> to an ambient temperature of 290°K (approximately 63°F). This specific noise temperature is designated by the symbol  $T_o$ . If the above network is operating in a standard environment, equation (B-5) becomes

$$F = 1 + \frac{\Delta N}{kT_o BG} \quad (B-6)$$

$\Delta N$ , the internal noise of the circuit, can now be defined in terms of the effective noise temperature of the circuit referred to the input terminals ( $T_e$ ).

$$\Delta N = kT_e BG \quad (B-7)$$

Substituting (B-7) into (B-6) the circuit noise figure becomes

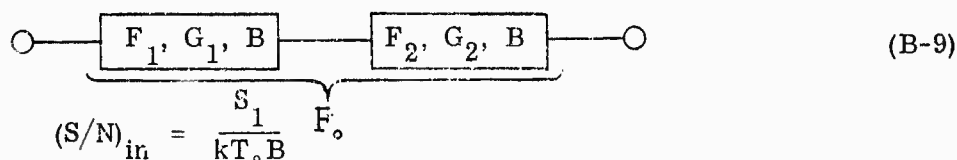
$$F = 1 + \frac{T_e}{T_o} \quad (B-8)$$

The term  $\frac{T_e}{T_o}$  is sometimes referred to as excess noise temperature since it represents a deviation from the standard ambient temperature ( $T_o$ ).

### 3. CASCADED CIRCUITS

In any electronic system, the overall noise figure must be determined from the components comprising the system. Since these components are usually cascaded, the noise interaction must be considered.

With two circuits operating in tandem, the input signal-to-noise ratio follows from (B-3).



<sup>1</sup> "IRE Dictionary of Electronics Terms and Symbols" Institute of Radio Engineers, New York 1961.

The signal-to-noise ratio out of the first circuit and into the second follows from the single circuit case.

$$\frac{S_2}{N_2} = \frac{G_1 S_1}{kT_o B G_1 + \Delta N_1}$$

where:  $\Delta N_1 = kT_1 B G_1$

therefore: 
$$\frac{S_2}{N_2} = \frac{G_1 S_1}{k B G_1 (T_o + T_1)}$$

and the signal-to-noise ratio at the output of the second circuit becomes

$$(S/N)_{out} = \frac{G_1 G_2 S_1}{k B G_1 G_2 (T_o + T_1) + \Delta N_2} = \frac{G_1 S_1}{k B G_1 (T_o + T_1) + k T_2 B} \quad (B-10)$$

since  $\Delta N_2 = k T_2 B G_2$

The overall noise figure ( $F_o$ ) is found by taking the ratio of equations (B-9) and (B-10).

$$F_o = \frac{\frac{S_1}{k T_o B}}{\frac{G_1 S_1}{k (T_o + T_1) B G_1 + k T_2 B}} = \frac{(T_o + T_1) G_1 + T_2}{T_o G_1}$$

or 
$$F_o = \left(1 + \frac{T_1}{T_o}\right) + \frac{T_2}{T_o G_1}$$

but from (B-8)

$$F_1 = 1 + \frac{T_1}{T_o} \quad \text{and} \quad F_2 = 1 + \frac{T_2}{T_o}$$

therefore: 
$$F_o = F_1 + \frac{(F_2 - 1)}{G_1} \quad (B-11)$$

If this basic two circuit analysis is extended to the general n-circuit case, the overall noise figure can be determined.

$$F_o = F_1 + \frac{(F_2 - 1)}{G_1} + \frac{(F_3 - 1)}{G_1 G_2} + \dots + \frac{(F_n - 1)}{G_1 G_2 \dots G_{n-1}} \quad (B-12)$$

or by substituting from equation (B-8)

$$T_e = (F_o - 1) T_o$$

$$T_e (\text{overall}) = T_1 + \frac{T_2}{G_1} + \frac{T_3}{G_1 G_2} + \dots + \frac{T_n}{G_1 G_2 \dots G_{n-1}} \quad (B-13)$$

#### 4. LOSSY CIRCUITS

In the foregoing analysis, it was assumed that the circuits are active with a value of gain (G) greater than unity. A passive lossy component, such as a transmission line section, has a gain of less than unity or a loss factor (L) greater than unity ( $L = 1/G$ ). As in the active component case, the lossy component has an effective noise temperature ( $T_e$ ). Assuming that the ambient temperature of the lossy network is T, the effective noise temperature of the circuit is related to T and L. The total noise out of the circuit is

$$N_{out} = kT_e B = \frac{kT_o B}{L} + \Delta N \quad (B-14)$$

With no internal active components, the noise in the passive circuit comes only from the loss, therefore:

$$\Delta N = kT_o B - \frac{kT_o B}{L} = kT_o B(1 - \frac{1}{L}) \quad (B-15)$$

Substituting (B-15) into the basic noise figure equation (B-6), the overall noise figure of the lossy component becomes

$$F_e = 1 + \frac{(\Delta N)L}{kT_o B} = 1 + L(1 - \frac{1}{L}) = L \quad (B-16)$$

Lossy components can be considered in cascade with active components by applying equation (B-16) to the generalized equation (B-12) for the appropriate networks.

#### 5. COMBINATION NETWORK - ACTIVE AND PASSIVE COMPONENTS

Using the cascaded circuit approach outlined above, an active circuit with gain (G) and a passive circuit with loss (L) can be considered as two discrete cases.

Case I - The lossy component ( $F_e$ ) is placed in front of the active circuit ( $F_a$ ) in the signal flow path. From equation (B-11) we have

$$F_o = F_e + (F_a - 1) L \text{ since } G = 1/L$$

and from (B-16)  $F_e = L$

therefore  $F_o = L + (F_a - 1) L = LF_a \quad (B-17)$

Case II - The active component precedes the lossy component in the signal flow path. Again from equation (B-11)

$$F_o = F_a + \frac{F_e - 1}{G} \quad \text{and } F_e = L \quad (B-18)$$

The general noise figures for the two cases are given by equations (B-17) and (B-18). To realize the significance of component location, three conditions of the gain-loss relationship are considered.

Condition A -  $G \gg L$

$$\text{Case I} - F_o = LF_a$$

$$\text{Case II} - F_o = F_a$$

For any value of loss other than the trivial lossless case, it is advantageous to place the amplification ahead of the loss.

Condition B -  $L \gg G$

$$\text{Case I} - F_o = LF_a$$

$$\text{Case II} - F_o = F_a + L$$

In this improbable condition, it is still desirable to place the amplification first since the product of two numbers greater than unity is generally greater than or equal to their sum.

Condition C -  $L=G$

$$\text{Case I} - F_o = LF_a$$

$$\text{Case II} - F_o = F_a + \frac{(L-1)}{L}$$

The loss term can vary in magnitude from zero to unity (as a function of  $L$ ) therefore Case II is still preferable in the location of components.

## APPENDIX C

### CORRELATION COEFFICIENTS

The correlation coefficient for a linear discrete array is defined as:

$$R(d) = \frac{\frac{1}{4\pi} \int_{-\infty}^{\infty} \int_0^{2\pi} \int_0^{\pi} I(\theta, \phi) G(\theta, \phi) W(f) e^{j \frac{2\pi f d}{c} \cos \theta} \sin \theta d\theta d\phi df}{\int_{-\infty}^{\infty} W(f) df} \quad (C-1)$$

where

- $G(\theta, \phi)$  = the element power pattern, (normalized to unity)
- $I(\theta, \phi)$  = the noise power distribution over space, (normalized to unity)
- $W(f)$  = the power spectral density

The S/N ratio of the array output for a boresight beam is

$$S/N = \frac{\frac{1}{\sum_{n=1}^N \sum_{m=1}^N A_n A_m R_{n,m}}}{\left( \sum_{n=1}^N A_n \right)^2} \quad (C-2)$$

where the peak signal is taken as unity. A consequence of normalizing the peak signal to unity is that the restriction  $R=1$  at  $d=0$  must be applied.

If the noise power distribution is uniform, i. e.,  $I(\theta, \phi) = 1$  and only a single frequency is considered, the S/N of the array is identical to the directivity of the array.

The problem of determining the correlation coefficient for different models is primarily that of carrying out the integration indicated in equation (C-1).

For a single or multifrequency spectrum we have

$$W(f) = \sum_k A_k \delta(f - f_k) \quad (C-3)$$

$$\int_{-\infty}^{\infty} W(f) df = \sum_k A_k \quad (C-4)$$

for any element and noise power distribution.

For the case of an isotropic element, single frequency, and isotropic noise, equation (C-1) reduces to:



$$R(d) = \frac{1}{4\pi} \int_0^{2\pi} \int_0^\pi e^{j \frac{2\pi f_0 d}{c} \sin \theta} \sin \theta \, d\theta \, d\phi \quad (C-5)$$

Using a change of variable

$$u = \frac{\pi f_0 d}{c} \cos \theta$$

$$du = - \frac{\pi f_0 d}{c} \sin \theta \, d\theta \quad (C-6)$$

the correlation coefficient assumes the form:

$$R(d) = \frac{\sin \left( \frac{2\pi d}{\lambda} \right)}{\frac{2\pi d}{\lambda}} \quad (C-7)$$

For cases other than uniform noise and element power patterns, the reader is referred to Table C-1. The required integration is often difficult to attain, therefore the resulting expression is written out for each case in Table C-1.

Corresponding to the linear array case, a similar expression may be defined as the generalized correlation coefficient for a planar array.

$$R_{n,m,i,j} = K \int_{-\infty}^{\infty} \int_0^{2\pi} \int_0^\pi I(\theta, \phi) G(\theta, \phi) W(f) e^{j\psi} \sin \theta \, d\theta \, d\phi \, df \quad (C-8)$$

where

$$\psi = \frac{2\pi}{\lambda} \sin \theta [d(n-i) \cos \phi + D(m-j) \sin \phi] \quad (C-9)$$

and  $K$  is a normalizing factor such that  $R_{n,m,i,j} = 1$  for  $i=n$  and  $j=m$ .  $I(\theta, \phi)$ ,  $G(\theta, \phi)$  and  $W(f)$  are defined as in equation (C-1). The main difference between equation (C-8) and equation (C-1) is that for the two dimensional case, the array geometry must be considered.

Corresponding to the derivations of specific correlation coefficients for the linear array case, it is possible to illustrate a mathematical derivation of two specific correlation coefficients. These are (C-1), a planar array with isotropic radiators, a uniform spatial noise source, and narrow bandwidth; and (C-2), the same conditions but with a flat spectral noise bandwidth.

For the first case we have:

$$G(\theta, \phi) = 1$$

$$I(\theta, \phi) = 1$$

$$W(f) = \delta(f - f_0) \quad (C-10)$$

The correlation coefficient is

$$R_{n,m,i,j} = K \int_0^{2\pi} \int_0^\pi e^{j \frac{2\pi}{\lambda} \sin \theta (d_x \cos \phi + d_y \sin \phi)} \sin \theta d\theta d\phi \quad (C-11)$$

where

$$d_x = d_n - d_i$$

$$d_y = D_m - D_j$$

By introducing a change of variable in (C-11) and simplifying, we obtain:

$$R_{n,m,i,j} = K \int_0^\pi \sin \theta d\theta \int_0^{2\pi} e^{j Z \sin \theta \cos (\phi - \alpha)} d\phi \quad (C-12)$$

Further simplification is possible if we use the identity for the nth order Bessel function of the first kind given by

$$J_n(Z \sin \theta) = \frac{j^{-n}}{2\pi} \int_0^{2\pi} e^{j Z \sin \theta \cos \phi} e^{jn\phi} d\phi \quad (C-13)$$

Equation (C-12) becomes

$$R_{n,m,i,j} = K \int_0^\pi 2\pi J_0(Z \sin \theta) \sin \theta d\theta \quad (C-14)$$

or in terms of original variables,

$$R_{n,m,i,j} = K \int_0^\pi 2\pi J_0 \left( \frac{2\pi}{\lambda} \sin \theta \sqrt{d_x^2 + d_y^2} \right) \sin \theta d\theta \quad (C-15)$$

If  $Z = \frac{2\pi}{\lambda} \sqrt{d_x^2 + d_y^2}$  is small, we write the Maclaurin expansion of  $J_0$  as

$$J_0(Z \sin \theta) = \frac{1}{(0!)^2} - \frac{(Z \sin \theta)^2}{(1!)^2 (2)^2} + \frac{(Z \sin \theta)^4}{(2!)^2 (2)^4} - \frac{(Z \sin \theta)^6}{(3!)^2 (2)^6} + \dots \quad (C-16)$$

Evaluating the integral in (C-15) by integrating, term by term, and imposing on  $\phi$  the limits 0 and  $\pi$ , we obtain

$$R_{n,m,i,j} = \frac{\sin \left( \frac{2\pi}{\lambda_o} \sqrt{d_x^2 + d_y^2} \right)}{\frac{2\pi}{\lambda_o} \sqrt{d_x^2 + d_y^2}} \quad (C-17)$$

where the normalizing factor, K, has been applied so that  $R_{n,m,i,j} = 1$  for  $d_x = d_y = 0$ . This equation is analogous to the one for the linear case (equation C-7).

Equation (C-17) can be extended to include a flat spectral noise bandwidth. The correlation coefficient becomes

$$R_{n,m,i,j} = \int_{-\infty}^{\infty} W(f) \frac{\sin \left( \frac{2\pi f}{c} \sqrt{d_x^2 + d_y^2} \right)}{\frac{2\pi f}{c} \sqrt{d_x^2 + d_y^2}} \quad (C-18)$$

or

$$R_{n,m,i,j} = \frac{1}{\frac{2\pi}{\lambda_o} P \sqrt{d_x^2 + d_y^2}} \left\{ \text{Si} \left[ \frac{2\pi}{\lambda_o} \sqrt{d_x^2 + d_y^2} (1 + P/2) \right] - \text{Si} \left[ \frac{2\pi}{\lambda_o} \sqrt{d_x^2 + d_y^2} (1 - P/2) \right] \right\} \quad (C-19)$$

where P is the bandwidth ratio and  $\lambda_o$  is the center frequency wavelength.

Table C-1 and Figures C-1 through C-16 give the mathematical form and graphical representation of the correlation coefficients corresponding to various conditions of antenna element function, noise distribution, and signal bandwidth. These examples are not intended to be all inclusive, but representative of the type of variations which may be expected in a wide range of array applications.

# APPENDIX C

TABLE C-1. ARRAY CONDITIONS AND CORRELATION FUNCTION

Case		Fig.
I Isotropic Element Isotropic Noise Single Frequency	$G(\theta, \phi) = 1, \quad I(\phi, \theta) = 1, \quad W(f) = \delta(f - f_0)$ $R(d) = \left[ \sin\left(\frac{2\pi d}{\lambda}\right) \right] / \left( \frac{2\pi d}{\lambda} \right)$	C-1
II Isotropic Element Isotropic Noise Double Frequency	$G(\theta, \phi) = 1, \quad I(\phi, \theta) = 1, \quad W(f) = \sum_{k=1}^2 \delta(f - f_k); \text{ where } f_2 = (1 + p) f_1$ $R(d) = \frac{1}{2} \left[ \frac{\sin\left[\frac{2\pi d}{\lambda} (1 + P/2)\right]}{\frac{2\pi d}{\lambda} (1 + P/2)} + \frac{\sin\left[\frac{2\pi d}{\lambda} (1 - P/2)\right]}{\frac{2\pi d}{\lambda} (1 - P/2)} \right]$	C-2
III Isotropic Element Isotropic Noise Flat Bandwidth	$G(\theta, \phi) = 1, \quad I(\phi, \theta) = 1, \quad W(f) = 50\% \text{ flat bandwidth; } P = .50 = \Delta f$ $R(d) = \left( \frac{1}{\frac{2\pi d}{\lambda_0} P} \right) \left\{ \text{Si} \left[ \frac{2\pi d}{\lambda_0} (1 + P/2) \right] - \text{Si} \left[ \frac{2\pi d}{\lambda_0} (1 - P/2) \right] \right\}$	C-3
IV Parallel Dipole Isotropic Noise Single Frequency	$G(\theta, \phi) = 1 - \sin^2 \theta \sin^2 \phi, \quad I(\phi, \theta) = 1, \quad W(f) = \delta(f - f_0)$ $R(d) = \frac{3}{2} \left( \frac{\lambda}{2\pi d} \right)^2 \left[ \frac{2\pi d}{\lambda} \sin\left(\frac{2\pi d}{\lambda}\right) + \cos\left(\frac{2\pi d}{\lambda}\right) - \sin\left(\frac{2\pi d}{\lambda}\right) / \frac{2\pi d}{\lambda} \right]$	C-4
V Parallel Dipole Isotropic Noise Double Frequency	$G(\theta, \phi) = 1 - \sin^2 \theta \sin^2 \phi, \quad I(\phi, \theta) = 1, \quad W(f) = \sum_{k=1}^2 \delta(f - f_k); \quad p = .25 = \Delta f$	C-5

TABLE C-1. ARRAY CONDITIONS AND CORRELATION FUNCTION (Continued)

Case		Fig.
V (Continued)	$R(d) = \frac{3}{4 \left( \frac{2\pi d}{\lambda} \right)^2} \left\{ \frac{1}{(1 + P/2)^2} \left[ \frac{2\pi d}{\lambda} (1 + P/2) \sin \left[ \frac{2\pi d}{\lambda} (1 + P/2) \right] \right. \right. \\ + \cos \left[ \frac{2\pi d}{\lambda} (1 + P/2) \right] - \frac{\sin \left[ \frac{2\pi d}{\lambda} (1 + P/2) \right]}{\frac{2\pi d}{\lambda} (1 + P/2)} \left. \left. + \frac{1}{(1 - P/2)^2} \right] \right. \\ \left. \left[ \frac{2\pi d}{\lambda} (1 - P/2) \sin \left[ \frac{2\pi d}{\lambda} (1 - P/2) \right] + \cos \left[ \frac{2\pi d}{\lambda} (1 - P/2) \right] \right] \right. \\ \left. - \frac{\sin \left[ \frac{2\pi d}{\lambda} (1 - P/2) \right]}{\frac{2\pi d}{\lambda} (1 - P/2)} \right\}$	C-5 (Cont)
VI Colinear Dipole Isotropic Noise Single Frequency	$G(\theta, \phi) = \sin^2 \theta, \quad I(\phi, \theta) = 1, \quad W(f) = \delta(f - f_0)$ $R(d) = \frac{3}{\left( \frac{2\pi d}{\lambda} \right)^2} \left[ \sin \left( \frac{2\pi d}{\lambda} \right) / \left( \frac{2\pi d}{\lambda} \right) - \cos \left( \frac{2\pi d}{\lambda} \right) \right]$	C-6
VII Colinear Dipole Isotropic Noise Double Frequency	$G(\theta, \phi) = \sin^2 \theta, \quad I(\phi, \theta) = 1, \quad W(f) = \sum_{k=1}^2 \delta(f - f_k), \quad P = .25 = \Delta f$ $R(d) = \frac{3}{4 \left( \frac{2\pi d}{\lambda} \right)^2} \left\{ \frac{1}{(1 + P/2)^2} \left[ \frac{2\pi d}{\lambda} (1 + P/2) \sin \left[ \frac{2\pi d}{\lambda} (1 + P/2) \right] \right. \right. \\ + \cos \left[ \frac{2\pi d}{\lambda} (1 + P/2) \right] - \frac{\sin \left[ \frac{2\pi d}{\lambda} (1 + P/2) \right]}{\frac{2\pi d}{\lambda} (1 + P/2)} \left. \left. + \frac{1}{(1 - P/2)^2} \right] \right. \\ \left. \left[ \frac{2\pi d}{\lambda} (1 - P/2) \sin \left[ \frac{2\pi d}{\lambda} (1 - P/2) \right] + \cos \left[ \frac{2\pi d}{\lambda} (1 - P/2) \right] \right] \right. \\ \left. - \frac{\sin \left[ \frac{2\pi d}{\lambda} (1 - P/2) \right]}{\frac{2\pi d}{\lambda} (1 - P/2)} \right\}$	C-7

TABLE C-1. ARRAY CONDITIONS AND CORRELATION FUNCTION (Continued)

Case		Fig.
V (Continued)	$R(d) = \frac{3}{4 \left( \frac{2\pi d}{\lambda} \right)^2} \left\{ \frac{1}{(1 + P/2)^2} \left[ \frac{2\pi d}{\lambda} (1 + P/2) \sin \left[ \frac{2\pi d}{\lambda} (1 + P/2) \right] \right. \right. \\ + \cos \left[ \frac{2\pi d}{\lambda} (1 + P/2) \right] - \frac{\sin \left[ \frac{2\pi d}{\lambda} (1 + P/2) \right]}{\frac{2\pi d}{\lambda} (1 + P/2)} \left. \left. + \frac{1}{(1 - P/2)^2} \right] \right. \\ \left. \left[ \frac{2\pi d}{\lambda} (1 - P/2) \sin \left[ \frac{2\pi d}{\lambda} (1 - P/2) \right] + \cos \left[ \frac{2\pi d}{\lambda} (1 - P/2) \right] \right] \right. \\ \left. \left. - \frac{\sin \left[ \frac{2\pi d}{\lambda} (1 - P/2) \right]}{\frac{2\pi d}{\lambda} (1 - P/2)} \right] \right\}$	C-5 (Cont)
VI Colinear Dipole Isotropic Noise Single Frequency	$G(\theta, \phi) = \sin^2 \theta, \quad I(\phi, \theta) = 1, \quad W(f) = \delta(f - f_0)$ $R(d) = \frac{3}{\left( \frac{2\pi d}{\lambda} \right)^2} \left[ \sin \left( \frac{2\pi d}{\lambda} \right) / \left( \frac{2\pi d}{\lambda} \right) - \cos \left( \frac{2\pi d}{\lambda} \right) \right]$	C-6
VII Colinear Dipole Isotropic Noise Double Frequency	$G(\theta, \phi) = \sin^2 \theta, \quad I(\phi, \theta) = 1, \quad W(f) = \sum_{k=1}^2 \delta(f - f_k), \quad P = .25 = \Delta f$ $R(d) = \frac{3}{4 \left( \frac{2\pi d}{\lambda} \right)^2} \left\{ \frac{1}{(1 + P/2)^2} \left[ \frac{2\pi d}{\lambda} (1 + P/2) \sin \left[ \frac{2\pi d}{\lambda} (1 + P/2) \right] \right. \right. \\ + \cos \left[ \frac{2\pi d}{\lambda} (1 + P/2) \right] - \frac{\sin \left[ \frac{2\pi d}{\lambda} (1 + P/2) \right]}{\frac{2\pi d}{\lambda} (1 + P/2)} \left. \left. - \frac{\sin \left[ \frac{2\pi d}{\lambda} (1 + P/2) \right]}{\frac{2\pi d}{\lambda} (1 + P/2)} \right] \right\}$	C-7

TABLE C-1. ARRAY CONDITIONS AND CORRELATION FUNCTION (Continued)

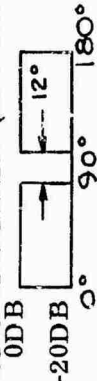
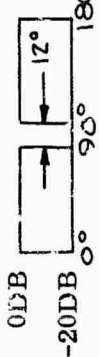
Case		Fig. C-9 (Cont)
IX (Continued)	$-2 \cos \left( \frac{2\pi d}{\lambda} \right) - 2 \left( \frac{2\pi d}{\lambda} \right) \text{Si} \left[ \frac{2\pi d}{\lambda} \right] \left\{ \right.$	
X Extended Element (2λ-Length) Isotropic Noise Single Frequency	$G(\theta, \phi) = \left[ \frac{\sin \frac{\pi A}{\lambda} \cos \theta}{\frac{\pi A}{\lambda} \cos \theta} \right]^2, \quad A = 720^\circ; I(\theta, \phi) = 1; W(f) = \delta(f - f_0)$ $R(d) = \frac{1}{2 \left[ \cos \left( \frac{2\pi A}{\lambda} \right) + \frac{2\pi A}{\lambda} \text{Si} \left( \frac{2\pi A}{\lambda} \right) - 1 \right]} \left\{ \cos \left[ \frac{2\pi}{\lambda} (A + d) \right] \right.$ $+ \frac{2\pi}{\lambda} (A - d) \text{Si} \left[ \frac{2\pi}{\lambda} (A - d) \right] + \cos \left[ \frac{2\pi}{\lambda} (A + d) \right] + \frac{2\pi}{\lambda} (A + d) \text{Si} \left[ \frac{2\pi}{\lambda} (A + d) \right]$ $\left. - 2 \cos \left( \frac{2\pi d}{\lambda} \right) - 2 \left( \frac{2\pi d}{\lambda} \right) \text{Si} \left( \frac{2\pi d}{\lambda} \right) \right\}$	C-10
XI Isotropic Element Single Frequency Non-Isotropic Noise	$G(\theta, \phi) = 1, W(f) = \delta(f - f_0),$ $R(d) = \frac{1}{(1 + B \sin \alpha)} \frac{2\pi d}{\lambda} \left[ \sin \left( \frac{2\pi d}{\lambda} \right) + B \sin \left( \frac{2\pi d}{\lambda} \sin \alpha \right) \right]$ <p>Noise Distribution (non-isotropic)</p>  <p><math>\alpha = 12^\circ, B</math> represents 20 DB step</p>	C-11
XII Isotropic Element Double Frequency Non-Isotropic Noise	$G(\theta, \phi) = 1, W(f) = \sum_{k=1}^2 \delta(f - f_k); \text{ where } f_2 = 1.25 f_1, P = .25, P = \Delta f$ <p>Noise Distribution</p>  <p><math>\alpha = 12^\circ</math> <math>B = 20 \text{ DB}</math></p>	C-12

TABLE C-1. ARRAY CONDITIONS AND CORRELATION FUNCTION (Continued)

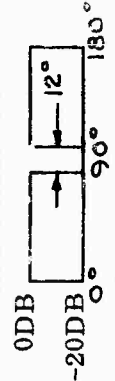
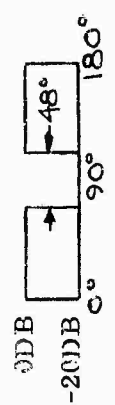
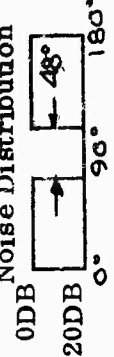
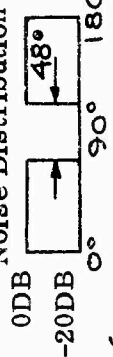
Case		Fig.
XII (Continued)	$R(d) = \frac{1}{2(1+B \sin \alpha) \frac{2\pi d}{\lambda}} \left\{ \frac{1}{1+P/2} \left[ \sin \left[ \frac{2\pi d}{\lambda} (1+P/2) \right] \right. \right. \\ \left. \left. + B \sin \left[ \frac{2\pi d}{\lambda} \sin \alpha (1+P/2) \right] \right] + \frac{1}{1-P/2} \left[ \sin \left[ \frac{2\pi d}{\lambda} (1-P/2) \right] \right. \right. \\ \left. \left. + B \sin \left[ \frac{2\pi d}{\lambda} \sin \alpha (1-P/2) \right] \right] \right\}$	C-12 (Cont)
XIII Isotropic Element Flat Bandwidth Non-Isotropic Noise	<p><math>G(\theta, \phi) = 1</math>, <math>W(f) = \text{flat bandwidth}</math>; <math>P = .5</math> (50% bw), <math>P = \Delta f</math></p> <p>Noise Distribution</p>  <p><math>\alpha = 12^\circ</math> B -20 DB</p> $R(d) = \frac{1}{P(1+B \sin \alpha) \frac{2\pi d}{\lambda}} \left\{ \text{Si} \left[ \frac{2\pi d}{\lambda} (1+P/2) \right] - \text{Si} \left[ \frac{2\pi d}{\lambda} (1-P/2) \right] \right. \\ \left. + B \text{Si} \left[ \frac{2\pi d}{\lambda} \sin \alpha (1+P/2) \right] - B \text{Si} \left[ \frac{2\pi d}{\lambda} \sin \alpha (1-P/2) \right] \right\}$	C-13
XIV Isotropic Element Single Frequency Non-Isotropic Noise	<p><math>G(\theta, \phi) = 1</math>, <math>W(f) = \delta(f-f_0)</math>, <math>P = \Delta f</math></p> <p>Noise Distribution</p>  <p><math>\alpha = 48^\circ</math> B -20 DB</p> $R(d) = \frac{1}{(1+B \sin \alpha) \frac{2\pi d}{\lambda}} \left[ \sin \left( \frac{2\pi d}{\lambda} \right) + B \sin \left( \frac{2\pi d}{\lambda} \sin \alpha \right) \right]$	C-14



TABLE C-1. ARRAY CONDITIONS AND CORRELATION FUNCTION (Continued)

Case		Fig.
XV Isotropic Elements Double Frequency Non-Isotropic Noise	$G(\theta, \phi) = 1, W(f) = \sum_{k=1}^2 \delta(f - f_k): f_2 = 1.25 f_1, P = \Delta f$ <p style="text-align: center;">Noise Distribution</p>  $R(d) = \frac{1}{2(1 + B \sin \alpha) \frac{2\pi d}{\lambda}} \left\{ \frac{1}{1 + P/2} \left[ \sin \left[ \frac{2\pi d}{\lambda} (1 + P/2) \right] \right. \right. \\ \left. \left. + B \sin \left[ \frac{2\pi d}{\lambda} \sin \alpha (1 + P/2) \right] + \frac{1}{1 + P/2} \left[ \sin \left[ \frac{2\pi d}{\lambda} (1 - P/2) \right] \right. \right. \right. \\ \left. \left. \left. + B \sin \left[ \frac{2\pi d}{\lambda} \sin \alpha (1 - P/2) \right] \right] \right\}$ <p style="text-align: right;"><math>\alpha = 48^\circ</math> B -20 DB</p>	C-15
XVI Isotropic Element Flat Bandwidth Non-Isotropic Noise	$G(\theta, \phi) = 1, W(f) = \text{flat bandwidth: } P = .5 (50\%), P = \Delta f$ <p style="text-align: center;">Noise Distribution</p>  $R(d) = \frac{1}{P(1 + B \sin \alpha) \frac{2\pi d}{\lambda}} \left\{ \text{Si} \left[ \frac{2\pi d}{\lambda} (1 + P/2) \right] \right. \\ \left. - \text{Si} \left[ \frac{2\pi d}{\lambda} (1 - P/2) \right] + B \text{Si} \left[ \frac{2\pi d}{\lambda} \sin \alpha (1 + P/2) \right] \right. \\ \left. - B \text{Si} \left[ \frac{2\pi d}{\lambda} \sin \alpha (1 - P/2) \right] \right\}$ <p style="text-align: right;"><math>\alpha = 48^\circ</math> B -20 DB</p>	C-16

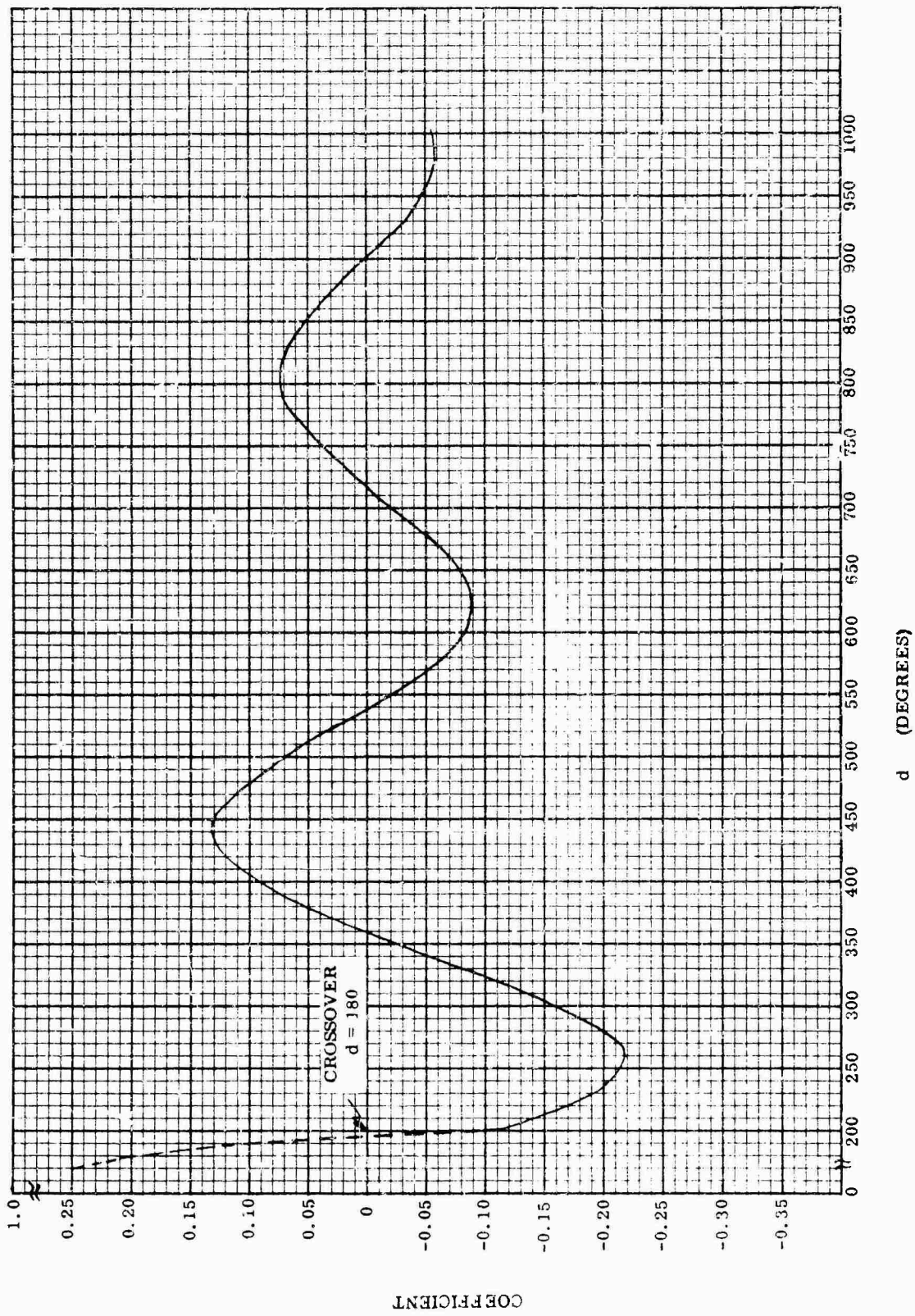


Figure C-1. Correlation Coefficient  $R$  (d)

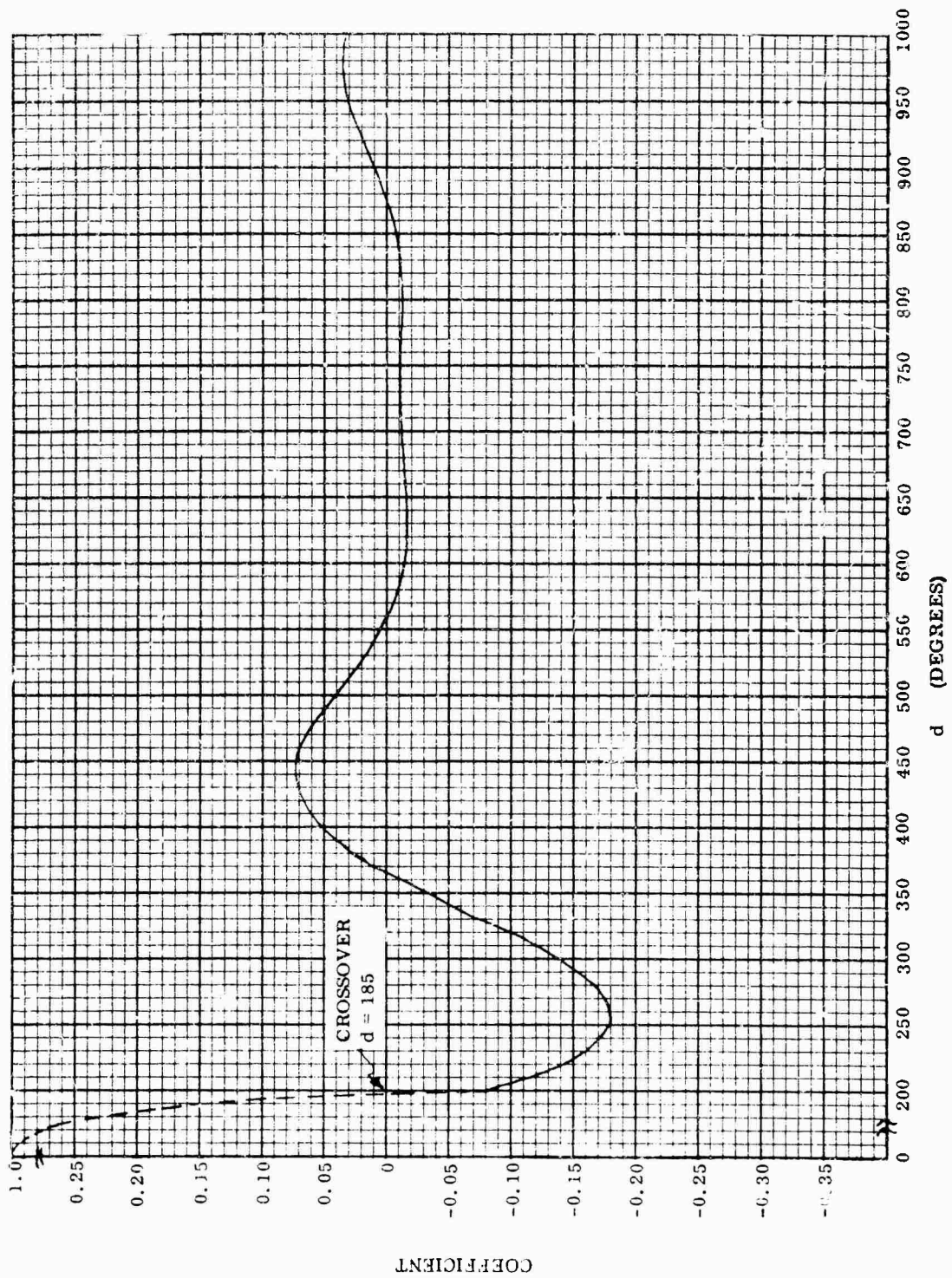


Figure C-2. Correlation Coefficient  $R(d)$

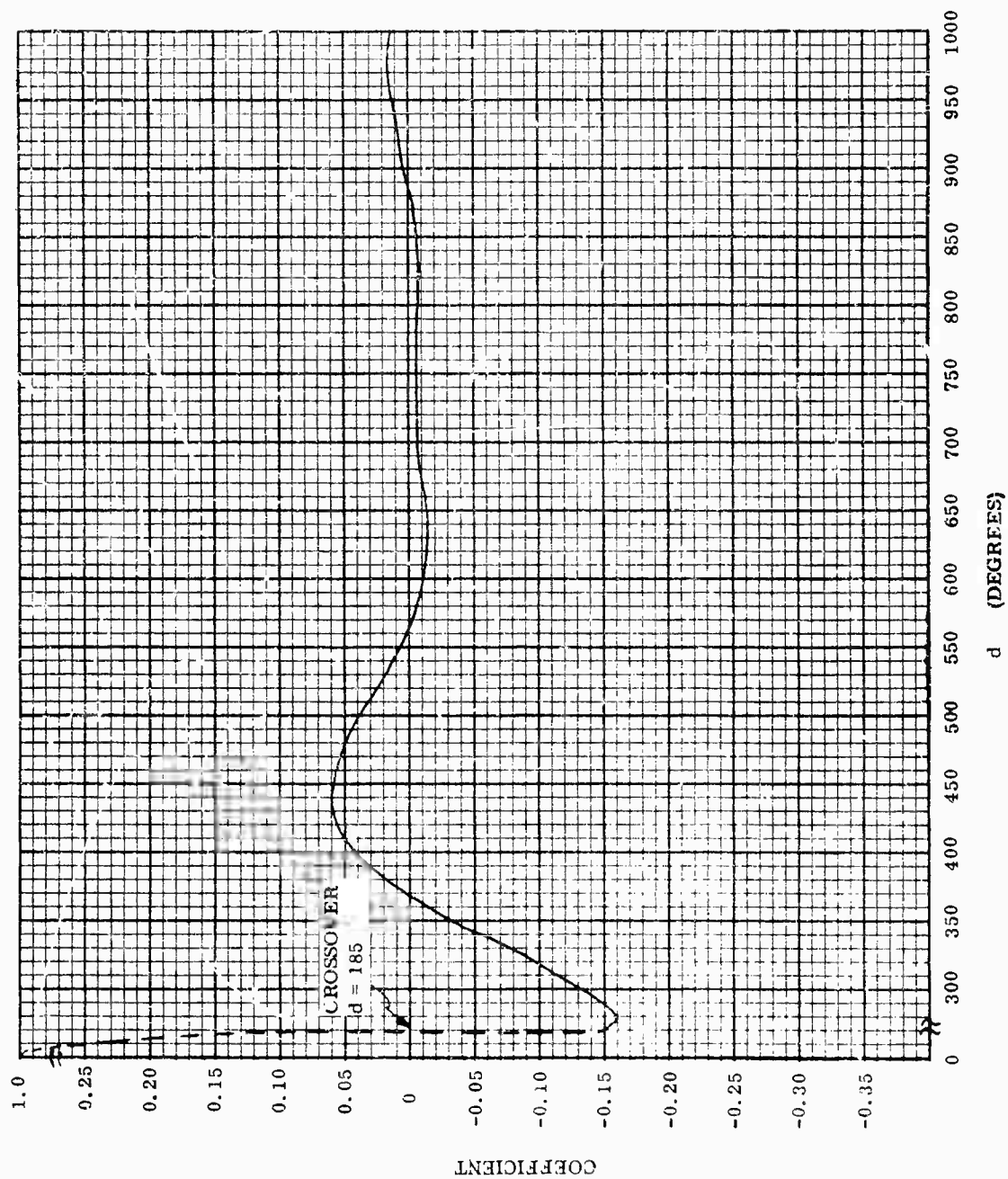


Figure C-3. Correlation Coefficient  $R(d)$

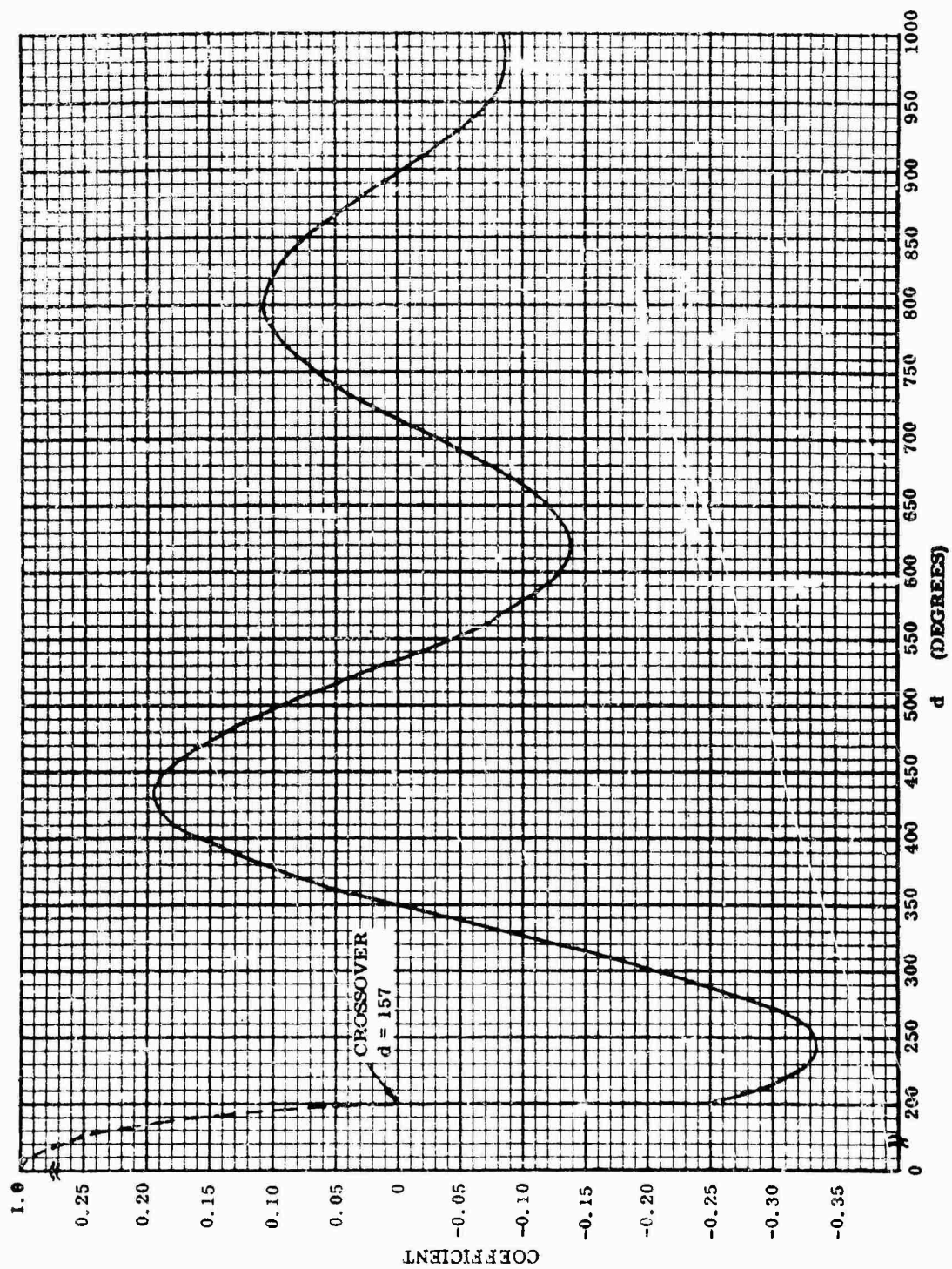


Figure C-4. Correlation Coefficient  $R(d)$



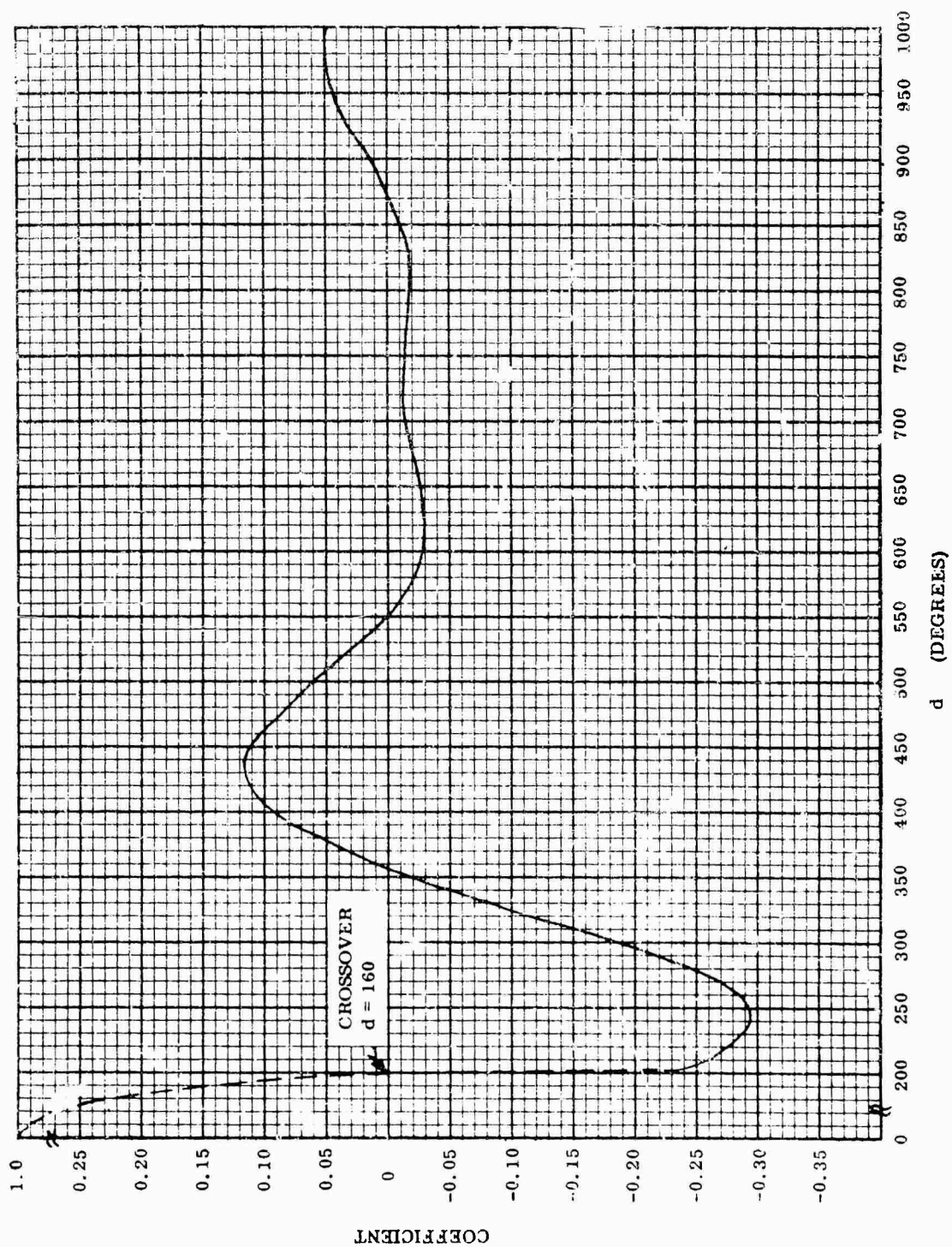


Figure C-5. Correlation Coefficient  $R(d)$

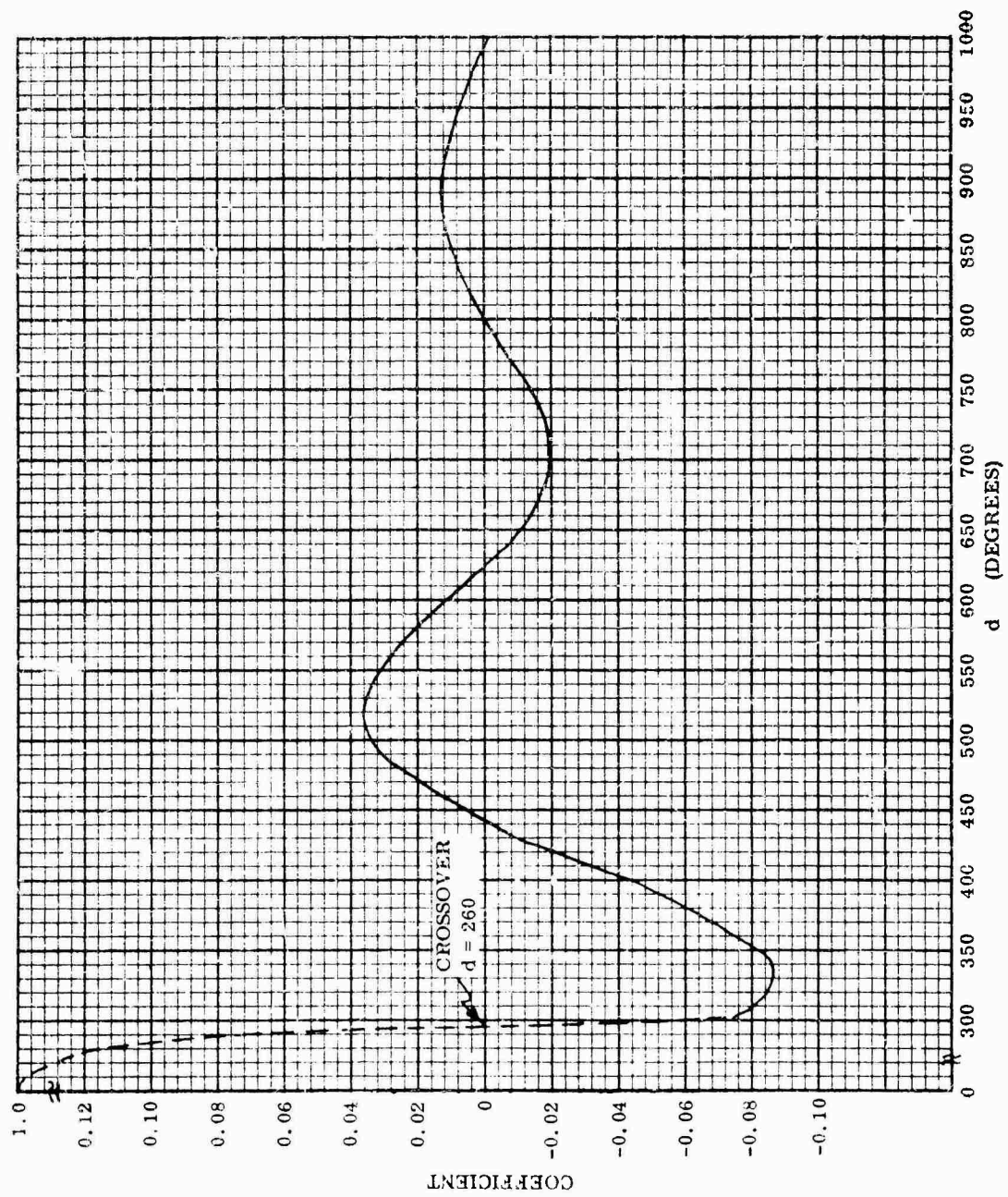


Figure C-6. Correlation Coefficient  $R(d)$

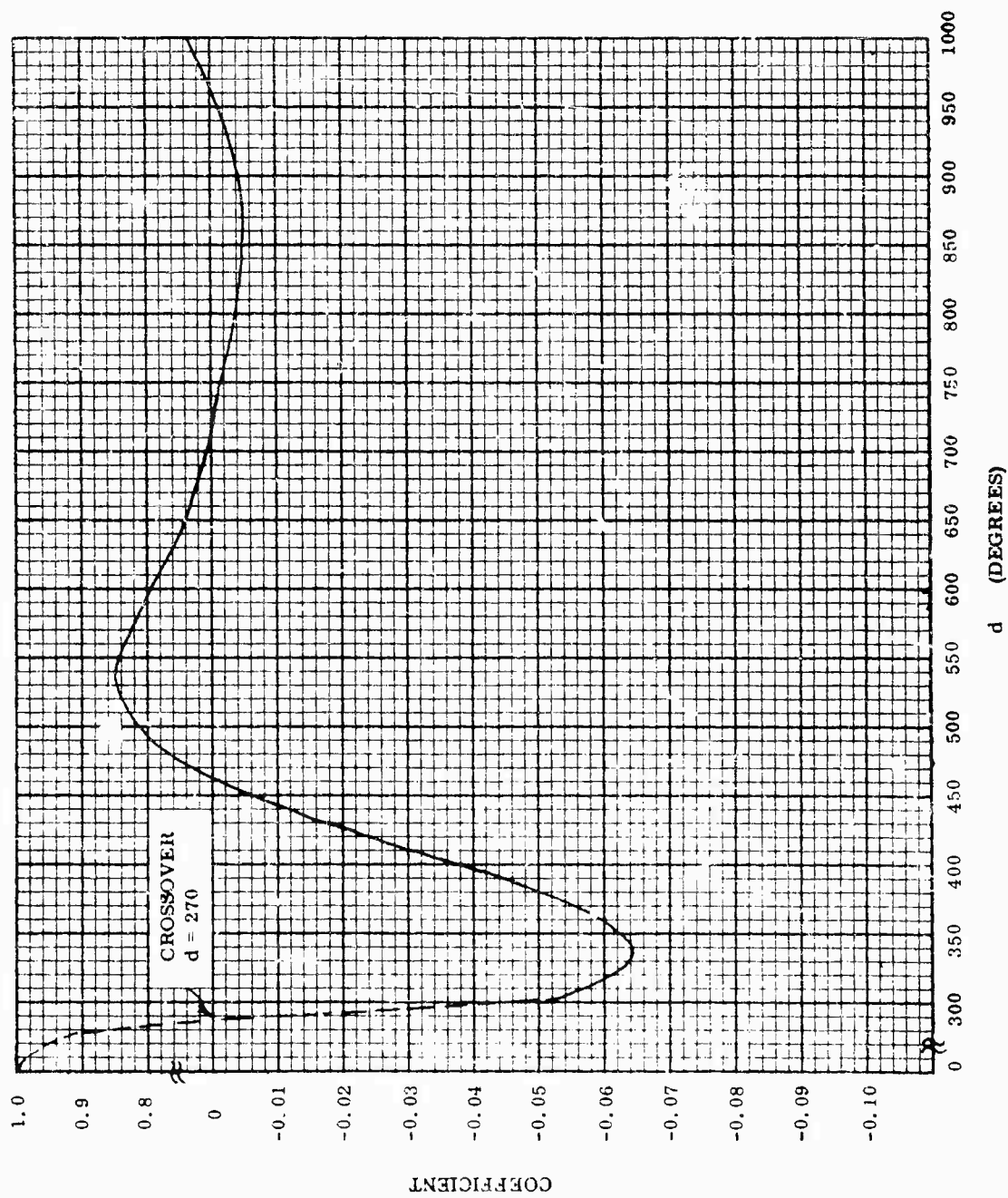


Figure C-7. Correlation Coefficient  $R$  ( $d$ )



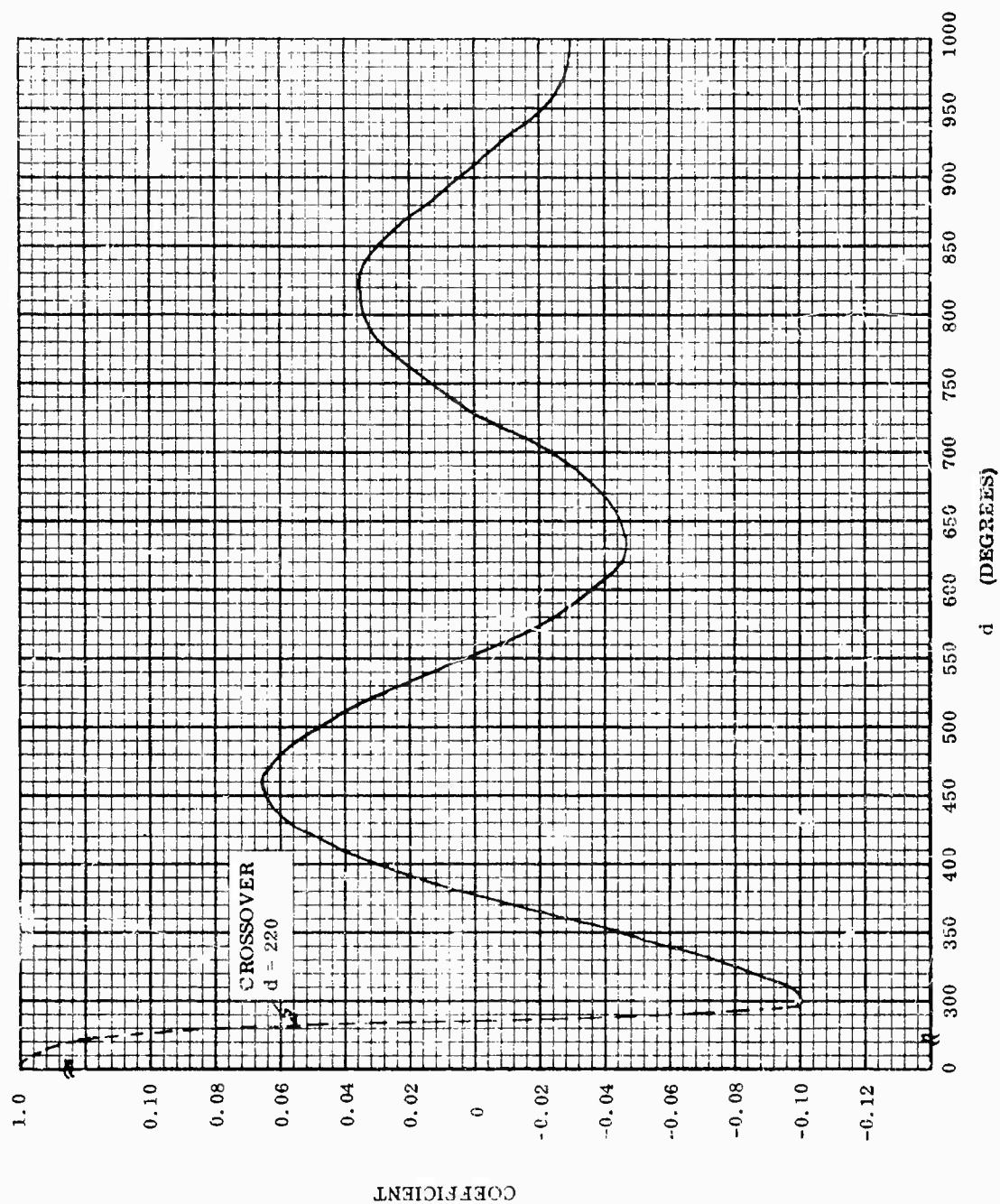


Figure C-8. Correlation Coefficient  $R$  ( $d$ )

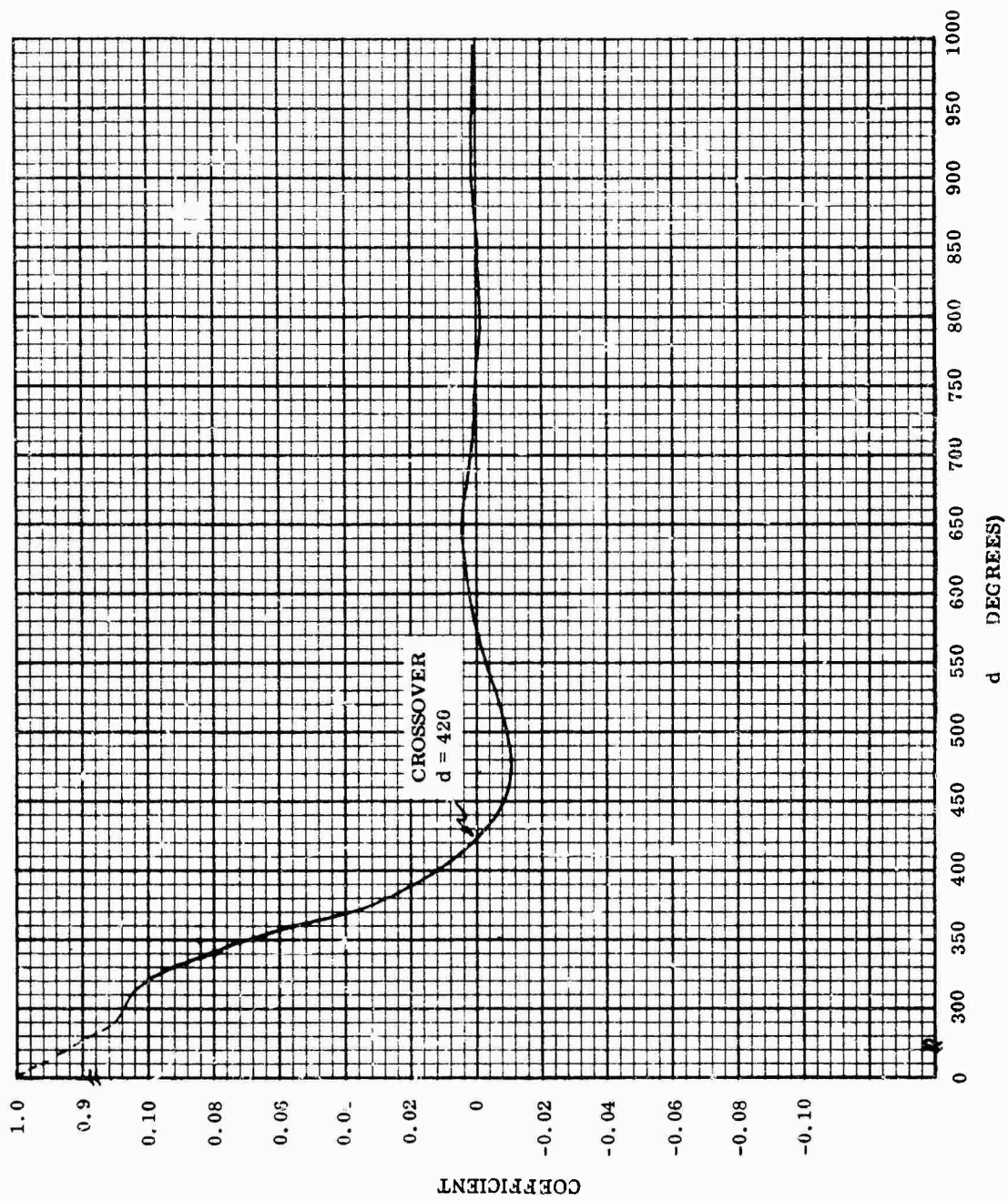


Figure C-9. Correlation Coefficient R (d)

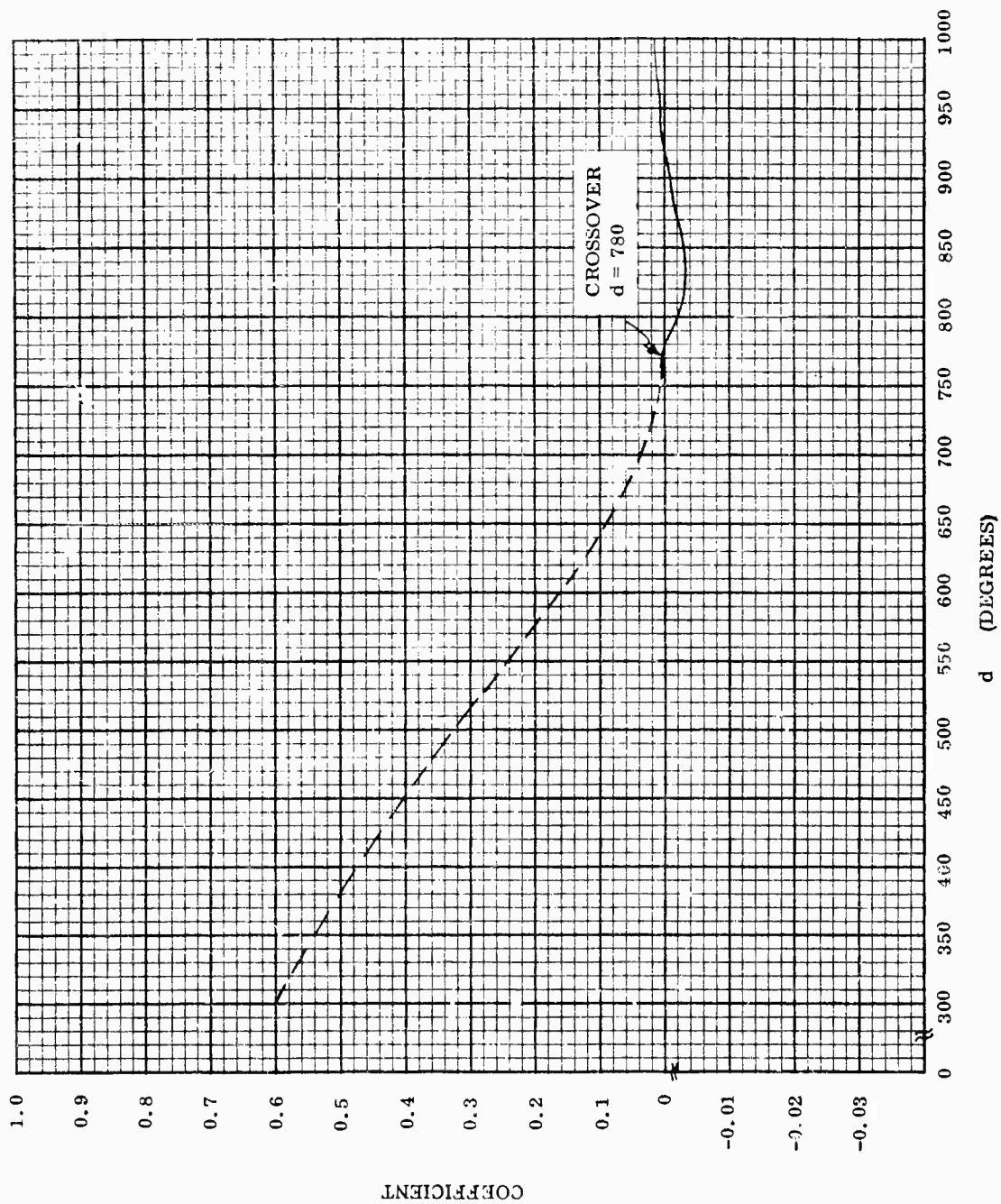


Figure C-10. Correlation Coefficient  $R(d)$

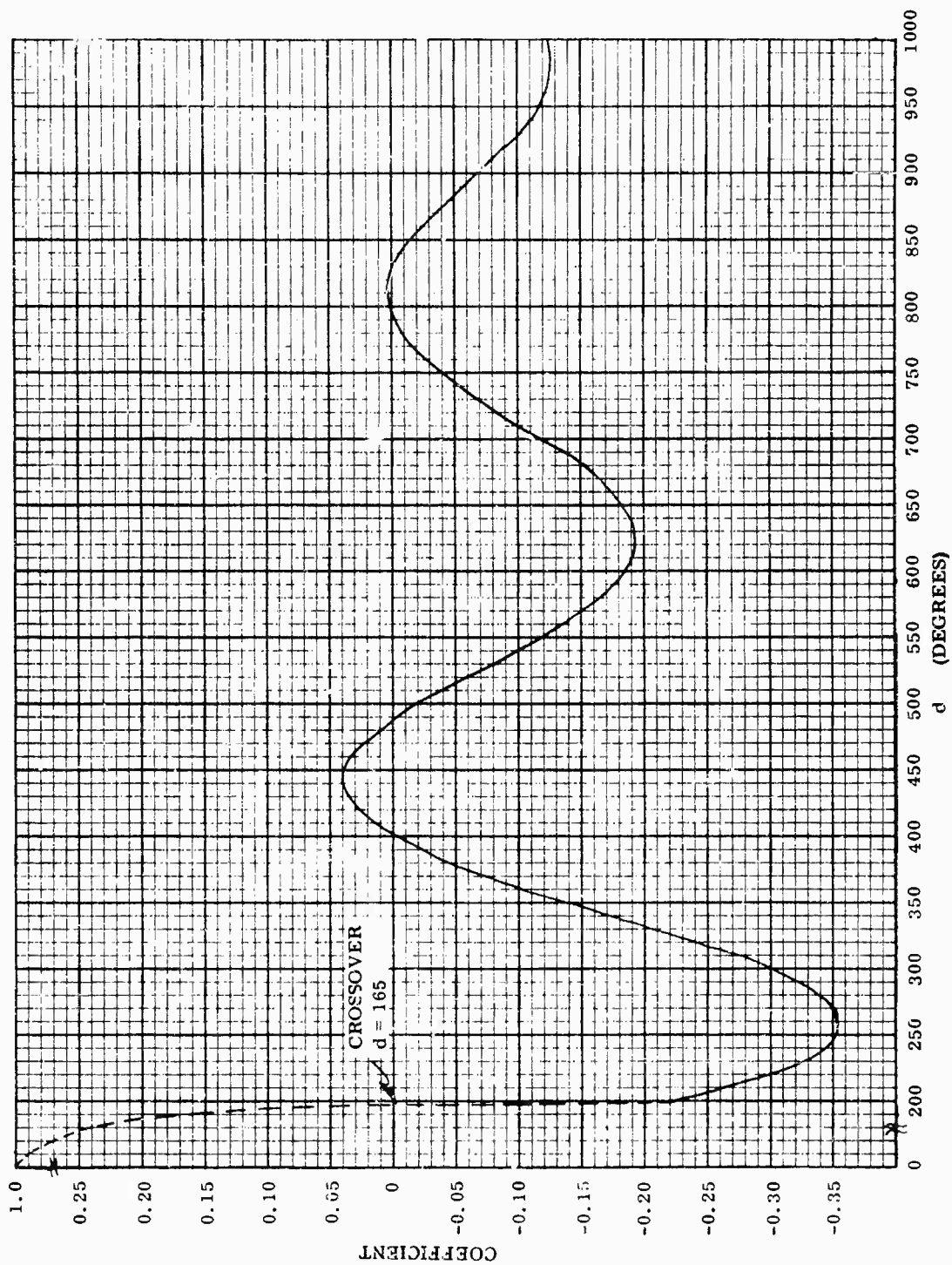


Figure C-11. Correlation Coefficient  $R$  (d)

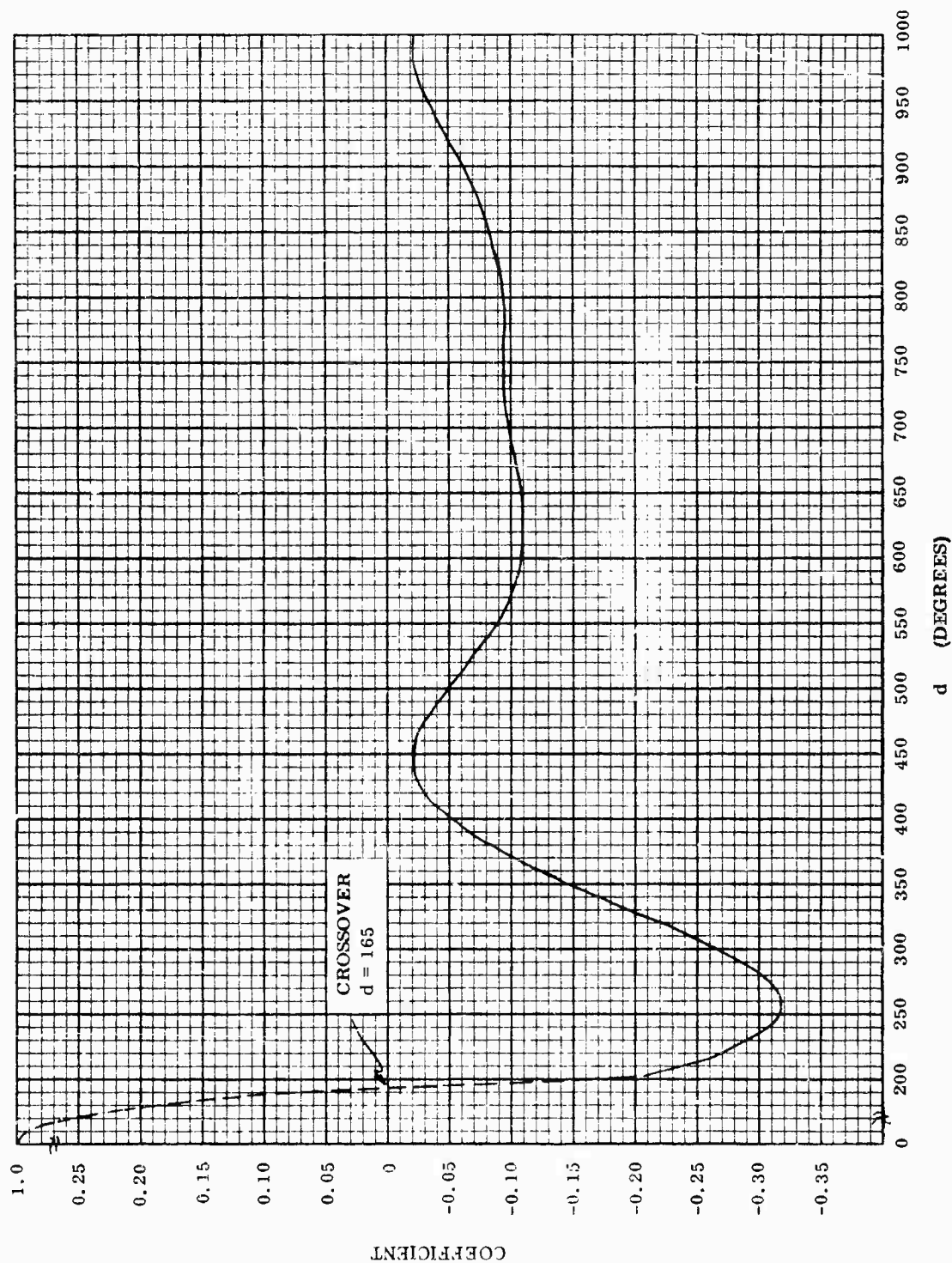


Figure C-12. Correlation Coefficient R (d)

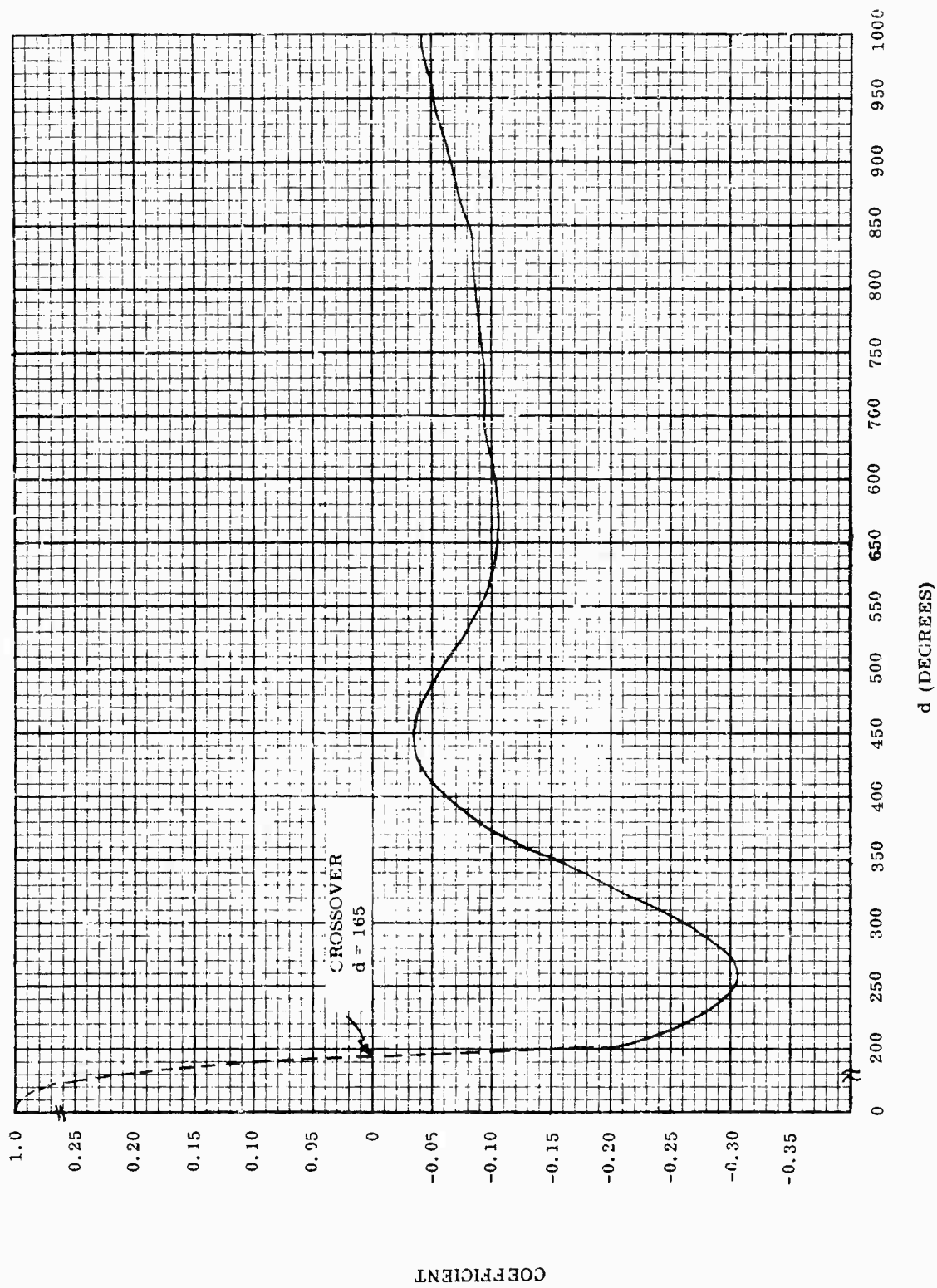


Figure C-13. Correlation Coefficient  $R$  ( $d$ )

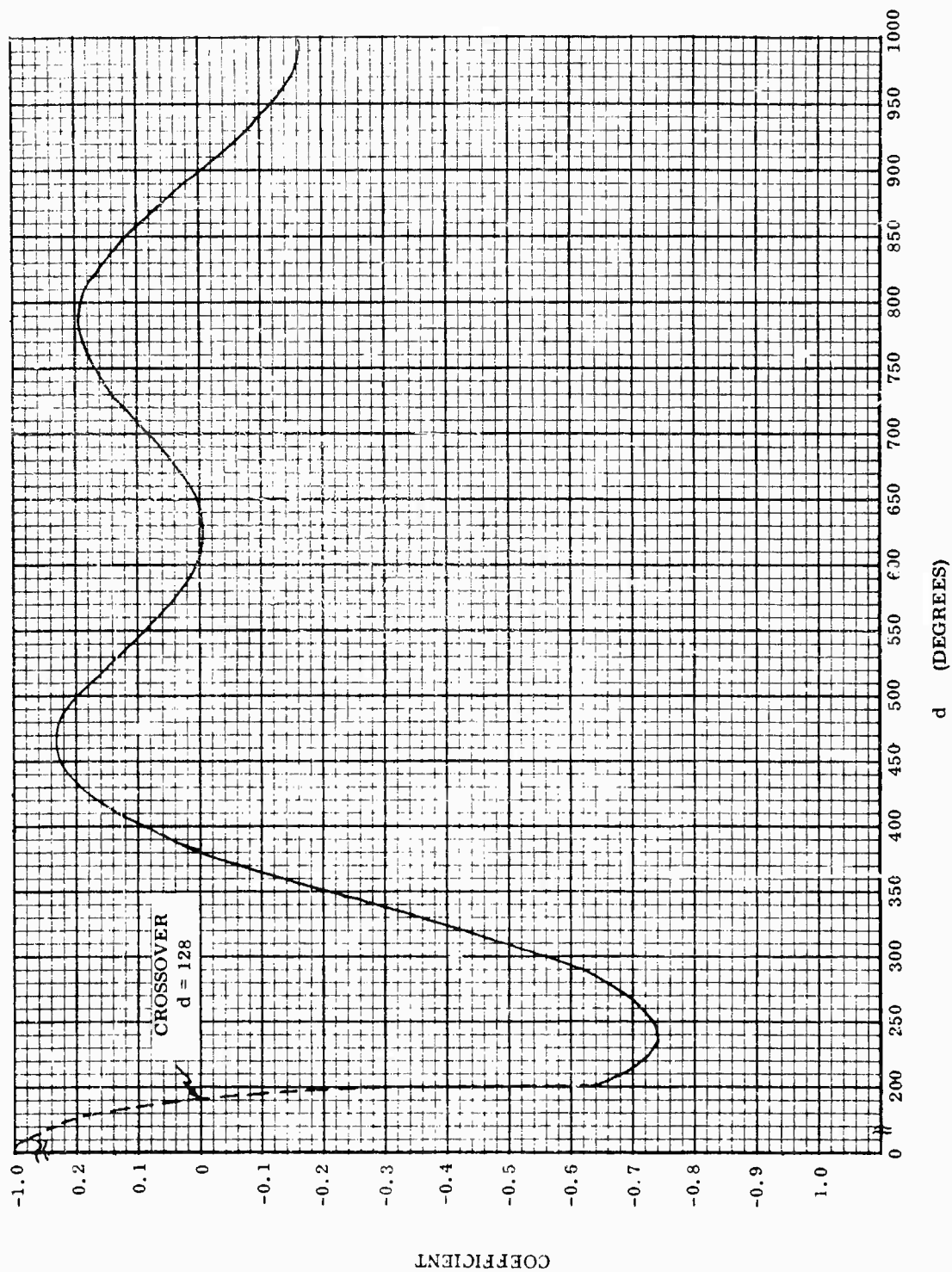


Figure C-14. Correlation Coefficient  $R$  ( $d$ )



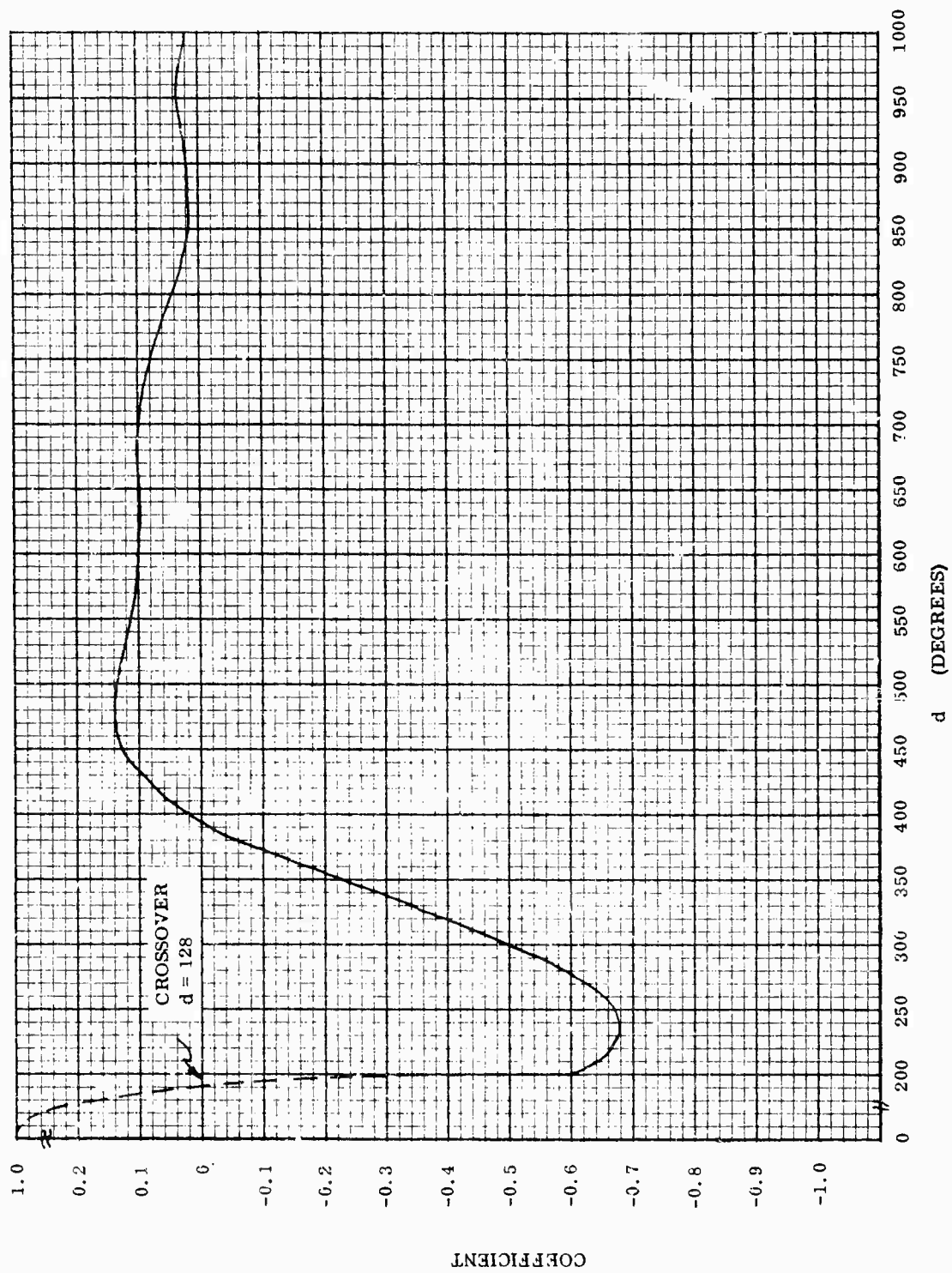


Figure C-15. Correlation Coefficient  $R$  ( $d$ )



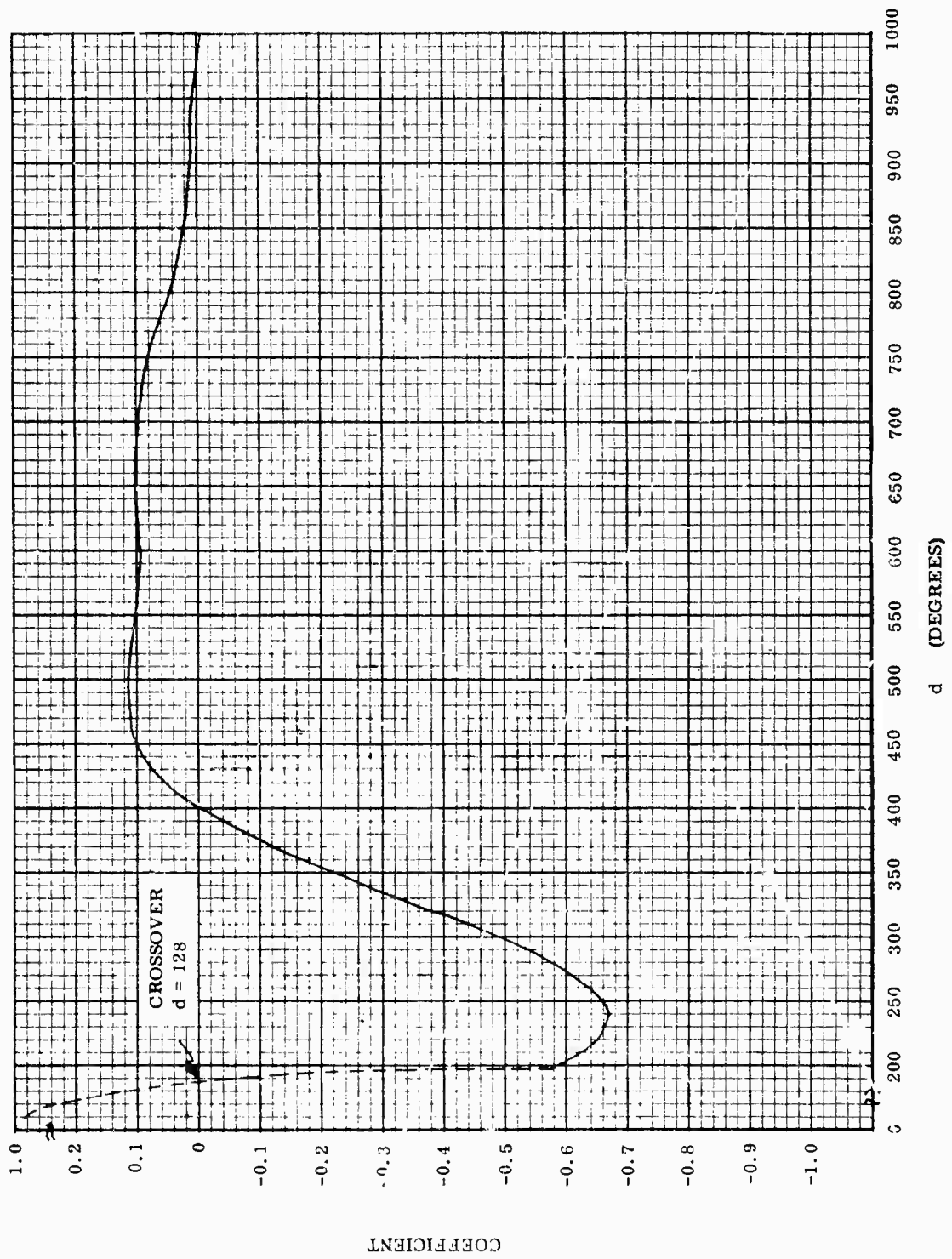


Figure C-16. Correlation Coefficient  $R$  ( $d$ )

Unclassified

Security Classification

DOCUMENT CONTROL DATA - R & D		
Security classification of title, body of abstract and indexing annotation must be entered when the overall report is classified		
1. ORIGINATING ACTIVITY (Corporate author)		2a. REPORT SECURITY CLASSIFICATION
The Bendix Corporation Communications Products Division Baltimore, Maryland		Unclassified
2. REPORT TITLE		2b. GROUP
Wideband Element Spacing and Weighting		- - -
3. DESCRIPTIVE NOTES (Type of report and inclusive dates)		
Final Report 4 April 1966 to 4 April 1967		
4. AUTHOR(S) (First name, middle initial, last name)		
Rupp, William E. Schneider, Wilfred E. Randolph, Philip L.		
5. REPORT DATE	7a. TOTAL NO. OF PAGES	7b. NO. OF PAGES
July 1967	158	26
6a. CONTRACT OR GRANT NO.	9a. ORIGINATOR'S REPORT NUMBER(S)	
AF30(602)-4206	471-929-841	
6b. PROJECT NO	9b. OTHER REPORT NO(S) (Any other numbers that may be assigned this report)	
4506	RADC-TR-67-347	
10. DISTRIBUTION STATEMENT		
This document is subject to special export controls and each transmittal to foreign governments, foreign nationals or representatives thereto may be made only with prior approval of RADC (EMLI), GAFB, N.Y. 13440.		
11. SUPPLEMENTARY NOTES		12. SPONSORING MILITARY ACTIVITY
Joseph Lovecchio EMATS/330-3685		Rome Air Development Center Techniques Branch (EMAT) Griffiss Air Force Base, New York 13440
13. ABSTRACT		
<p>This study was initiated to determine the effects of antenna element weighting (amplitude control) and spacing on the signal-to-noise ratio of wideband systems. The initial analysis is directed toward the linear array operating in an environment of white noise, uniformly distributed in space. These confinements are later removed to illustrate application to planar arrays, and non-uniform noise conditions.</p> <p>It is shown that the signal-to-noise ratio of an antenna system operating in a uniform noise environment is optimized when the array directivity is maximum. Optimization involves the application of a specific illumination function which can be achieved by element weighting element spacing or a combination.</p> <p>The application of wideband signals modifies the array pattern in the time space domain. Although the nature of the modification is dependent on waveform, the sidelobe displacement in time and space is a function of the number of elements comprising the array.</p> <p>An iterative technique of mathematical analysis is developed which permits solutions to large array problems where matrix inversion is difficult. Several examples of possible applications of the analysis are presented including a spectral detection technique, an approach to secure communications, and a concept of array adaptation to a non-uniform noise environment.</p>		

DD FORM 1473

Unclassified

Security Classification

Unclassified

Security Classification

1a	KEY WORDS	LINK A		LINK B		LINK C	
		ROLE	WT	ROLE	WT	ROLE	WT
	Antenna Arrays Signal-to-Noise Ratio Optimum Directivity Wideband Antennas Matrix Inversion						

Unclassified

Security Classification